

DOCTORAL SCHOOL OF EARTH SCIENCES
FACULTY OF SCIENCE AND INFORMATICS
UNIVERSITY OF SZEGED

**TOWARD CLIMATE-RESILIENT AGRICULTURE IN NORTHERN KAZAKHSTAN:
INTEGRATING SNOWMELT-BASED DROUGHT MITIGATION, CROP MODELING,
AND YIELD IMPACT ASSESSMENT**

PhD Dissertation

TELEUBAY ZHANASSYL

Supervisor:

PROF. DR. ZOLTÁN KOVÁCS

SZEGED

2025

Table of Contents

1. Introduction	9
1.1. Background	9
1.1.1. <i>Climate Change and Agricultural Vulnerability in Northern Kazakhstan</i>	9
1.1.2. <i>Snowpack as a Potential Resource for Agricultural Resilience</i>	10
1.1.3. <i>Snowmelt Harvesting as an Adaptive Strategy</i>	11
1.1.4. <i>Study area</i>	13
1.2. Problem Statement	14
1.3. Research Objectives	15
1.4. Data and Methods	16
1.5. Dissertation outline	17
2. Comparison of Climate Change Effects on Wheat Production under Different Representative Concentration Pathway Scenarios in North Kazakhstan	18
2.1. Introduction	20
2.2. Materials and Methods	22
2.2.1. <i>Study Area</i>	23
2.2.2. <i>Data Sources</i>	23
2.2.3. <i>Methodology</i>	26
2.3. Results	26
2.4. Discussions	30
2.5. Conclusions	32
3. Comparison of Snow Indices in Assessing Snow Cover Depth in Northern Kazakhstan	32
3.1. Introduction	34
3.2. Materials and Methods	36
3.2.1. <i>Study Area</i>	36
3.2.2. <i>Data Sources</i>	37
3.2.3. <i>Methodology</i>	39
3.3. Results	42
3.3.1. <i>Calculation of the Snow Spectral Indices</i>	42
3.3.2. <i>Estimation of SCF</i>	44
3.3.3. <i>Snow Depth Modeling</i>	45
3.3.4. <i>SWE Calculation</i>	47
3.4. Discussions	48

3.5.	Conclusions	49
3.6.	Appendix A	51
4.	Identification of Potential Farm Pond Sites for Spring Surface Runoff Harvesting Using an Integrated Analytical Hierarchy Process in a GIS Environment in Northern Kazakhstan	59
4.1.	Introduction	60
4.2.	Materials and Methods	64
4.2.1.	<i>Study Area</i>	64
4.2.2.	<i>Data Sources</i>	64
4.2.3.	<i>Methodology</i>	67
4.3.	Results	74
4.3.1.	<i>Hydrogeology</i>	75
4.3.2.	<i>Slope</i>	76
4.3.3.	<i>Drainage Density</i>	76
4.3.4.	<i>Land Use/Land Cover</i>	77
4.3.5.	<i>Soil</i>	78
4.3.6.	<i>Snow Water Equivalent</i>	79
4.3.7.	<i>Overall Assessment of Potential Farm Pond Sites</i>	80
4.3.8.	<i>Validation of Potential Farm Pond Sites Map</i>	82
4.4.	Discussions	83
4.5.	Conclusions	84
4.6.	Appendix B	84
5.	Conclusions	88
5.1.	Summary of Key Findings	88
5.2.	Implications	89
5.3.	Limitations, Recommendations, and Future Research.....	90

List of Tables

Table 1.1. Summary of Datasets Used in the Study	17
Table 2.1. Planting methods in four soil and farming zones of North Kazakhstan region.....	25
Table 2.2. Average wheat yield in the North Kazakhstan region and each soil and farming zone under RCPs 2.6, 4.5, and 8.5 in 2050	26
Table 3.1. Snow survey dates and numbers of measured points in the territories of the three limited liability partnerships	37
Table 3.2. Specifications of the Sentinel-2 multispectral instrument.....	39
Table 3.3. Snow indices and their definitions	41
Table 3.4. Modeled snow depth error assessments	47
Table 4.1. A quick summary of recent studies on identification of potential rainwater harvesting sites	62
Table 4.2. Snow survey dates and number of measured points in the study area	65
Table 4.3. Specifications of the Sentinel-2 multispectral instrument.....	66
Table 4.4. Analytical hierarchy process significance scale by Saati	72
Table 4.5. Relative weights of input layers compiled with expert judgment	73
Table 4.6. Evaluation of pairwise matrix consistency.....	73

List of Figures

Figure 1.1. Study area and the soil map of the Republic of Kazakhstan.....	14
Figure 2.1. Study area and digitized wheat fields in 2021	23
Figure 2.2. The flowchart of the future spatial wheat yield prediction	26
Figure 2.3. Predicted wheat yield in kg/ha under RCP 2.6 in the North Kazakhstan region for the midcentury	27
Figure 2.4. Predicted wheat yield in kg/ha under RCP 4.5 in the North Kazakhstan region for the midcentury	28
Figure 2.5. Predicted wheat yield in kg/ha under RCP 8.5 in the North Kazakhstan region for the midcentury	29
Figure 2.6. Predicted wheat yield difference in kg/ha between RCPs 2.6–4.5 (a), 4.5–8.5 (b), and 2.6–8.5 (c) in the North Kazakhstan region. Blue and red circles indicate favorable and unfavorable areas, respectively	30
Figure 3.1. Study area and soil map of the Republic of Kazakhstan.....	37
Figure 3.2. Waypoints of snow survey over the territories of the three agricultural enterprises: (a) limited liability partnership (LLP) North Kazakhstan Agricultural Experimental Station, (b) LLP Naidorovskoe, and (c) LLP A.I. Barayev Research and Production Cent Center for Grain Farming.....	37
Figure 3.3. Process of measuring the snow height and density	38
Figure 3.4. Flowchart of the data processing methods in the present study.....	40
Figure 3.5. Spectral snow indices at “North Kazakhstan Agricultural Experimental Station”: (a) normalized-difference snow index [NDSI]-1, (b) NDSI-2, (c) normalized-difference snow and ice index [NDSII]-1, (d) NDSII-2, (e) difference snow index [DSI]-1, (f) DSI-2,	43
Figure 3.6. Agricultural field at the “North Kazakhstan Agricultural Experimental Station” after applying the snow retention technique. Source: Captured by the authors during the field-snow survey	44
Figure 3.7. Snow cover fraction (SCF) maps at the “North Kazakhstan Agricultural Experimental Station” generated from different snow cover indices: (a) NDSI-1, (b) NDSI-2, (c) NDSII-1, (d) NDSII-2, (e) DSI-1, (f) DSI-2, (g) RSI-1, and (h) RSI-2	45
Figure 3.8. Snow depth maps at “North Kazakhstan Agricultural Experimental Station” generated from the SCFs of (a) NDSI-1, (b) NDSI-2, (c) NDSII-1, (d) NDSII-2, (e) DSI-1, (f) DSI-2, (g) RSI-1, and (h) RSI-2	46
Figure 3.9. Snow water equivalent (kg/m ²) maps of the “North Kazakhstan Agricultural Experimental Station” generated from the SDs of (a) NDSI-1, (b) NDSI-2, (c) NDSII-1, (d) NDSII-2, (e) DSI-1, (f) DSI-2, (g) RSI-1, and (h) RSI-2	48
Figure 4.1. Study area and the soil map of the Republic of Kazakhstan.....	64
Figure 4.2. Waypoints of snow survey over the territory of Akkayin district, North Kazakhstan Region (a) between 25 and 27 January 2023 and (b) between 25 and 27 February 2023.....	65
Figure 4.3. The conceptual framework of the research	68
Figure 4.4. Digitized boundaries of agricultural fields in the study area	69
Figure 4.5. Flow chart of the methodology for calculating the snow water equivalent	71
Figure 4.6. Hierarchy structure of the identification of potential farm pond sites	72
Figure 4.7. Reclassified hydrogeological map of Akkayin district.....	75
Figure 4.8. Reclassified slope map of Akkayin district.....	76
Figure 4.9. Reclassified drainage density map of Akkayin district.....	77
Figure 4.10. Reclassified land use/land cover map of Akkayin district.....	78

Figure 4.11. Reclassified soil map of Akkayin district	79
Figure 4.12. Reclassified snow water equivalent map of Akkayin district	80
Figure 4.13. The relative weights of the potential farm pond site indicators	81
Figure 4.14. Overall potential farm pond sites for melt and flood water reservation map of Akkayin district, North Kazakhstan region, overlaid on agricultural fields.....	82

Abbreviations and acronyms

AHP	Analytical hierarchy process
AEGIS/WIN	Agricultural mad Environmental Geographic Information System for Windows
APSIM	Agricultural Production Systems sIMulator
BioMA	Biophysical Models Applications
CC BY	Creative Commons Attribution License
CI	Consistency index
CILOS	Criterion impact loss
CR	Consistency ratio
CRAFT	CCAFS Regional Agricultural Forecasting Toolbox
DD	Drainage density
DEM	Digital elevation model
DSI	Difference Snow Index
DSM	Digital surface model
DSSAT	Decision Support System for Agrotechnology Transfer
ESM	Earth System Model
FAO UN	Food and Agriculture Organization of the United Nations
GCP	Ground control points
GEE	Google earth engine
GEPIC	GIS-based Environmental Policy Integrated Climate
GFDL	Geophysical Fluid Dynamics Laboratory
GIS	Geographic information system
GPS	Global positioning system
GYGA	Global Yield Gap Atlas
IPCC	Intergovernmental Panel on Climate Change
LULC	Land use and land cover
MCDA	Multi-criteria decision analysis
MEREC	Method based on the removal effects of criteria
MSI	Multispectral instrument
NDSI	Normalized Difference Snow Index
NDSII	Normalized Difference Snow and Ice Index
PFPS	Potential farm pond sites
RCP	Representative Concentration Pathway
RI	Random index

RS	Remote sensing
RSI	Ratio Snow Index
SAPEVO-M	Simple aggregation of preferences expressed by ordinal vectors group decision making
SCF	Snow cover fraction
SD	Snow depth
SDGs	Sustainable Development Goals
STICS	Simulateur mulTIdisciplinaire pour les Cultures Standard
SWE	Snow water equivalent
UAV	Unmanned aerial vehicle
UNESCO	United Nations Educational, Scientific and Cultural Organization

1. Introduction

1.1. Background

1.1.1. Climate Change and Agricultural Vulnerability in Northern Kazakhstan

In recent decades, climate change has emerged as a global crisis transcending national borders and economic systems, reshaping ecosystems, and threatening food security worldwide (IPCC, 2021). Agriculture, a cornerstone of human civilization, is particularly vulnerable, given its direct dependency on climatic variables such as temperature, precipitation, and atmospheric CO₂ levels. Changes in these factors can disrupt crop development, shift phenological cycles, and destabilize yields, posing significant risks to both subsistence farming and global food trade networks (Teleubay et al., 2024). Northern Kazakhstan, and particularly the North Kazakhstan Region (NKR), plays a pivotal role in this equation. It is one of the country's most productive agricultural zones, contributing approximately one-quarter (24%) of Kazakhstan's total wheat output (U.S. Department of Agriculture, 2022). The region's rainfed wheat systems are highly sensitive to climatic changes, especially to rising temperatures, prolonged droughts, and altered rainfall patterns. Studies show that if left unaddressed, these shifts may compromise regional and Central Asian food security, as Kazakhstan supplies substantial wheat exports (nearly half of all production) to neighboring countries such as Uzbekistan, Afghanistan, and Iran (U.S. Department of Agriculture, 2023).

Multiple crop models have been developed to quantify the influence of climate change on crop production. Tools like DSSAT (Decision Support System for Agrotechnology Transfer), APSIM (Agricultural Production Systems sIMulator), and STICS (Simulateur mulTidisciplinaire pour les Cultures Standard) integrate climate data, agronomic parameters, and management practices to estimate yield outcomes under varying scenarios (Fraga et al., 2015; Xiang et al., 2020). The Decision Support System for Agrotechnology Transfer (DSSAT), in particular, has been widely applied for wheat yield simulations under future climate conditions. In Northern Kazakhstan, the DSSAT model was implemented through the CCAFS Regional Agricultural Forecasting Toolbox (CRAFT v3.4) to assess wheat yield responses to RCP 2.6, RCP 4.5, and RCP 8.5 climate scenarios by 2050 (Shelia et al., 2019; Teleubay et al., 2024). The simulation results reveal that wheat yields are projected to decrease under both moderate and high-emission scenarios, with more severe declines observed in arid steppe and small hilly zones. These findings are consistent with broader regional trends indicating that increasing temperatures, shortened growth periods, and greater evapotranspiration stress will reduce the productivity of spring wheat, the dominant crop in the region (Attia et al., 2021; Bureau of National Statistics, Agency for Strategic Planning and Reforms of the Republic of Kazakhstan, 2023; Mubeen et al., 2020; North Kazakhstan Agricultural Experimental Station, 2022). Importantly, the results highlight a geographic disparity in vulnerability, suggesting that some districts, due to soil properties, microclimate, or elevation, will be more affected than others (Teleubay et al., 2024). This spatial variability supports the need for site-specific adaptation strategies. Without intervention, food insecurity risks may extend beyond Kazakhstan's borders, affecting more than 80 million people in Central Asia dependent on regional grain trade.

Given these projections, there is an urgent need to explore alternative or supplemental water management solutions capable of reducing climate exposure. Traditional irrigation infrastructure is largely absent across Northern Kazakhstan's wheat-growing belt, making large-scale irrigation infeasible. Instead, adaptive strategies must work with existing hydrological and climatic conditions. Among these, snowmelt harvesting, examined in detail in the following sections, emerges as a practical and scalable response.

1.1.2. Snowpack as a Potential Resource for Agricultural Resilience

Snowmelt runoff serves as a vital hydrological resource in many cold-region agricultural systems, and Northern Kazakhstan is no exception. The region receives substantial snowfall during the winter months, with typical average snow depths ranging between 20 to 40 cm. As this snowpack melts rapidly in spring, it often results in flood events that damage infrastructure and inundate rural settlements (Nurbatsina et al., 2025; Terekhov et al., 2023). Simultaneously, the summer months are characterized by severe moisture deficits that limit crop yields (Karatayev et al., 2022). This duality, water abundance during snowmelt and scarcity during peak agricultural demand, presents a critical opportunity, managing snowmelt runoff for spring water harvesting and agricultural use (Dietz et al., 2012).

Yet, the spatial extent of the North Kazakhstan Region (approximately 97,000 km²) poses a serious challenge for direct in-situ monitoring of snowpack conditions. Therefore, remote sensing has become a cornerstone of snow monitoring efforts. Accurate estimation of snow depth and SWE is essential for evaluating runoff potential and water availability in cold-region agricultural systems. Researchers around the world have employed a range of methods, spanning in-situ field observations, geographic information systems, and remote sensing techniques, to quantify snowpack characteristics. These efforts generally fall into two methodological approaches: direct measurement of snow properties and indirect estimation using remote sensing, derived indices and empirical modeling. From the direct measurement perspective, field-based experiments such as the Nordic Snow Radar Experiment (NoSREx) have advanced our understanding of snowpack dynamics. Lemmetyinen et al. (2016) demonstrated that gamma water instruments deployed at intensive observation sites can yield real-time estimates of snow depth, density, and SWE. Gan et al. (2021) compared SWE retrievals from two passive microwave sensors, the Advanced Technology Microwave Sounder (ATMS) and the Advanced Microwave Scanning Radiometer 2 (AMSR2), and proposed parameterized equations for estimating snow depth in both forested and open landscapes. These products were particularly effective at elevations below 900 meters and snow depths under 20 cm, making them applicable to regions like Northern Kazakhstan with similar snow conditions. UAV-mounted radar systems have also emerged as a promising tool for direct snowpack monitoring. Jenssen & Jacobsen (2021) used an ultra-wide-band radar (0.7–4.5 GHz) on an unmanned aerial vehicle to measure snow depths up to 5.5 meters with high precision ($R > 0.92$). However, the system's ability to estimate snow density lagged due to algorithmic limitations, suggesting further development is needed before such tools are widely operationalized.

On the other hand, indirect estimation methods using satellite-derived snow indices and Snow Cover Fraction (SCF) equations offer broader spatial coverage, albeit with certain trade-offs in precision. These methods are particularly valuable in large and data-scarce regions like Kazakhstan. Lin et al. (2012) applied a set of snow indices, including the RSI, DSI, and the widely used NDSI, to estimate snow cover fraction in northwestern China. Their results showed that exponential regression ($R^2 > 0.79$) outperformed linear regression models, highlighting the potential of non-linear approaches for snow cover modeling. Romanov & Tarpley (2004) also found strong exponential relationships between snowpack depth and fractional snow cover. Their SCF-based modeling achieved a mean absolute error of just 5 cm across the U.S. Great Plains and Canadian Prairies, which share some climatic similarities with Kazakhstan's steppe zone. Similarly, Kim et al. (2017) evaluated linear, quadratic, and exponential functions of NDSI to estimate snow depth in South Korea. While the quadratic function produced the lowest RMSE (2.37 cm), the linear model (RMSE = 3.43 cm) was deemed more robust under high-snowfall conditions due to better stability. Additional improvements in snow cover delineation were proposed by Dixit et al. (2019), who compared NDSI, NDSII, and a newer S3 index in the Indian Himalayas. They ultimately introduced the Snow Water Index (SWI), which integrates green, NIR, and SWIR bands to enhance snow discrimination accuracy. The SWI achieved an overall classification accuracy of 93%, outperforming existing indices and offering better performance in forested regions.

Snowmelt-derived water is crucial for alleviating water stress during dry periods and reducing reliance on rainfall-fed systems. In Northern Kazakhstan, the agricultural calendar is tightly coupled with snowmelt timing; delays or accelerations in melt can significantly affect planting schedules and soil moisture availability. Importantly, identifying the spatial patterns of SWE can help prioritize zones for runoff harvesting infrastructure such as farm ponds or seasonal reservoirs. From a broader climate adaptation perspective, integrating SWE estimates into water management planning can substantially enhance the resilience of agroecosystems. This is particularly critical in light of the predicted increase in temperature and precipitation variability across Central Asia. By establishing a validated remote sensing workflow for SWE estimation, our work lays the groundwork for assessing the feasibility of snowmelt harvesting in the region. This evidence-based approach not only helps protect rural infrastructure from flood damage but also introduces a promising adaptation pathway: converting a portion of the snow-derived runoff into a productive irrigation source. Ultimately, the strategic monitoring and management of snow resources should be considered a foundational pillar of climate-resilient agriculture in Northern Kazakhstan.

1.1.3. Snowmelt Harvesting as an Adaptive Strategy

Northern Kazakhstan is experiencing a growing paradox at the intersection of climate variability and agricultural water management. Springtime floods caused by rapid snowmelt juxtaposed with severe summer droughts that endanger crop productivity. This dual exposure is symptomatic of broader climate trends affecting cold semi-arid regions globally, where seasonal precipitation is highly skewed and water management infrastructure is often underdeveloped

(Alwan et al., 2020; Maina & Raude, 2016). According to data from the CACILM-2 project of the FAO, between 2001 and 2022, the Akkayin district in North Kazakhstan experienced drought conditions in 14 out of 22 years. The few drought-free years were clustered in the early 2000s and 2018. These trends reflect broader Central Asian climate patterns characterized by increasing aridity, rising temperatures, and unpredictable precipitation, all of which disproportionately affect rainfed agricultural systems (Shen et al., 2019). The absence of major rivers in the region has left agricultural production almost entirely reliant on rainfed systems, rendering cereal, legume, and oilseed crops highly vulnerable to warm-season moisture deficits. Meanwhile, heavy snowfall in winter, followed by abrupt thaws, has resulted in damaging spring floods, such as the catastrophic 2017 event that displaced 4,000 residents and inundated 15 rural settlements (Berezhnaya, 2020). The climatic duality between excess water in spring and scarcity in summer presents a compelling opportunity, capturing and storing snowmelt runoff for later agricultural use through farm pond systems. While the concept of runoff harvesting is well established in tropical and arid regions (e.g., India, Iraq, Kenya), snowmelt harvesting in cold steppe environments remains understudied. Reviews by Chou et al. (2014), Kadam et al. (2012), Sayl et al. (2020) demonstrate that runoff harvesting has been successful in diverse settings, improving water productivity, reducing erosion, and enhancing local livelihoods. However, most studies rely on rainfall-based inputs and overlook snow-related hydrological parameters, making them inapplicable to cold-region contexts like Kazakhstan. Historical data indicate that snowmelt collection was once widespread in the region. During the Soviet era, thousands of farm ponds were constructed to harness runoff for agricultural use. These systems were largely abandoned post-1991, leading to issues such as water salinization and infrastructure decay. Moreover, they were not designed with current or future climate change projections in mind, limiting their utility for modern flood and drought mitigation. Contemporary adaptation strategies must now combine traditional water management practices with modern spatial analysis tools to optimize design and placement.

This study fills a critical research gap by adapting runoff harvesting frameworks to a cold, semi-arid steppe environment, using SWE as a central parameter. Unlike prior studies in tropical or desert regions (e.g., Balkhair & Ur Rahman (2021), Wu et al. (2018), this work introduces SWE-derived inputs, thus accounting for seasonal snow accumulation and spring discharge. The method employs a Geographic Information System (GIS)-based Analytical Hierarchy Process (AHP), a robust Multi-Criteria Decision Analysis (MCDA) tool. AHP has been successfully applied to prioritize dam site selection (Esavi et al., 2012; Jozaghi et al., 2018; Yasser et al., 2013), solar farm suitability (Elboshy et al., 2022; Mehdaoui et al., 2022; Noorollahi et al., 2016; Sindhu et al., 2017; Uyan, 2013), and groundwater potential mapping (Doke et al., 2021; Lentswe & Molwalefhe, 2020; Murmu et al., 2019; Subbarayan et al., 2020; Upwanshi et al., 2023), offering both transparency and scalability. The AHP remains especially suited to regions with limited field data and the need for expert-informed decision-making (T. Saaty, 2008).

Our analysis incorporates six spatial parameters: hydrogeology, slope, drainage density, LULC, soil texture, and snow water equivalent, each known to influence water accumulation, runoff behavior, and infiltration rates. The SWE layer was derived from previously validated snow

depth estimation models using Sentinel-2 indices (Teleubay et al., 2022). Using pairwise comparisons and expert judgments, each criterion was weighted based on relative importance, and suitability zones for snowmelt harvesting were classified as low, moderate, high, or very high. Validation using the location of existing farm ponds confirmed the accuracy of the suitability map, reinforcing its value as both a decision-support tool and a practical framework for sustainable water management. In this context, snowmelt harvesting could transition regional agricultural strategies from yield maximization to income stabilization. Experiments with deficit irrigation, where water is applied during only the most drought-sensitive crop stages, have shown remarkable results globally. In Turkey, such practices increased wheat yield by 65% and doubled water productivity compared to rainfed systems (Ilbeyi et al., 2006). Similar outcomes have been documented in China, Syria, and Bangladesh (Ali et al., 2007; Kang et al., 2002; H. Zhang & Oweis, 1999). Importantly, this work also contributes to early flood warning and drought preparedness, while supporting socio-economic development.

1.1.4. Study area

The study focuses on the Akkayin district, located in the North Kazakhstan Region, one of the most agriculturally productive zones in the country (Figure 1.1). Climatically, the area is characterized by a sharply continental climate with pronounced seasonal extremes. Winters are long and frigid, with average January temperatures ranging from -14.1°C to -18.7°C , while summers are hot and dry, with July averages of $+18.5^{\circ}\text{C}$ to $+20.9^{\circ}\text{C}$. Annual precipitation is highly variable, averaging 225–335 mm, with historical extremes ranging from 204 mm to over 600 mm. Approximately two-thirds (66%) of precipitation occurs between April and October. Snow cover typically lasts for five months (November to March), with average snow depths ranging from 20 to 40 cm. The topography of the district is shaped by the West Siberian Lowland, featuring relatively flat terrain interspersed with closed basins and seasonal lakes, which make the area prone to spring flooding. Strong winds often redistribute snow, creating spatially heterogeneous snowpacks. These spring snowmelt events, though occasionally destructive, represent a significant yet underutilized water resource that could be harnessed for agricultural drought mitigation. Soil types follow a zonal distribution, with ordinary loamy chernozems dominating the northern part of the district and gradually transitioning into southern chernozems to the south. During summer, dry winds accelerate soil moisture loss, contributing to frequent agricultural droughts.

Crops cultivated in the region include spring wheat, barley, oats, lentils, peas, clover, alfalfa, and oilseeds like safflower and sunflower, with cereals and legumes occupying about 70% of the total sown area. In recent years, the region has averaged over 4.3 million hectares under major crop cultivation. The Akkayin district mirrors this agricultural profile on a smaller scale but faces acute climate stress due to the lack of major rivers and reliance on rainfed agriculture. Given this confluence of climatic volatility, seasonal water imbalance, and agricultural importance, the Akkayin district presents a compelling case for exploring snowmelt harvesting strategies as an adaptive water management solution under increasing climate uncertainty.

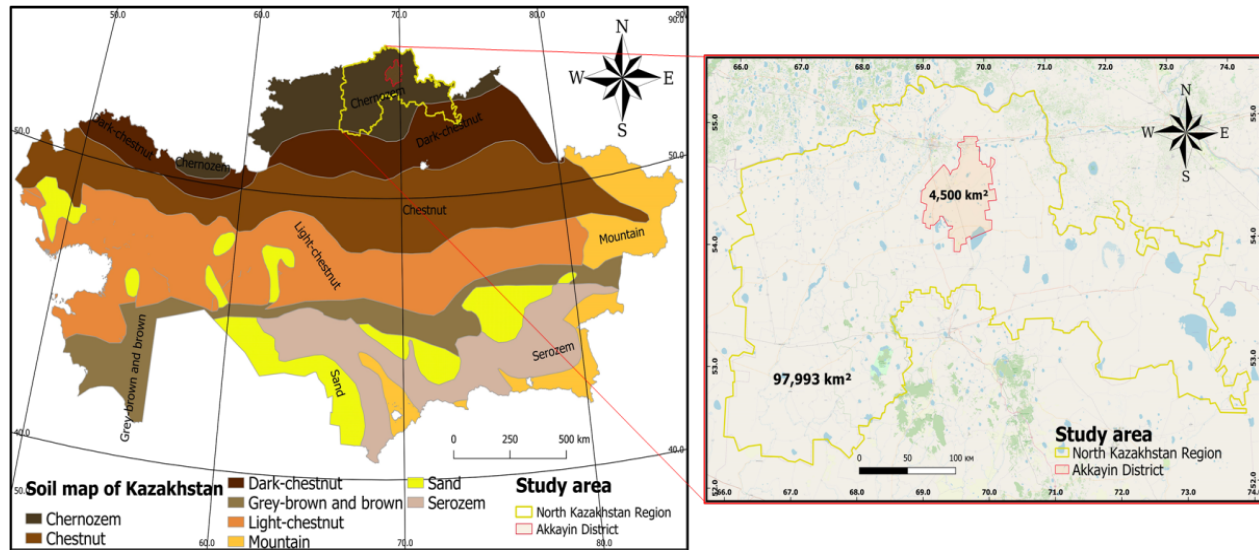


Figure 1.1. Study area and the soil map of the Republic of Kazakhstan.

1.2.Problem Statement

Agriculture in Northern Kazakhstan faces a profound and growing challenge at the intersection of climate change, water scarcity, and agricultural sustainability. The region, particularly the Akkayin district in the North Kazakhstan Region, is a vital contributor to national and regional food security, supplying nearly a quarter of Kazakhstan's wheat production. Yet, its rainfed cropping systems remain highly vulnerable to climatic extremes, including prolonged summer droughts and devastating spring floods, exacerbated by rising temperatures and erratic precipitation patterns. These dual stressors, compounded by the absence of large-scale irrigation infrastructure, create an urgent need for locally adapted, climate-resilient solutions to maintain and improve agricultural productivity. Conventional crop modeling studies have shown that under high-emission climate scenarios, spring wheat yields in the region are likely to decline significantly due to shortened growing seasons and increased evapotranspiration (Shelia et al., 2019; Teleubay et al., 2024). However, while models such as DSSAT and APSIM provide important forecasts, they lack integration with spatial water management strategies that reflect the unique hydrology of cold steppe environments. Specifically, these models do not account for seasonal snowmelt runoff, a key but underutilized water source in Northern Kazakhstan. At the same time, a critical paradox exists in the region's hydrological cycle: excess water during spring snowmelt often leads to floods, while acute water deficits during summer droughts limit crop growth and yields. This mismatch in temporal water availability represents a missed opportunity. Historically, snowmelt runoff was captured through farm pond infrastructure, but these systems have been largely abandoned since the collapse of the Soviet Union. Contemporary attempts to reintroduce water harvesting have focused primarily on rainwater collection in arid and tropical regions, failing to account for cold-region dynamics such as snow cover, SWE, and rapid spring thaw patterns. Moreover, despite the promise of RS and GIS technologies to map and monitor snow resources, there remains a lack of integrated, spatially explicit frameworks for snowmelt-

based water harvesting site selection in cold semi-arid steppe zones. Most studies to date have emphasized tropical, monsoonal, or desert environments and rely on rainfall-derived parameters, making them inapplicable to snow-dominated systems like Northern Kazakhstan. The limited inclusion of snowpack properties in runoff harvesting models further undermines the region's capacity to design effective water management interventions. Therefore, the central problem addressed by this research is the lack of adaptive, snowmelt-based water harvesting strategies tailored to the cold, semi-arid conditions of Northern Kazakhstan. In a climate-constrained future, failure to address this issue will result in worsening crop failures, diminished food security, and socio-economic decline in one of Central Asia's most important breadbaskets. Bridging this gap requires not only accurate SWE estimation through remote sensing but also a robust, multi-criteria decision-making approach for identifying optimal snowmelt harvesting zones.

This dissertation responds to this need by integrating snowmelt runoff estimation, spatial modeling via GIS-AHP, and crop simulation using DSSAT, forming a comprehensive, interdisciplinary framework for climate-resilient agriculture in Northern Kazakhstan. By strategically converting spring runoff into a productive water resource, this work aims to inform policy, empower local stakeholders, and lay the groundwork for sustainable drought mitigation and adaptive agricultural planning in cold-region environments.

1.3. Research Objectives

The primary objective of this dissertation is to develop an integrated framework for enhancing climate resilience in Northern Kazakhstan's rainfed agricultural systems by linking snowmelt hydrology, drought vulnerability assessment, and crop yield modeling. This research addresses a critical knowledge gap in cold semi-arid agroecosystems, where the simultaneous occurrence of springtime water surplus (via snowmelt and floods) and summertime water scarcity (due to drought and rising evapotranspiration) poses a complex challenge for sustainable agriculture. By incorporating high-resolution remote sensing, spatial decision support models, and process-based crop simulations, this dissertation offers a novel, interdisciplinary approach to agro-climatic adaptation.

Specifically, the research pursues the following objectives:

- 1) To quantify the potential impacts of climate change on wheat yields in Northern Kazakhstan under various Representative Concentration Pathways (RCPs) using the DSSAT model. This includes the identification of highly vulnerable zones in yield reduction due to shifting precipitation regimes and increased heat stress.
- 2) To develop and validate a remote sensing-based method for estimating snow depth and deriving SWE in the Akkayin district using remote sensing data. This includes the refinement of snow index functions (e.g., NDSI, RSI, and DSI) for application in flat, open, snow-drift-prone landscapes typical of the West Siberian Lowland.
- 3) To identify and spatially map optimal farm pond locations for snowmelt runoff harvesting in the study area through a GIS-based AHP. This objective integrates multiple criteria,

including slope, drainage density, LULC, soil type, hydrogeology, and SWE distribution, to delineate high-suitability zones for snow meltwater retention and agricultural reuse.

Through the achievement of these objectives, the dissertation aims to inform not only regional water and food security strategies but also contribute to the broader scientific discourse on climate adaptation in cold-steppe agroecosystems. It proposes an integrated, transferable methodology that can be replicated across similar high-latitude, snow-dominated agricultural regions facing dual threats of drought and flood.

1.4.Data and Methods

To estimate the effects of climate change on spring wheat yields, the DSSAT model was used. The CERES-Wheat module within DSSAT was calibrated for the dominant local wheat variety using field data from the North Kazakhstan Agricultural Experimental Station (NKAES). Calibration inputs included daily weather data (temperature, solar radiation, precipitation), soil physical and chemical properties (texture, depth, water-holding capacity), management practices (sowing date, fertilizer input, irrigation), and crop phenological data. Weather data were sourced from local meteorological stations and downscaled CMIP6 projections for RCP2.6, RCP4.5, and RCP8.5 scenarios using the CRAFT v3.4 tool. The model was validated with historical yield data from 2000 to 2020 (sourced from the National Bureau of Statistics) and then run forward under the three RCP scenarios up to 2050. Yield simulations were used to identify the most vulnerable zones within the study area and examine potential yield declines due to increased temperature and reduced soil moisture.

Estimation of snow depth and SWE was performed using multi-temporal Sentinel-2 Level-2A surface reflectance imagery from ESA's Copernicus Open Access Hub. Pre-processing included cloud masking using the QA60 band and top-of-atmosphere to surface reflectance conversion. Several snow indices were tested for estimating snowpack properties, including the NDSI, NDSII, DSI, and RSI. A pixel-wise regression models were developed and validated against field snow survey data collected during March 2022 and 2023. The quadratic function showed the best performance ($R^2 > 0.88$, $RMSE < 5.4$ cm) and was used to generate a district-wide snow depth map. SWE was calculated by combining estimated snow depth with assumed bulk snow density (200–300 kg/m³), adjusted by terrain slope using SRTM 30m elevation data.

To identify optimal snowmelt harvesting locations, a GIS-based AHP was employed. Six parameters were selected based on expert opinion and literature: slope, drainage density, soil texture, LULC, hydrogeology, and SWE. Each layer was resampled to a 30m resolution and normalized to a 0-1 scale. Pairwise comparisons were conducted among parameters to derive weights, following Saaty's consistency ratio threshold of <0.1 . Weights were applied to each factor in a weighted linear combination (WLC) using raster algebra in ArcGIS Pro. The resulting composite suitability index ranged from 0 (unsuitable) to 1 (very suitable), and the district was reclassified into four categories: low, moderate, high, and very high suitability. Validation was performed using geolocated existing farm ponds and expert ground-truthing conducted in 2023.

Table 1.1 provides a summary of the datasets used in this study, including their sources, spatial and temporal coverage, and primary applications in snowmelt estimation, biophysical characterization, and suitability analysis. Additionally, a range of software tools was employed depending on the specific requirements of each task, including R and Python for statistical analysis and data processing, DSSAT and CRAFT for crop modeling and climate impact assessment, JavaScript within the Google Earth Engine (GEE) platform for remote sensing analysis, and GIS software for spatial data integration and multi-criteria evaluation.

Table 1.1. Summary of Datasets Used in the Study

Dataset	Description	Source
Sentinel-2	10m multispectral imagery	Copernicus Open Access Hub
SWE	10m snow water equivalent	Derived from the Sentinel-2
SRTM DEM	30m elevation data	USGS Earth Explorer
Slope	30 m slope	Derived from the SRTM DEM
Drainage density	30 m drainage density	Derived from the SRTM DEM
Hydrogeology	Digitized hydrogeological map (1:25 000)	Ministry of Geology
Soil map	Soil texture and type	FAO Harmonized World Soil Database
Meteorological data	Daily T, P, radiation	Kazhydromet, CMIP6 (CRAFT)
Land use	2021 LULC classification	ESRI 2021 LULC
Snow survey	In-situ snow depth measurements (2022–2023)	Field survey, authors' data
Crop data	Yield, phenology, soil	Bureau of Statistics

1.5. Dissertation outline

This dissertation is structured around three peer-reviewed scientific articles, each addressing a key aspect of climate-resilient agriculture in Northern Kazakhstan. While each chapter presents an independent research investigation, together they form a cohesive narrative that integrates climate impact assessment, remote sensing-based snow monitoring, and spatial decision-making for drought mitigation. The chapters are designed to build upon one another, culminating in a comprehensive synthesis of findings and future research directions.

Chapter 1 introduces the dissertation by providing a comprehensive background on the impacts of climate change on agriculture in cold semi-arid regions, with a particular focus on Northern Kazakhstan. It includes a literature review on snowpack monitoring, snowmelt harvesting, and crop yield modeling, and lays out the research problem, objectives, and study area. The chapter also describes the data sources, analytical tools, and methodological framework used across the dissertation.

Chapter 2 examines how future climate scenarios may impact wheat yields across different agroecological zones in Northern Kazakhstan. Using the DSSAT crop modeling framework, simulations were conducted under multiple RCPs to project yield outcomes by mid-century. The findings reveal significant spatial variability in climate sensitivity, with some zones facing much sharper productivity declines than others. This chapter highlights the importance of site-specific

adaptation strategies and serves as a foundation for targeted climate risk management in the region's wheat-growing systems.

Chapter 3 focuses on estimating snow depth using remote sensing techniques, particularly Sentinel-2 imagery. Various snow indices and regression models were evaluated for their accuracy in detecting snowpack conditions in the study area. The results indicate that quadratic regression applied to the DSI-2 provides the most reliable estimates. This work underscores the potential of satellite-derived snow indicators for operational snow monitoring in cold, data-scarce agricultural environments and lays the groundwork for integrating snowpack information into water resource planning.

Chapter 4 identifies suitable zones for snowmelt harvesting through a GIS-based AHP. By combining snow depth estimates from Chapter 3 with other key parameters such as slope, drainage density, soil texture, and land use, this chapter maps out potential locations for farm pond construction. The methodology provides a practical and replicable tool for optimizing water harvesting infrastructure in dryland agricultural regions. The results not only support drought mitigation efforts but also reintroduce snowmelt as a strategic resource in climate adaptation planning.

Chapter 5 synthesizes the key findings of the previous chapters, discusses the broader implications for climate adaptation in cold-region agriculture, and outlines the methodological and contextual limitations of the study. It also offers recommendations for policymakers, stakeholders, and future research, emphasizing the need for integrated, site-specific, and scalable strategies to enhance agricultural resilience in Northern Kazakhstan and similar environments.

2. Comparison of Climate Change Effects on Wheat Production under Different Representative Concentration Pathway Scenarios in North Kazakhstan

This article is published in Sustainability journal as: **Zhanassyl Teleubay**, Farabi Yermekov, Arman Rustembayev, Sultan Topayev, Askar Zhabayev, Ismail Tokbergenov, Valentina Garkushina, Amangeldy Igilmanov, Vakhtang Shelia and Gerrit Hoogenboom. 2024

Comparison of Climate Change Effects on Wheat Production under Different Representative Concentration Pathway Scenarios in North Kazakhstan

Sustainability Volume 16, December 2023, 293

<https://doi.org/10.3390/su16010293>

Journal CiteScore (Scopus): 7.7

Author Contributions: Conceptualization, Z.T., A.R. and V.S.; methodology, Z.T., V.S. and G.H.; software, A.R. and A.Z.; formal analysis, I.T.; investigation, Z.T. and S.T.; resources, I.T. and F.Y.; data curation, A.R. and Z.T.; writing—original draft preparation, S.T., A.R., A.Z. and Z.T.; writing—review and editing, Z.T., V.G. and A.I.; visualization, Z.T.; supervision, I.T., V.S. and G.H.; project administration, I.T.; funding acquisition, I.T. and F.Y.

Article

Comparison of Climate Change Effects on Wheat Production under Different Representative Concentration Pathway Scenarios in North Kazakhstan

Zhanassyl Teleubay ^{1,*}, Farabi Yermekov ², Arman Rustembayev ², Sultan Topayev ², Askar Zhabayev ², Ismail Tokbergenov ², Valentina Garkushina ³, Amangeldy Igilmanov ³, Vakhtang Shelia ⁴ and Gerrit Hoogenboom ⁴

¹ Department of Geography and Atmospheric Sciences, The Ohio State University, Columbus, OH 43210, USA

² Center for Technological Competence in the Field of Digitalization of the Agro-Industrial Complex, S.Seifullin Kazakh Agrotechnical Research University, Astana 010000, Kazakhstan

³ Faculty of Land Management, Architecture and Design, S.Seifullin Kazakh Agrotechnical Research University, Astana 010000, Kazakhstan

⁴ Department of Agricultural and Biological Engineering, Global Food Systems Institute, University of Florida, Gainesville, FL 32611, USA

* Correspondence: teleubay.1@buckeyemail.osu.edu or zhanassyl.kz@gmail.com



Citation: Teleubay, Z.; Yermekov, F.; Rustembayev, A.; Topayev, S.; Zhabayev, A.; Tokbergenov, I.; Garkushina, V.; Igilmanov, A.; Shelia, V.; Hoogenboom, G. Comparison of Climate Change Effects on Wheat Production under Different Representative Concentration Pathway Scenarios in North Kazakhstan. *Sustainability* **2024**, *16*, 293. <https://doi.org/10.3390/su16010293>

Abstract: Adverse weather conditions, once rare anomalies, are now becoming increasingly commonplace, causing heavy losses to crops and livestock. One of the most immediate and far-reaching concerns is the potential impact on agricultural productivity and global food security. Although studies combining crop models and future climate data have been previously carried out, such research work in Central Asia is limited in the international literature. The current research aims to harness the predictive capabilities of the CRAFT (CCAFS Regional Agricultural Forecasting Toolbox) to predict and comprehend the ramifications stemming from three distinct RCPs, 2.6, 4.5, and 8.5, on wheat yield. As a result, the arid steppe zone was found to be the most sensitive to an increase in greenhouse gases in the atmosphere, since the yield difference between RCPs 2.6 and 8.5 accounted for almost 110 kg/ha (16.4%) and for 77.1 kg/ha (10.4%) between RCPs 4.5 and 8.5, followed by the small hilly zone with an average loss of 90.1 and 58.5 kg/ha for RCPs 2.6–8.5 and RCPs 4.5–8.5, respectively. The research findings indicated the loss of more than 10% of wheat in the arid steppe zone, 7.6% in the small hilly zone, 7.5% in the forest steppe zone, and 6% in the colo steppe zone due to climate change if the modeled RCP 8.5 scenario occurs without any technological modernization and genetic modification. The average wheat yield failure in the North Kazakhstan region accounted for 25.2, 59.5, and 84.7 kg/ha for RCPs 2.6–4.5, 4.5–8.5, and 2.6–8.5, respectively, which could lead to food disasters at a regional scale. Overall, the CRAFT using the DSSAT crop modeling system, combined with the climate predictions, showed great potential in assessing climate change effects on

Abstract: Adverse weather conditions, once rare anomalies, are now becoming increasingly commonplace, causing heavy losses to crops and livestock. One of the most immediate and far-reaching concerns is the potential impact on agricultural productivity and global food security. Although studies combining crop models and future climate data have been previously carried out, such research work in Central Asia is limited in the international literature. The current research aims to harness the predictive capabilities of the CRAFT (CCAFS Regional Agricultural Forecasting Toolbox) to predict and comprehend the ramifications stemming from three distinct RCPs, 2.6, 4.5, and 8.5, on wheat yield. As a result, the arid steppe zone was found to be the most sensitive to an increase in greenhouse gases in the atmosphere, since the yield difference between RCPs 2.6 and 8.5 accounted for almost 110 kg/ha (16.4%) and for 77.1 kg/ha (10.4%) between RCPs 4.5 and 8.5, followed by the small hilly zone with an average loss of 90.1 and 58.5 kg/ha for RCPs 2.6–8.5 and RCPs 4.5–8.5, respectively. The research findings indicated the loss of more than 10% of wheat in the arid steppe zone, 7.6% in the small hilly zone, 7.5% in the forest steppe zone, and 6% in the colo steppe zone due to climate change if the modeled RCP 8.5 scenario occurs

without any technological modernization and genetic modification. The average wheat yield failure in the North Kazakhstan region accounted for 25.2, 59.5, and 84.7 kg/ha for RCPs 2.6–4.5, 4.5–8.5, and 2.6–8.5, respectively, which could lead to food disasters at a regional scale. Overall, the CRAFT using the DSSAT crop modeling system, combined with the climate predictions, showed great potential in assessing climate change effects on wheat yield under different climate scenarios in the North Kazakhstan region. We believe that the results obtained will be helpful during the development and zoning of modified, drought-resistant wheat varieties and the cultivation of new crops in the region.

Keywords: agriculture; food security; crop modeling; RCP; wheat yield prediction

2.1. Introduction

The global community has awakened to a looming crisis transcending borders, economies, and ecosystems in recent decades: climate change (Mirzabaev et al., 2023; Murken & Gornott, 2022). As atmospheric greenhouse gas concentrations continue to rise, the planet's climate is undergoing rapid transformations, triggering a cascade of effects that ripple across diverse sectors of society (Nunes, 2023). One of the most immediate and far-reaching concerns is the potential impact on agricultural productivity and global food security (Ejaz Qureshi et al., 2013; Hadley et al., 2023). Studies of such influence have been conducted for many countries, reaching conclusions on the complexity of the situation and the requirement of particular policies to mitigate the consequences (Alkolibi, 2002; Chauhan et al., 2014; Schlenker et al., 2006; Sugiura et al., 2012). As a cornerstone of human civilization, agriculture sustains livelihoods, economies, and societies worldwide. Yet, this intricate web of sustenance is inextricably tied to climatic conditions. Rising temperatures, altered precipitation patterns, and changing atmospheric carbon dioxide levels challenge agricultural systems' stability and predictability (Arisco et al., 2023; Kabir et al., 2023; Malhi et al., 2021; Ngaba et al., 2023). The consequences of such shifts can potentially disrupt the delicate balance between food production and population growth, compromising our ability to feed a burgeoning global population (Rehman et al., 2021).

Extreme weather events, once rare anomalies, are now becoming distressingly familiar, exacting heavy tolls on crops and livestock (Furtak & Wolińska, 2023; Pangapanga-Phiri & Mungatana, 2021; Schmitt et al., 2022). Prolonged droughts, unpredictable rainfall, and intensified storms disrupt planting cycles and reduce yields (Gömann, 2015; Perondi et al., 2022; Powell & Reinhard, 2016). The nexus between climate change and food security is multifaceted. It extends beyond the fields to impact post-harvest storage, transportation, and distribution systems (Weber et al., 2023). These disruptions disproportionately affect vulnerable communities, particularly in developing nations, given their reliance on subsistence agriculture and limited adaptive capacity (Nugroho et al., 2023). The global food trade, a lifeline for many countries, faces disruptions as production centers shift and supply chains strain under pressure (Saboori et al., 2022; Steinbach, 2023). These mounting concerns necessitate urgent action, not only in mitigating the drivers of climate change but also in enhancing the resilience of agricultural systems to its impacts.

Numerous models and software tools have been developed to predict crop yields in response to temperature changes and other environmental factors. These tools use a combination of climate data, agronomic knowledge, and mathematical models to estimate the potential crop production. Here are a few notable ones:

1. DSSAT (Decision Support System for Agrotechnology Transfer) 4.7.5 is a widely used program that simulates the growth of crops and their response to various management practices, including temperature changes. It includes a suite of crop models that can affect the impact of temperature, rainfall, and other factors on crop yields. Xiang et al. (2020) used the DSSAT model in combination with the MODFLOW groundwater flow model to facilitate assessments of irrigation technology changes, crop choices, and strategies for adapting to climate change in various regions. Mubeen et al. (2020) adapted the DSSAT model to determine the impact of climate change through the elevated CO₂ condition. The authors suggest that cultivating wheat and cotton varieties with high water use efficiency could be pivotal in sustaining crop production. Attia et al. (2021), following the DSSAT calibration and evaluation algorithms for maize cultivation, believe that compost application with retained crop residues is a promising strategy for enhancing agronomic outcomes and environmental sustainability in maize cultivation on arid soils.

2. APSIM (Agricultural Production Systems sIMulator) is another comprehensive software tool that models various aspects of agricultural systems, including crop growth, soil processes, and climate interactions. It can be used to assess the impact of temperature changes on crop yields and inform adaptation strategies. Vogeler et al. (2023) found that for well-drained soils in regions with high precipitation and no water limitations, the APSIM model displays low sensitivity to soil hydraulic parameters and suggests that general data from databases may be justifiable instead of relying solely on site-specific measurements of hydraulic properties. Research by Wimalasiri et al. (2022) highlights the potential of selecting specific cultivars and adjusting planting dates as climate change adaptation strategies based on APSIM crop model simulation results.

3. STICS (Simulateur mulTIdisciplinaire pour les Cultures Standard) is a crop model for simulating various crops and cropping systems. It considers temperature, precipitation, and other environmental factors to predict crop growth and yield (Brisson et al., 2003). Fraga et al. (2015) adapted the STICS model to suit the unique conditions of Portuguese wine growing and its diverse grapevine varieties. The authors assume that the STICS model holds potential as a decision-support tool for both short- and long-term strategic planning in the Portuguese viticulture sector.

4. Global Yield Gap Atlas (GYGA): While not a standalone piece of software, the Global Yield Gap Atlas provides an online platform where users can access global and regional data on actual and potential crop yields. It offers insights into the yield gaps that exist and how they might change under different scenarios, including temperature changes. In the research of Grassini et al. (2017), the authors followed the idea of achieving maximum yield potential under sustainable usage of water resources and natural ecosystem protection. It was found that GYGA successfully estimated yield potential, yield gaps, and water productivity for 13 crops across 70 countries around the world (Wageningen University & Research, University of Nebraska-Lincoln, n.d.).

As we transition from evaluating various crop models for agricultural simulations, it is imperative to consider the broader environmental context. Climate change is a pivotal factor that can significantly impact crop growth and yield (Long et al., 2022). Current research includes wheat yield estimation under three different Representative Concentration Pathway (RCP) scenarios defined by the Intergovernmental Panel on Climate Change (IPCC) for the year 2050 (IPCC, n.d.; Tan et al., 2014). RCP scenarios offer a spectrum of future climate projections, ranging from stringent mitigation efforts in RCP 2.6 to business-as-usual emissions in RCP 8.5.

Current research aims to harness the predictive capabilities of the CRAFT v3.4 (CCAFS Regional Agricultural Forecasting Toolbox) (Shelia et al., 2019) to forecast and comprehend the ramifications stemming from three distinct RCPs on wheat yield in the North Kazakhstan region (van Vuuren et al., 2011). The CRAFT v3.4 is a multifunctional software platform that can run pre-installed crop models from DSSAT, SARRA-H, and APSIM. By employing the CRAFT, we aim to unravel the intricate relationship between varying climatic conditions, as delineated by RCP 2.6, 4.5, and 8.5 scenarios, and the resulting alterations in wheat yield. This endeavor seeks to foresee potential changes in yield and deepen our understanding of the underlying mechanisms driving these shifts, thereby contributing to a more robust comprehension of the dynamic interplay between climate change and agricultural productivity (Govindaraj et al., 2015). Wheat is a staple crop and a significant contributor to Kazakhstan's economy and the region's food security (Raihan & Tuspekova, 2022). Given the country's vast geographical span and diverse climatic conditions, understanding how climate scenarios, such as those represented by RCPs 2.6, 4.5, and 8.5, could affect wheat production is crucial. The combination of rising temperatures, altered precipitation patterns, and increased water stress could profoundly impact wheat production in Kazakhstan (Shmelev et al., 2021; Wang et al., 2022).

Research based on the three RCP scenarios for modeling wheat yield in the North Kazakhstan Region for the year 2050 provides an opportunity to assess the impact of climate change on agriculture in the Republic of Kazakhstan and, accordingly, on the country's and Central Asia's food security. According to the USDA's Global Agricultural Information Network report, Kazakhstan harvested 16,404 million tons of wheat in 2022 and exported almost half of it (47%) (U.S. Department of Agriculture, 2023). Since the top five importers were Uzbekistan, Afghanistan, Tajikistan, Iran, and Turkmenistan, we can firmly state Kazakhstan's high importance in Central Asia's food security. If preventive and adaptive measures are not taken, about 80 million people in the region could be at risk of food insecurity.

This paper is organized as follows: (1) the materials and methods used in the current research for assessing the effects of climate change on wheat production in the North Kazakhstan region are explained, (2) the results of the simulations are presented, (3) the advantages, disadvantages, limitations, and possibilities of the work are discussed, and (4) conclusions and recommendations for future research are provided.

2.2. Materials and Methods

2.2.1. Study Area

The North Kazakhstan Region occupies the southern outskirts of the West Siberian Plain and a part of the Kazakh Uplands (Sary-Arka). The territory of the region covers around 98,000 square kilometers, which is equivalent to 3.6% of the total area of the Republic of Kazakhstan.

A pronounced continental nature characterizes the climate of northern Kazakhstan. Winters in this region are frigid, and summers are sweltering. The average air temperature in January from 2020 to 2022 was -14.1°C , while in July it was $+20.9^{\circ}\text{C}$. The average annual precipitation from 2020 to 2022 was 306.25 mm, with 66% of the rainfall occurring during the warm period of the year (from April to October). The region's snow cover usually lasts about five months, from November to March.

The area under cultivation of major crops in this region averages around 4325 thousand hectares (4361 thousand hectares in 2022, 4332 thousand hectares in 2021, and 4283 thousand hectares in 2020). Cereals and legumes accounted for about 70% of the total sown area, with the share of cereals, including winter and spring wheat, making up 55%.

The region's share of gross wheat harvest (including winter and spring wheat) accounted for 23% of the total wheat production in the country for the last three years. Figure 2.1 illustrates the wheat fields in 2021 in the study area. According to data from the National Statistics Bureau, the average wheat yield in the North Kazakhstan Region for the period from 2020 to 2022 was 1250 kg per hectare (Bureau of National Statistics, Agency for Strategic Planning and Reforms of the Republic of Kazakhstan, 2023).

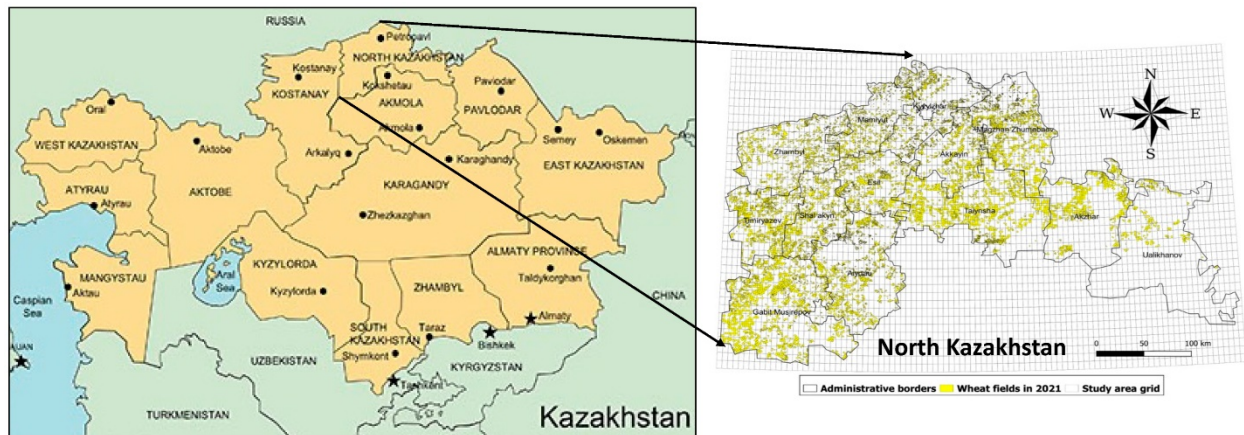


Figure 2.1. Study area and digitized wheat fields in 2021

2.2.2. Data Sources

The CRAFT requires a large set of input data to create a project and run the simulation. The Graphical User Interface contains such sections as Gridded User Dataset, Crop mask, Crop variety, Fertilizer, Planting, Weather, Soil, etc. The reference gridded dataset in the CRAFT is the WGS84 world grid in two spatial resolutions (5 and 30 arcminutes). The schema of the area of interest was automatically generated by uploading the shapefile in three different administrative

levels (larger region, region, county) of the study area, and cell IDs were assigned. The current research utilized five arcminute spatial resolution to obtain more accurate results. Further, using the digitized wheat fields for 2021, the share of wheat in each grid cell was calculated and uploaded as a crop mask layer. The date, type, quantity, and application methods of fertilizers were obtained from the recommendation developed by the North Kazakhstan Agricultural Experimental Station, “Features of cultivation of crops in the North Kazakhstan region,” for 2022, taking into account an increase in the use of fertilizer in the region by 25% by 2050 (North Kazakhstan Agricultural Experimental Station, 2022). Given the region’s vast territory and the soil and climate characteristics, farmers cultivate wheat differently. Hence, planting methods differ from one soil and farming zone to another. Accordingly, the study area was divided into four zones (forest steppe, colo steppe, arid steppe, and small hilly), and the corresponding planting methods were assigned. Since the region receives an enormous amount of snow during winter, rainfed agriculture predominates; thus, the current research did not consider irrigation regimes.

2.2.2.1. Weather Data

Despite the vast number of available models of the Earth system, daily climate data from two models, The Earth System Model (MPI-ESM1.2) for the High-Resolution Model Intercomparison Project (HighResMIP) (Gutjahr et al., 2019) and Geophysical Fluid Dynamics Laboratory’s (GFDL) Earth System Model Version 4.1 (ESM4.1) (*The GFDL Earth System Model Version 4.1 (GFDL-ESM 4.1)*, n.d.), were used in this work. The latter has been shown to be ineffective in predicting wheat yields under the three RCP scenarios in Central Asia, most likely due to the calibration of the model using large volumes of ground-based data from North and South America. The Max Planck Institute, Germany, developed the MPI-ESM1.2. This model is widely used in the intercomparison of high-resolution models (Bakhshandeh et al., 2022; Xu et al., 2018). The model is a comprehensive tool for studying climatic and environmental processes on Earth. A feature of this model is its high spatial resolution, which allows for a more detailed study of regional climate changes. Since our goal was to assess the impact of climate change on wheat cultivation in the northern regions of Kazakhstan by 2050, the study used daily climate data from 2036 to 2065 (30-year period). Daily weather data for the North Kazakhstan region from 2015 to 2100 used for the baseline scenario are stored in the GitHub repository and are available on request.

2.2.2.2. Soil Data

Soil profile properties of the study area were obtained from the global SOILGRIDS database (Batjes et al., 2020). For each grid, soil characteristics were compiled separately and entered into the CRAFT v3.4 program. The soil analysis data were divided into six layers and varied from 5 to 200 cm depth. Moreover, soil characteristics are indicated for lower limit, upper limit drained, upper limit saturated, root growth factor, sat. hydraulic conductivity macropore, bulk density moist, organic carbon, clay, silt, coarse fraction, total nitrogen, pH in water, pH in buffer, and cation exchange capacity.

2.2.2.3. Wheat Variety

For the simulation, the local soft spring wheat variety “Shortandy 95” was chosen since this variety is widespread in the Republic of Kazakhstan and is recommended for cultivation in

the Akmola and North Kazakhstan regions. According to the State Commission for Variety Testing of Agricultural Crops of the Ministry of Agriculture, the variety is medium-late, and the growing season is 95–100 days. According to approbation characteristics, it is a variety of *lutescens* (the ear is white, awnless, and hairless, and the grain is red). The yield in competitive variety testing for fallow was 2790 kg/ha, while the maximum yield was 4200 kg/ha (State Commission for Variety Testing of Agricultural Crops of the Ministry of Agriculture of the Republic of Kazakhstan, 2006). The advantage of this variety is its resistance to diseases and climatic conditions, such as drought and smut. In terms of milling qualities, the weight of 1000 grains is 38–42 g, bulk density is 808 g/L, protein content is 15.7%, and raw gluten is 32.2%. A genetic model was compiled for this wheat variety using the DSSAT program. The results of this model were integrated into the CRAFT system for further simulation of the impact of climate change on wheat cultivation in 2050.

2.2.2.4. Planting Method

Even though each farmer has their own approaches and traditions of wheat cultivation, which are passed down from generation to generation, in this study, we relied on the most optimal sowing methods recommended by the North Kazakhstan agricultural experimental station for four different soil and farming zones of the North Kazakhstan region (Table 2.1). Plant population at seeding varied between 250 and 400 seeds per square meter depending on the soil and climate properties of zones. The planting method (dry seeds) and plant distribution (row) were the same throughout the region, while planting depth increased from 5 cm in the forest steppe zone to 7 cm in hilly areas. As a rule, sowing should be carried out to the minimum permissible depth in a moist soil layer of at least 5 cm. When the top layer of soil dries out, the seeding depth increases to 7–8 cm. In this regard, when deepening the seeds, it is necessary to adjust the seeding rates by 10–15% upward, which was not considered in our model. Another essential element of spring sowing agricultural technology is compliance with optimal sowing dates. If there is an expected lack of moisture, it is possible to sow 2–3 days later than usual to allow plants to use precipitation during critical phases of development effectively. However, the model needed to be more flexible to implement it. Thus, a uniform planting date was set for May 13.

Table 2.1. Planting methods in four soil and farming zones of North Kazakhstan region

Soil and Farming Zone	Plant Seeding (PPOP), Seeds per sq. Meter	Planting Method (PLME)	Planting Distribution (PLDS)	Planting Row Spacing (PLRS), cm	Planting Depth (PLDP), cm
Forest steppe	400	Dry seeds	Row	17	5
Colo steppe	350	Dry seeds	Row	17	5
Arid steppe	300	Dry seeds	Row	17	6
Small hilly	250	Dry seeds	Row	17	7

2.2.3. Methodology

After preparing the above input data in the appropriate format (administrative boundaries in SHP, weather in WTG, soil in SOL, management in tabular form, etc.), we ran the crop model and calibrated wheat yield with the observed data to obtain a spatial future wheat yield for the study area with a resolution of 5 arcminutes (Figure 2.2).

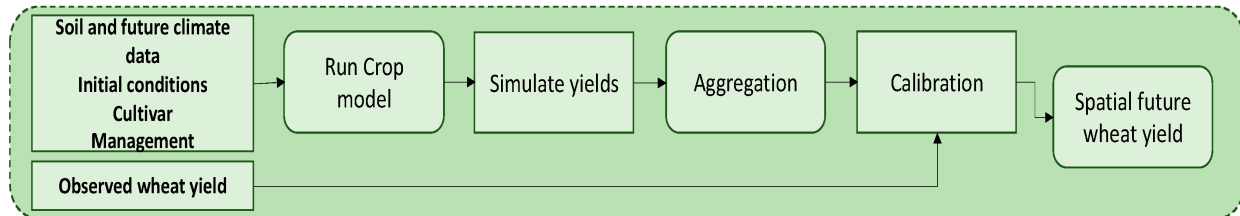


Figure 2.2. The flowchart of the future spatial wheat yield prediction

2.3. Results

Wheat yield in the North Kazakhstan region was predicted under three different RCP scenarios for 2050. The average yield was calculated for the entire study area and each soil-farming zone in the region to assess the vulnerability of each zone to climate change (Table 2.2). According to the results, the arid steppe zone was found to be the most sensitive to an increase in carbon dioxide in the atmosphere, since the yield difference between RCPs 2.6 and 8.5 accounted for almost 110 kg per hectare (16.4%) and for 77.1 kg per hectare (10.4%) between RCPs 4.5 and 8.5. The small hilly zone was the second most vulnerable area, and the results showed an average loss of 90.1 and 58.5 kg/ha for RCPs 2.6 and 8.5 and RCPs 4.5 and 8.5, respectively. Oddly enough, the forest steppe zone was more sensitive to climate change than the colo steppe region under all three scenarios, with an average wheat loss difference of 10 kg/ha. Since we consider RCP 4.5 as a stabilization scenario and 8.5 as a negative scenario with high greenhouse gas emissions, it is crucial to estimate the potential damages in case humanity fails to achieve the Sustainable Development Goals (SDGs) until 2030. Thus, potentially, we will lose more than 10% of wheat in the arid steppe zone, 7.6% in the small hilly zone, 7.5% in the forest steppe zone, and 6% in the colo steppe zone due to climate change if the modeled RCP 8.5 scenario comes true. Overall, the average wheat yield failure in the North Kazakhstan region accounted for 25.2, 59.5, and 84.7 kg/ha for RCPs 2.6–4.5, 4.5–8.5, and 2.6–8.5, respectively.

Table 2.2. Average wheat yield in the North Kazakhstan region and each soil and farming zone under RCPs 2.6, 4.5, and 8.5 in 2050

Soil and Farming Zone	Average Yield RCP 2.6, kg/ha	Average Yield RCP 4.5, kg/ha	Average Yield RCP 8.5, kg/ha	Difference RCPs 2.6–4.5, kg/ha	Difference RCPs 4.5–8.5, kg/ha	Difference RCPs 2.6–8.5, kg/ha	Difference RCPs 2.6–4.5, %	Difference RCPs 4.5–8.5, %	Difference RCPs 2.6–8.5, %
Forest steppe	847.6	829.7	766.9	–17.8	–62.8	–80.7	2.1	7.5	10.5

Soil and Farming Zone	Average Yield RCP 2.6, kg/ha	Average Yield RCP 4.5, kg/ha	Average Yield RCP 8.5, kg/ha	Difference RCPs 2.6–4.5, kg/ha	Difference RCPs 4.5–8.5, kg/ha	Difference RCPs 2.6–8.5, kg/ha	Difference RCPs 2.6–4.5, %	Difference RCPs 4.5–8.5, %	Difference RCPs 2.6–8.5, %
Colo steppe	856.3	830.2	780.0	–26.1	–50.1	–76.3	3.0	6.0	9.7
Arid steppe	767.7	736.1	659.0	–31.5	–77.1	–108.7	4.1	10.4	16.4
Small hilly	798.0	766.4	707.8	–31.6	–58.5	–90.1	3.9	7.6	12.7
Total	831.1	805.8	746.3	–25.2	–59.5	–84.7	3.0	7.3	11.3

According to Table 2.2, the average wheat yield under RCP 2.6 was 831.1 kg/ha in the North Kazakhstan region. To illustrate the spatial variability of wheat yield, a map was compiled based on the crop model and environmental data (Figure 2.3). The results demonstrated the homogeneous distribution of wheat yield over the study area, since around 70% of wheat fields had 800–900 kg/ha yield under RCP 2.6. Potentially, in almost 20% of the study area, which is primarily located in the southwestern part, farmers could harvest the highest yield of 900–1000 kg/ha of wheat without any technological modernizations and genetic modifications in the mid-century. Nevertheless, eastern and southwestern parts of the study area, which are located in the arid steppe zone, had the lowest yield of 600–700 kg/ha (<3%) and 700–800 kg/ha (10%), respectively.

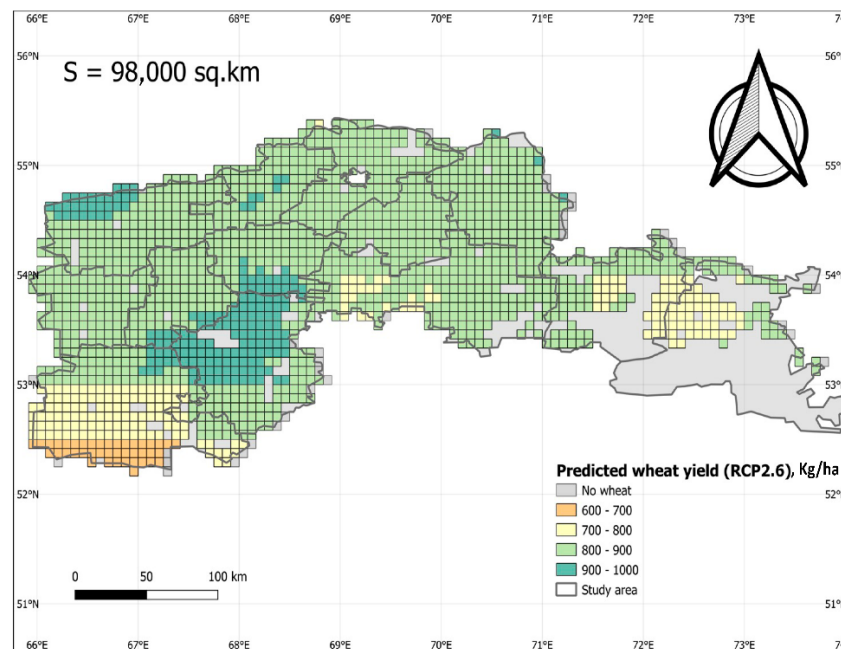


Figure 2.3. Predicted wheat yield in kg/ha under RCP 2.6 in the North Kazakhstan region for the midcentury

The spatial distribution of wheat yield in the study area under RCP 4.5 was still relatively homogeneous, with a predominant share of wheat fields with 800–900 kg/ha (64%) yield (Figure 2.4). However, this does not indicate a minor difference between RCPs 2.6 and 4.5, since we observed a dramatic decrease (7%) in wheat fields with 900–1000 kg/ha yield in the southwest and a substantial increase (25%) in the territories with a lower 700–800 kg/ha yield in the east, west, and central parts of the study area. This contributed to the stable share of the area with 800–900 kg/ha yield but, overall, demonstrated an average yield decrease of 25 kg/ha in the North Kazakhstan region. The far southwestern region with the lowest yield (600–700 kg/ha) faced minor change, and its area increased by only 1%.

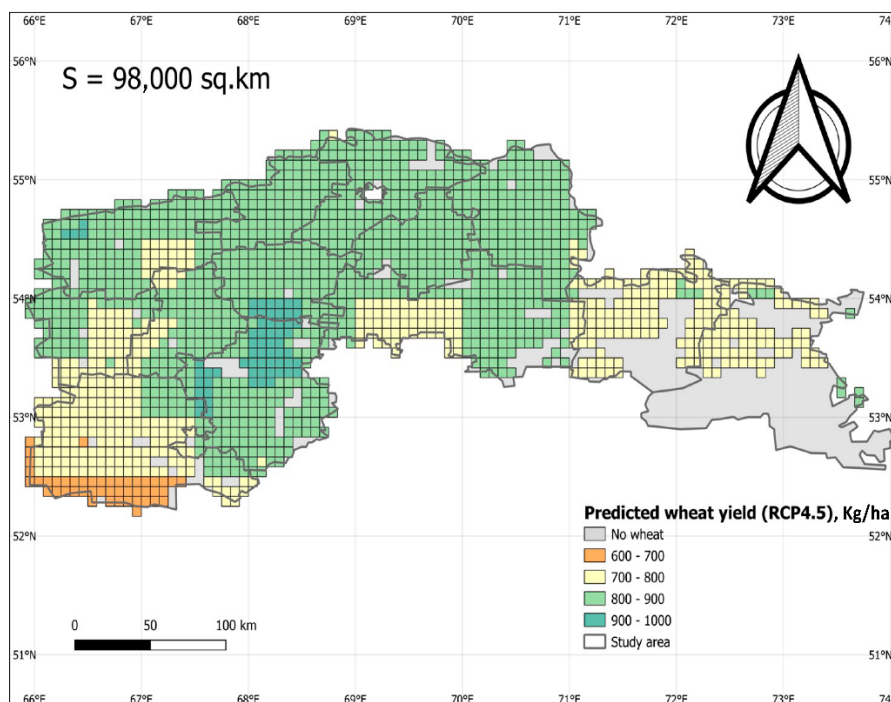


Figure 2.4. Predicted wheat yield in kg/ha under RCP 4.5 in the North Kazakhstan region for the midcentury

The average wheat yield in the study area under RCP 8.5 decreased to 746.3 kg/ha (on average, 60 kg/ha loss compared to RCP 4.5 and 85 kg/ha compared to RCP 2.6). According to Figure 2.5, the negative scenario with an increased concentration of carbon dioxide in the atmosphere and, consequently, increased temperature caused the most significant harm to the wheat fields of the study area. If we observed an increase of 15% in the fields with a yield of 700–800 kg/ha under RCP scenario 4.5 relative to 2.6, then in the abovementioned figure, this area reached almost half of Northern Kazakhstan and expanded in all directions. The model also showed that agricultural fields with a yield of more than 900 kg/ha will completely disappear. Instead, farmers will harvest a maximum yield of 800–900 kg/ha in limited areas (~30%) in the central and west-central colo steppe zones. According to the results of previous scenarios, the lowest yield of 600–700 kg/ha was observed only in the southwestern part of the North Kazakhstan region, while under the RCP

8.5 scenario, it increased to 20%, covering the eastern and southwestern parts of the study area. Moreover, a new class appeared on the map, showing meager yields of 500–600 kg/ha in the far southwestern part, and its area was equal to 4%.

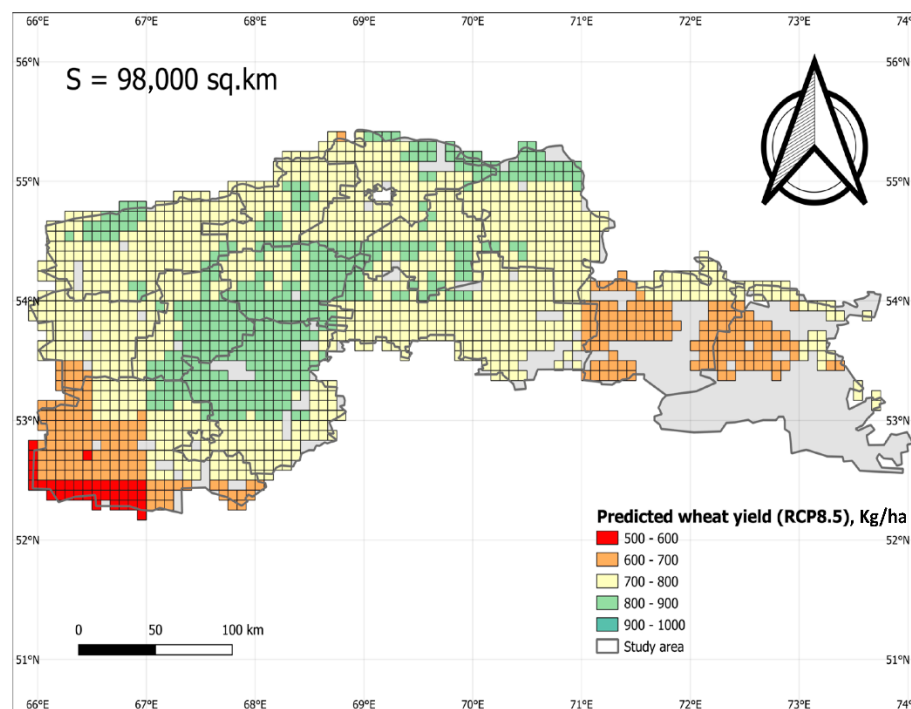


Figure 2.5. Predicted wheat yield in kg/ha under RCP 8.5 in the North Kazakhstan region for the midcentury

According to Table 2.2, the average wheat yield failure in the North Kazakhstan region accounted for 25.2, 59.5, and 84.7 kg/ha for RCPs 2.6–4.5, 4.5–8.5, and 2.6–8.5, respectively. To demonstrate the spatial variations, maps were compiled showing differences in wheat yield between three scenarios of RCP with a spatial resolution of 5 arcminutes (Figure 2.6). Nevertheless, since the climate data received from the Earth System Model version 1.2 from the Max Planck Institute had a 30 arcminute resolution interpolated to 5 arcminutes, the produced maps contained relatively similar yield difference results inside those square shapes. The highest predicted wheat yield difference between RCPs 2.6 and 4.5 was observed in the arid steppe zone located in the eastern part of the study area and east of the colo steppe zone, which varied from 40 to 60 kg/ha loss of wheat, while the northern and southwestern parts (predominantly in the forest steppe zone) faced only minor changes of 0–20 kg/ha loss. Dramatical yield decrease in the arid steppe zone could be explained by relatively low soil fertility (saline tertiary sediments), increased level of evaporation due to high air temperatures and strong steppe winds which exceed the amount of precipitation, and the low xerophilicity of the wheat varieties used. However, a comparison of RCP 4.5–8.5 results illustrated dramatic wheat yield failure (60–80 kg/ha) across the forest steppe and small hilly zones and severe yield anomalies (80–110 kg/ha) in the arid steppe zone both in the southwest and east parts of the study area. The most red-colored map (53% of the area had 80–

130 kg/ha loss) was the RCP 2.6–8.5 comparison map. Severe yield failure was observed along all edges and the western and eastern parts of the study area that primarily occupied the arid steppe, small hilly, and forest zones. As a result, it was found that the colo steppe zone in the central part of the study area has a higher resistance to climate change (20–60 kg/ha damage) when growing spring wheat using current technologies and varieties. This is because the colo steppe zone is predominantly located on the floodplain of the Ishim paleochannel, which has highly fertile soil and moisture reserves.

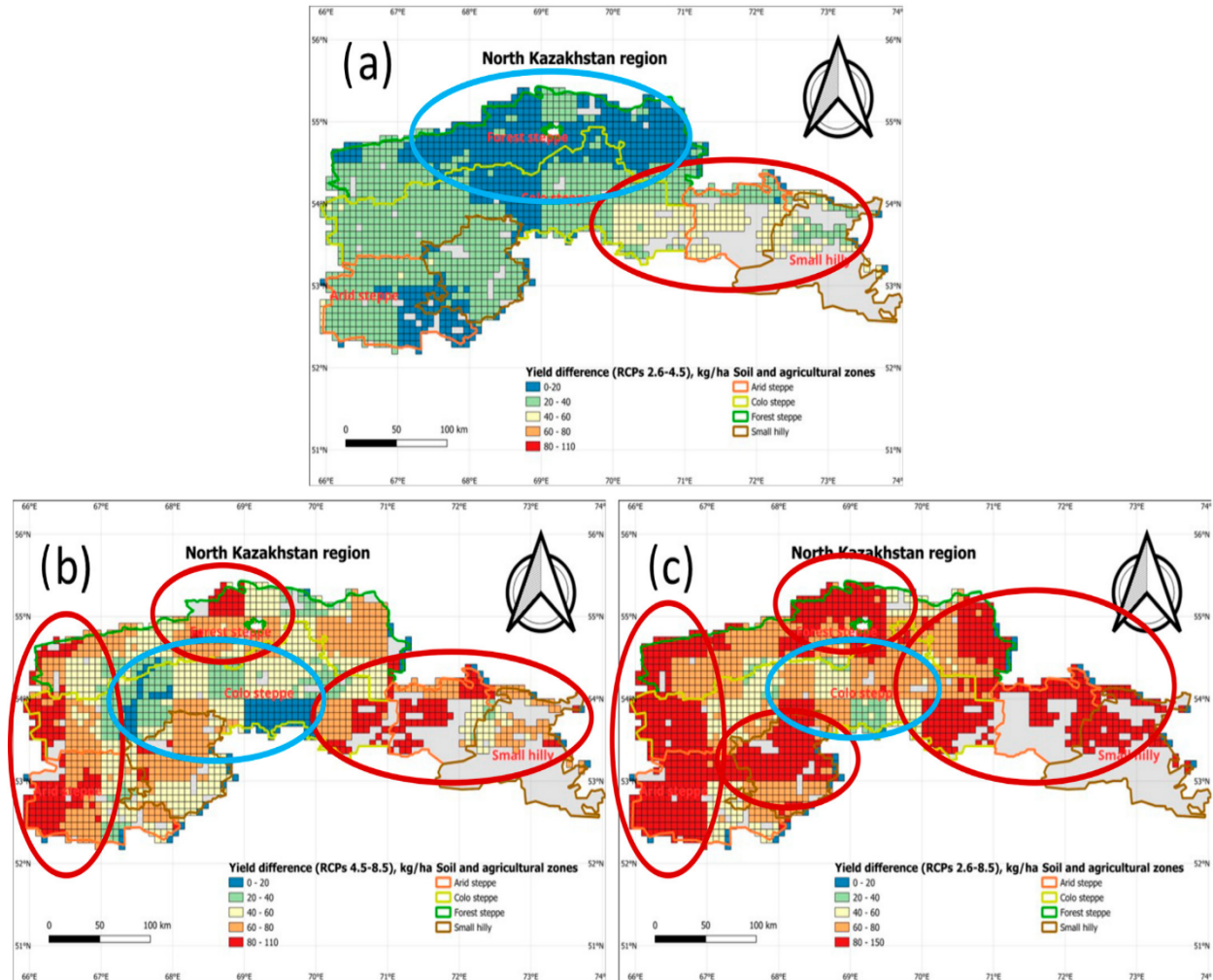


Figure 2.6. Predicted wheat yield difference in kg/ha between RCPs 2.6–4.5 (a), 4.5–8.5 (b), and 2.6–8.5 (c) in the North Kazakhstan region. Blue and red circles indicate favorable and unfavorable areas, respectively

2.4. Discussions

There has been a massive demand for modern geographic (spatial) yield forecasting tools in recent decades and a corresponding rise in the accessibility of global geospatial data sets from several data-gathering sources. Different tools utilizing various techniques have been effectively

assisted by statistical seasonal weather predictions (Donatelli et al., 2012; Lal et al., 1993; Liu et al., 2007; van der Velde et al., 2019). These involve utilizing crop models in conjunction with seasonal precipitation estimates based on GCMs (General Circulation Models) (Hansen et al., 2004; Mishra et al., 2008) and historical data (de Jager et al., 1998; Hammer et al., 2001). Although the CRAFT was designed with an integrated Climate Predictability Tool for seasonal forecasts, it is not limited to this. It allows one to enter external climate data from different sources. Unlike its predecessors (the Agricultural and Environmental Geographic Information System for Windows (AEGIS/WIN) (Engel et al., 1997), the Joint Research Centre's Biophysical Models Applications (BioMA) framework (Supit, 1997), and the GIS-based Environmental Policy Integrated Climate (GEPIC) model (Liu et al., 2007)), the CRAFT allows multiple pre-installed crop models such as DSSAT, APSIM, and SARRA-H to be run, thus being a successful product for predicting both seasonal and long-term crop yields with a sufficiently high spatial resolution.

The above results indicate that, by combining the DSSAT crop model and long-term climate predictions, the CRAFT can successfully assess the impact of climate change on agricultural production under different climate scenarios. Considering 2 million hectares of wheat fields in the North Kazakhstan region and the average wheat yield of 1250 kg/ha between 2020 and 2022 (Bureau of National Statistics, Agency for Strategic Planning and Reforms of the Republic of Kazakhstan, 2023), the world market receives 2.5 billion kilograms or 2.5 million tons of wheat annually. However, even if humanity can reduce carbon dioxide emissions into the atmosphere by zero and methane by half by 2100 (RCP 2.6), global temperatures will still continue to rise naturally to about 2 degrees, and according to our study based on spatial simulations using CRAFT, it will cause a loss of 837,800 tons of wheat or USD 167 million (the market price of wheat varies significantly due to different events worldwide, but for the calculation, an average price of USD 200 per ton was determined) annually in the mid-century. There is a debate among scientists worldwide if rising temperatures and a higher concentration of carbon dioxide in the atmosphere will boost or decrease wheat yield in different continents and soil and climate conditions. Even though the experiments conducted in the laboratory-chamber, greenhouse, and open- and closed-top field chamber demonstrate a positive effect of elevated CO₂ on wheat yield (Amthor, 2001; Broberg et al., 2019; Pandey et al., 2017; Shaheen et al., 2022; Shoukat et al., 2022), overall, direct and indirect effects of climate change will result in yield and nutritional quality decrease (Abdelhakim et al., 2022; Alsafadi et al., 2023; Daloz et al., 2021; T. Zhang et al., 2022; Zhou et al., 2023). Many scholars agreed that the RCP 4.5 is the most probable baseline scenario (Höök et al., 2010; Pielke Jr. et al., 2021), under which the simulation in the North Kazakhstan region demonstrated wheat failure of 25.2 kg/ha compared to RCP 2.6 or 888,400 tons (USD 177 million) relative to today's yield. Under the improbable but still possible RCP 8.5 scenario, the world market will receive around 1 million tons of wheat (USD 201 million) less annually, which may lead to regional food disasters. Nevertheless, the model and calculations we used do not consider future technological modernization and genetic modification aimed at adapting to climate change. Moreover, the limited availability of high-resolution climate data might cause spatial wheat yield bias.

2.5. Conclusions

In this study, the effects of three distinct Representative Concentration Pathways with 2.6 W/m², 4.5 W/m², and 8.5 W/m² on wheat production in the North Kazakhstan region were assessed using the DSSAT crop model spatial application using the CRAFT and daily forecasted climate data from the MPI-ESM1.2. As a result, the arid steppe zone was found to be the most sensitive to an increase in greenhouse gases in the atmosphere, since the yield difference between RCPs 2.6 and 8.5 accounted for almost 110 kg/ha (16.4%) and 77.1 kg/ha (10.4%) between RCPs 4.5 and 8.5, followed by the small hilly zone with an average loss of 90.1 and 58.5 kg/ha for RCPs 2.6–8.5 and RCPs 4.5–8.5, respectively. It was found that by the mid-century, potentially, we will lose more than 10% of wheat in the arid steppe zone, 7.6% in the small hilly zone, 7.5% in the forest steppe zone, and 6% in the colo steppe zone due to climate change if the modeled RCP 8.5 scenario comes true. The spatial variation maps for RCPs 2.6 and 4.5 demonstrated a homogeneous distribution of wheat yield over the study area since around 70% of wheat fields produced from 800 to 900 kg/ha yield. A comparison of RCP 4.5–8.5 results illustrated dramatic wheat yield failure (60–80 kg/ha) across the forest steppe and small hilly zones and severe yield anomaly (80–110 kg/ha) in the arid steppe zone both in the southwest and east parts of the study area. Lastly, it was found that the colo steppe zone in the central part of the study area has a higher resistance to climate change (20–60 kg/ha damage) when cultivating spring wheat using current technologies and wheat varieties.

Overall, the CRAFT v3.4 and DSSAT 4.7.5 software application program combined with the Earth System Model's climate predictions showed great potential in assessing climate change effects on wheat yield under different climate scenarios in the North Kazakhstan region. We believe that the results obtained will be helpful during the development and zoning of modified, drought-resistant wheat varieties and the cultivation of new crops in the region. Further work is required to improve simulation models and provide available and accurate environmental data at a high spatial resolution to consider the full range of factors affecting wheat production (e.g., flexible sowing date for each year, which changes automatically to effectively use rainfall during critical phases of crop development instead of fixed ones).

3. Comparison of Snow Indices in Assessing Snow Cover Depth in Northern Kazakhstan

This article is published in Sustainability journal as: **Zhanassyl Teleubay**, Farabi Yermekov, Ismail Tokbergenov, Zhanat Toleubekova, Amangeldy Igilmanov, Zhadyra Yermekova and Aigerim Assylkhanova. 2022

Comparison of Snow Indices in Assessing Snow Cover Depth in Northern Kazakhstan



Sustainability Volume 14, August 2022, 9643

<https://doi.org/10.3390/su14159643>

Journal CiteScore (Scopus): 7.7



Author Contributions: Z.T. (Zhanassyl Teleubay) analyzed the data and drafted the manuscript.

F.Y., I.T., Z.T. (Zhanat Toleubekova) and Z.Y. completed the manuscript and made major revisions; A.A. searched references; A.I. checked and proofread the manuscript.


sustainability


Article

Comparison of Snow Indices in Assessing Snow Cover Depth in Northern Kazakhstan

Zhanassyl Teleubay ^{1,*} , Farabi Yermekov ¹, Ismail Tokbergenov ¹ , Zhanat Toleubekova ², Amangeldy Igilmanov ², Zhadyra Yermekova ³ and Aigerim Assylkhanova ⁴

¹ Center for Technological Competence in the Field of Digitalization of the Agro-Industrial Complex, S.Seifullin Kazakh Agrotechnical University, Nur-Sultan 010000, Kazakhstan

² Faculty of Land Administration and Architecture, S.Seifullin Kazakh Agrotechnical University, Nur-Sultan 010000, Kazakhstan


³ Faculty of Physics and Technical Sciences, L.N.Gumilyov Eurasian National University, Nur-Sultan 010000, Kazakhstan

⁴ Faculty of Science and Informatics, University of Szeged, 6720 Szeged, Hungary

* Correspondence: zhanassyl.kz@gmail.com; Tel.: +7-(775)-860-06-80

Abstract: This study compares the performances of four existing snow indices (Normalized-Difference Snow Index, Normalized-Difference Snow and Ice Index, Difference Snow Index, and Ratio Snow Index) in estimating snow cover depth at three agricultural enterprises in different soil zones, namely, the “North Kazakhstan Agricultural Experimental Station”, A.I. Barayev “Research and Production Center for Grain Farming”, and “Naidorovskoe”. From 30 January to 9 February 2022, the snow cover thickness and density were measured at 410 and 285 points, respectively, throughout the agricultural enterprise territories. It was found that: (1) snow-covered territories were effectively classified using all spectral indices except both combinations of RSI; (2) the snow cover fraction maps generated from DSI most accurately classified the non-snow areas as forest plantations, settlements, and strongly blown uplands; (3) the maps generated from DSI-2 presented a clear pattern of objects in all three study areas; (4) the liquid water in snowpacks is available in excess for possible reservation and rational use in agriculture during the dry season. At the “North Kazakhstan AES”, A.I. Barayev “Research and Production Center for Grain Farming”, and “Naidorovskoe”, the RMSE varied from 5.62 (DSI-2) to 6.85 (NDSII-2), from 3.46 (DSI-2) to 4.86 (RSI-1), and from 2.86 (DSI-2) to 3.53 (NDSII-1), respectively. The DSI-2-based snow depths best matched the ground truth, with correlations of 0.78, 0.69, and 0.80, respectively.

Keywords: snow indices; snow depth; North Kazakhstan agricultural experimental station; research and production center for grain farming; Naidorovskoe



Citation: Teleubay, Z.; Yermekov, F.; Tokbergenov, I.; Toleubekova, Z.; Igilmanov, A.; Yermekova, Z.; Assylkhanova, A. Comparison of Snow Indices in Assessing Snow Cover Depth in Northern Kazakhstan. *Sustainability* **2022**, *14*, 9643. <https://doi.org/10.3390/su14159643>

Academic Editors: Ayyoob Sharifi, Baojie He, Chi Feng and Jun Yang

Abstract: This study compares the performances of four existing snow indices (Normalized-Difference Snow Index, Normalized-Difference Snow and Ice Index, Difference Snow Index, and Ratio Snow Index) in estimating snow cover depth at three agricultural enterprises in different soil zones, namely, the “North Kazakhstan Agricultural Experimental Station”, A.I. Barayev “Research and Production Center for Grain Farming”, and “Naidorovskoe”. From 30 January to 9 February 2022, the snow cover thickness and density were measured at 410 and 285 points, respectively, throughout the agricultural enterprise territories. It was found that: (1) snow-covered territories were effectively classified using all spectral indices except both combinations of RSI; (2) the snow cover fraction maps generated from DSI most accurately classified the non-snow areas as forest plantations, settlements, and strongly blown uplands; (3) the maps generated from DSI-2 presented a clear pattern of objects in all three study areas; (4) the liquid water in snowpacks

is available in excess for possible reservation and rational use in agriculture during the dry season. At the “North Kazakhstan AES”, A.I. Barayev “Research and Production Center for Grain Farming”, and “Naidorovskoe”, the RMSE varied from 5.62 (DSI-2) to 6.85 (NDSII-2), from 3.46 (DSI-2) to 4.86 (RSI-1), and from 2.86 (DSI-2) to 3.53 (NDSII-1), respectively. The DSI-2-based snow depths best matched the ground truth, with correlations of 0.78, 0.69, and 0.80, respectively.

Keywords: snow indices; snow depth; North Kazakhstan agricultural experimental station; research and production center for grain farming; Naidorovskoe

3.1. Introduction

Kazakhstan’s largest crop production areas are found in the northern and central regions, which permanently suffer from spring and summer droughts. The dry climate reduces crop yield and quality and lowers Kazakhstan’s socio-economic situation. Given the current realities of climate change and the agrarian practice of rainfed agriculture on the great steppe of Kazakhstan, spring melt water can be a primary source of water for irrigated agriculture. To do this, estimating the amount of snow and snow water equivalent and retaining melt water in small reservoirs is necessary. In addition, this decision would help prevent the annual spring floods of settlements. The region receives a stable amount of snow cover for up to six months a year, potentially allowing the use of melt water for agricultural purposes.

Methods for obtaining reliable, large-area snow cover information with high spatial and temporal resolution are essential because snow cover naturally has high spatio-temporal variability and shows rapid directional changes under the influence of climate change (Armstrong & Brun, 2008; Dong, 2018; Lettenmaier et al., 2015; Sturm, 2015). Owing to its extreme thermophysical characteristics, highly variable parameters, and duration of occurrence on vast land areas, snow cover affects almost all interactions between the atmosphere and the underlying surfaces at temperate and high latitudes in the cold season (Jones et al., 2001; Vavrus, 2007). Climate warming causes earlier than normal snowmelt and shortens the period of stable snow cover, with adverse effects on natural and anthropogenic systems (Duan et al., 2021; Kumar et al., 2022; Mote et al., 2005). Mountainous regions and plains in temperate regions, where the snow cover is susceptible to temperature fluctuations, will most likely suffer from increased snow melting (Barnett et al., 2005; Popova et al., 2015). Regime changes in snow accumulation and snow melting alter the level of spring floods and increase the potential for evaporation, thus affecting water resources and the agriculture sectors that depend on them (Rood et al., 2008). Snow cover is an essential water supply for plants, as it prevents freezing winter crops, perennial grasses, and the root systems of fruits and berries (Groffman et al., 2001; Pilon et al., 1994; T. Zhang, 2005).

Researchers worldwide have estimated snow depth from ground observations, geographic information systems, and remote sensing. These investigations are primarily conducted from two perspectives: direct measurements of actual snow depth and indirect estimates using snow indices and modeling equations. From the first perspective, the Nordic Snow Radar Experiment (NoSREx) conducted by Lemmetyinen et al. (2016) estimates the snow depth, snow density, and snow water equivalent (SWE) in real-time from gamma water instruments at intensive observation points. Gan et al. (2021) compared two passive microwave-estimated snow depths with SWE retrievals from

the Advanced Technology Microwave Sounder and the Advanced Microwave Scanning Radiometer 2. They proposed two equations for calculating the snow depth in forested and non-forested territories. Both products captured the temporal variability of the SWE at elevations lower than 900 m and snow depths lower than 20 cm well. Jenssen & Jacobsen (2021) measured the snow depth, snow density, and SWE in Norway using an ultra-wide-band (0.7–4.5 GHz) radar mounted on an unmanned aerial vehicle (UAV). They found that pseudo-noise radar can measure snow depths up to 5.5 m with high precision ($R > 0.92$) (Jenssen & Jacobsen, 2021). However, the frequency–wavenumber migration algorithm proved insufficient for estimating the snow density, and system improvements were required. From the second perspective, various snow indices and snow cover fraction (SCF) equations have been proposed for snow depth estimation. Analogously to the ratio vegetation index and difference vegetation index, Lin et al. (2012) employed the ratio snow index (RSI), the difference snow index (DSI), and the existing normalized-difference snow index (NDSI) to estimate the SCF in northwestern China. They discovered that an exponential fitting ($R^2 > 0.79$) outperforms the linear fitting ($R^2 > 0.15$). Romanov & Tarpley (2004) found a strong correlation between snowpack depth and FSC. After fitting the relationship to an exponential equation and formulating a parametrization, they achieved a mean absolute error of 5 cm over the U.S. Great Plains and Canadian prairies. Kim et al. (2017) compared the abilities of three existing SCF equations, namely linear, quadratic and exponential functions of NDSI, to estimate snow depth over South Korea. Although the quadratic function obtained the lowest root mean squared error (RMSE = 2.37 cm), the authors recommended the linear equation (RMSE = 3.43 cm) because the error of the snow depth map calculated by the quadratic equation will increase when using satellite images with high snowfall. Additionally, Dixit et al. (2019) compared NDSI, NDSII, and S3 to delineate snow cover over the Beas River basin, India, and proposed a new Snow Water Index (SWI). According to their findings, S3 could delineate snow and non-snow pixels more accurately (89%) compared with NDSI (80%) and NDSII (85%). The S3 index has a huge advantage in assessing snow cover in the forest zone, combining Red, NIR, and SWIR bands. However, since the authors needed to minimize the snow-water mixing, they proposed SWI (overall accuracy 93%), which utilizes green, NIR, and SWIR bands.

Although there are methods for snow cover assessment, new approaches are needed in the steppe zone, where there is no snow–water, snow–vegetation, or snow–shadow mixing. Consistently, within the framework of this study, we set a goal to develop an approach that allows assessing the snow cover (1) over large areas (>10,000 ha), (2) with high temporal resolution (<7 days), and (3) without field snow surveys, which are time- and resource-consuming. This paper compares snow indices for estimating snow depth at three agricultural enterprises in different soil zones, namely, the limited liability partnerships (LLPs) North Kazakhstan Agricultural Experimental Station, A.I. Barayev Research and Production Center for Grain Farming, and Naidorovskoe. The selected snow indices were the NDSI, NDSII, DSI, and RSI from the Sentinel-2 multispectral instrument (MSI). The choice of these indices is justified because each has its advantages and disadvantages, which are suitable for use in the steppe zone and have not been compared before. NDSI is the most widely used snow index, which identifies snow cover by

ignoring cloud cover and reducing the influence of atmospheric effects, while NDSII is used to determine not only snow cover, but also ice. In turn, knowing that snow density is greater than ice density, we intend to evaluate and compare the performance of NDSII in calculating the snow water equivalent. The use of such simple snow indices as DSI and RSI are bottomed because they are both susceptible to the amount of snow and can distinguish snow from soil differently. If DSI does not consider the difference between reflectance and radiance caused by the atmosphere or shadows, RSI takes advantage of the reduced influence of the atmosphere and topography. The modeled results were compared with actual snow survey results to assess the possibility of estimating the snowpack depth from the SCF–snow depth relationship. The objective of this study was to compare the snow depths estimated from the existing snow indices with parametrization in three different soil zones. The study outcomes form a scientific basis for early warning of spring floods, combating meteorological and agricultural droughts, and developing more accurate approaches for estimating snow depths over vast territories using geographic information systems (GISs) and remote sensing methods. Moreover, in addition to a new approach for snow cover assessment in the steppe zone, field snow survey data from three soil zones for independent testing and comparative studies by the international research community have been published under the CC BY license (see the Data Availability Statement).

3.2. Materials and Methods

3.2.1. Study Area

The study sites (see Figure 3.1) were three agricultural enterprises in different soil zones, the LLP North Kazakhstan Agricultural Experimental Station (Akkayin district, North Kazakhstan region), the LLP A.I. Barayev Research and Production Center for Grain Farming (Shortandy district, Akmola region) and the LLP Naidorovskoe (Osakarov district, Karagandy region). The climate is extremely continental and arid in all three regions, with hot summers and cold winters. The daily and annual temperatures fluctuate sharply. The average annual precipitation in the North Kazakhstan and Akmola regions is 350 mm, of which around 80% falls during the warm season (April–October). The Karaganda region receives only around 200 mm. Snow cover on the studied agricultural enterprises resides for approximately 150 days (November–March) and reaches average depths of 20–25 cm by the end of the winter season. Snow melt begins in mid-March and is completed at the end of April. The A.I. Barayev Research and Production Center for Grain Farming and the Naidorovskoe LLPs each have approximately 20,000 ha of cultivated land, while the North Kazakhstan Agricultural Experimental Station sows around 25,000 ha of arable land. Three main crop types are grown in the studied enterprises: cereals (wheat, oat, barley, and millet), legumes (peas, lentils, alfalfa, clover, and sweet clover), and oilseeds (safflower, sunflower, rapeseed, and flax). The sowing campaign typically begins in mid-May and ends in October.

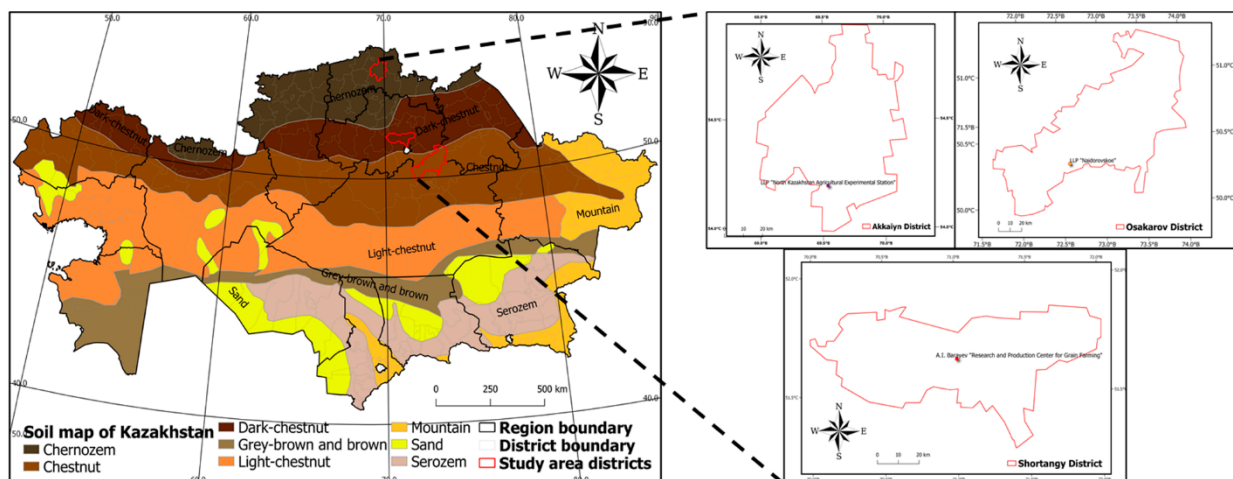


Figure 3.1. Study area and soil map of the Republic of Kazakhstan

3.2.2. Data Sources

3.2.2.1. In situ surveying

Field snow at the key sites was surveyed from 30 January to 9 February 2022 in the territories of the three agricultural enterprises (Figure 3.2). The snow cover thickness was measured at 410 points, and the snow density was measured at 285 points (Table 3.1).

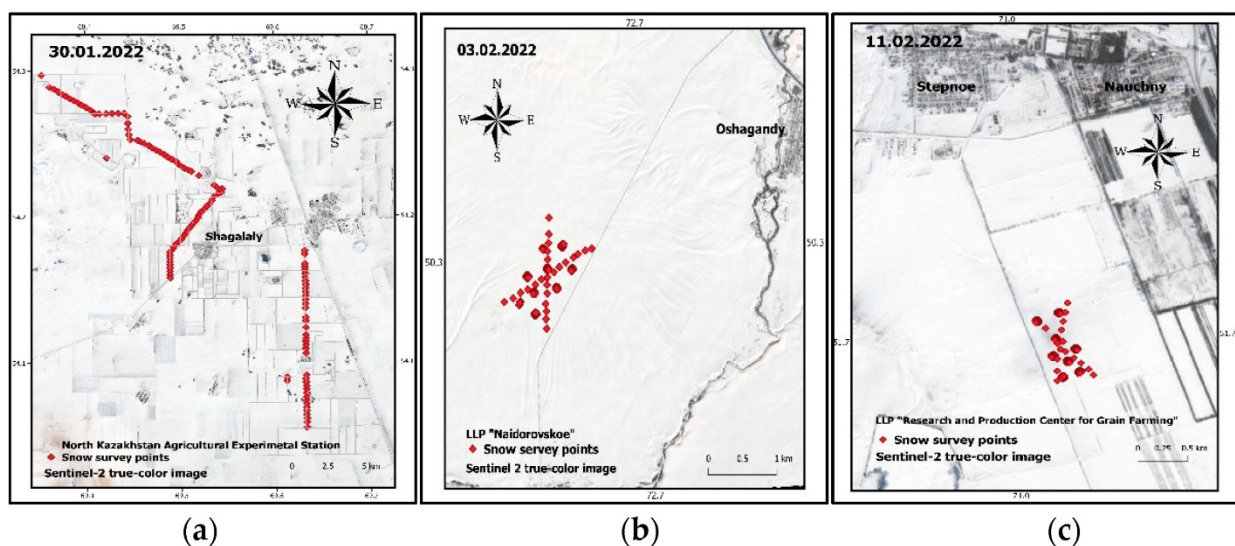


Figure 3.2. Waypoints of snow survey over the territories of the three agricultural enterprises: (a) limited liability partnership (LLP) North Kazakhstan Agricultural Experimental Station, (b) LLP Naidorovskoe, and (c) LLP A.I. Barayev Research and Production Cent Center for Grain Farming

Table 3.1. Snow survey dates and numbers of measured points in the territories of the three limited liability partnerships

Study Area/Snow Survey Dates and the Number of Points	30 January 2022		7 February 2022		9 February 2022	
	Depth	Density	Depth	Density	Depth	Density
LLP North Kazakhstan Agricultural Experimental Station	118	118				
LLP A.I. Barayev Research and Production Center for Grain Farming			144	19		
LLP Naidorovskoe					148	148

The snow thickness was measured with a metal ruler with a 1 mm scale, and the snow density was calculated using a weight snow gauge (VS-43M). The actual snow density ρ (kg/m³) was calculated from the snow mass m (kg), the snow depth SD (m), and the area S (m²) of the VS-43M weight snow gauge cylinder as:

$$\rho = \frac{m}{SD \times S} \quad (1)$$

For convenient and quick movement in the study area, we operated our snowmobile (RM Vector 551i). To measure the actual snow height and density and determine the geolocation during snow surveys, we employed an M-103 II snow gauge, a VS-43M weight snow gauge, and a Garmin Montana 610 system (see Figure 3.3).



Figure 3.3. Process of measuring the snow height and density

3.2.2.2.Digital Satellite Image Dataset

As the remote sensing data for estimating the snow cover thickness, we used wide-swath and high-resolution multispectral images of the Sentinel-2 MSI. Images with the nearest dates to the field-snow surveying dates were downloaded and processed. At the LLP North Kazakhstan Agricultural Experimental Station, the satellite images and field work dates coincided,

but to cover the large territory of the study area, we constructed a mosaic of two satellite images with different cloud cover percentages. At the A.I. Barayev Research and Production Center for Grain Farming and Naidorovskoe, satellite images were taken four days earlier and two days later than the field-snow survey, respectively. The cloud coverage in the satellite image excluded the study area of the three agricultural enterprises. Table 3.2 provides the details of the Sentinel-2 MSI specifications. All satellite images were downloaded from the Google Earth Engine cloud-based geospatial platform.

Table 3.2. Specifications of the Sentinel-2 multispectral instrument

Sensor	Acquisition Date	Spectral Band with Wavelet (μm)	Cloud Cover
Sentinel-2	30 January 2022, 42UWE	Coastal (0.443)	26%
		Blue (0.490)	
	30 January 2022, 42UWF	Green (0.560)	60%
		Red (0.665)	
	3 February 2022, 43UCR	Vegetation red edge (0.705)	1%
		Vegetation red edge (0.740)	
	11 February 2022, 42UCX	Vegetation red edge (0.783)	84%
		Near-infrared (0.842)	
		Vegetation red edge (0.865)	
		SWIR-Cirrus (1.375)	
		SWIR-1 (1.610)	
		SWIR-2 (2.190)	

3.2.3. Methodology

The methodology of the present study included selecting an appropriate study site, collecting satellite and ground data, applying snow cover indices, calculating SCF maps from the snow cover indices, and estimating snow depth and SWE (Figure 3.4). The accuracy of each snow depth map was assessed through field-data validation. All the computations and analysis were applied to the satellite images using the Google Earth Engine cloud-based geospatial platform, ERDAS IMAGINE was used for stack image generation, and the final maps were produced in Quantum GIS software.

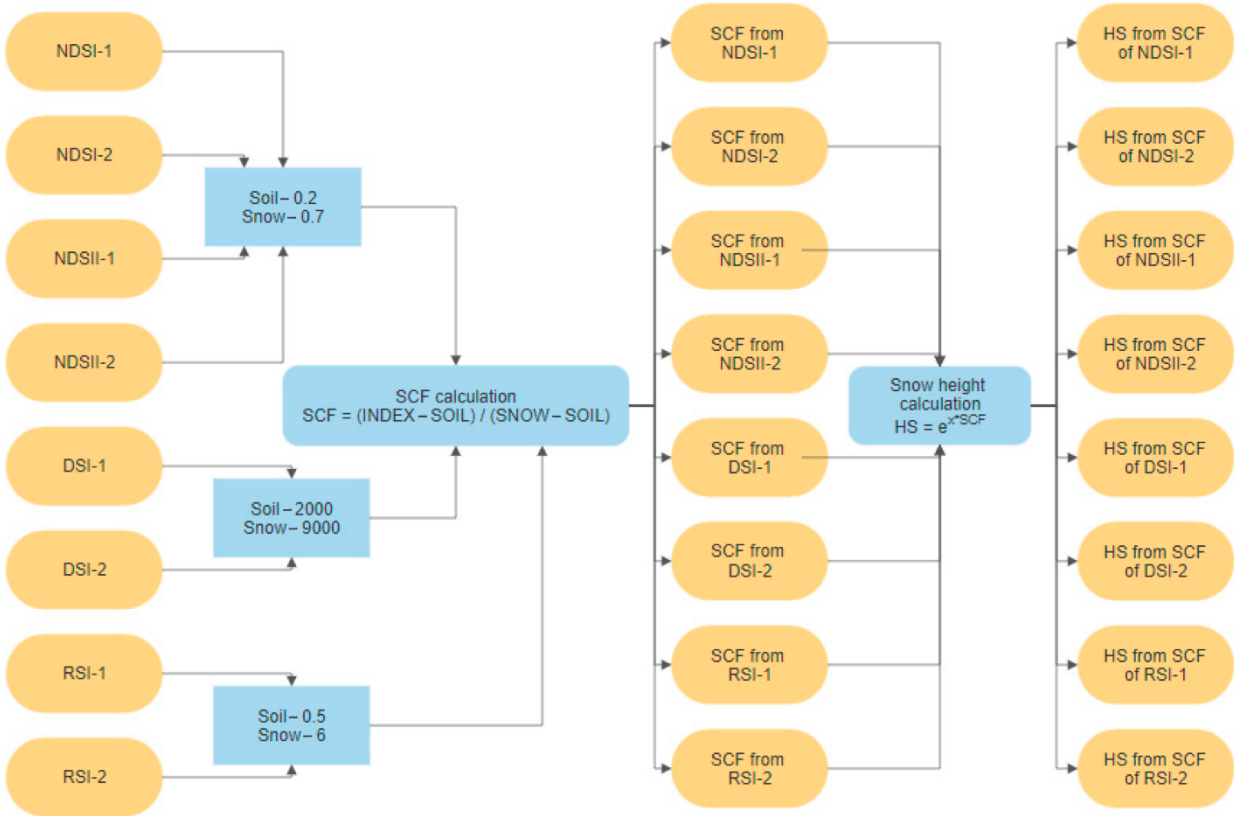


Figure 3.4. Flowchart of the data processing methods in the present study

3.2.3.1. Spectral Snow Indices

The spectral reflectivity of snow has a distinct spectral variability, being high in the green band of visible light (0.543–0.578 μm) and low in the shortwave infrared region (SWIR) (1.565–2.280 μm). Therefore, we can automatically detect and extract snow cover extent using various snow spectral indices (Dozier, 1989; Hall et al., 1995, 1998, 2002; H. S. Negi et al., 2010). As mentioned above, we adopted the NDSI, NDSII, DSI, and RSI (see Table 3.3). Using the NDSI, we can not only distinguish snow from non-snow pixels, but can also reduce the effects of clouds, atmospheric noise, and geometric distortion (Negi et al., 2009; Salomonson & Appel, 2004). In addition, the NDSI accounts for the topographic effect and can map snow in mountain shadows (Negi et al., 2010). Hall et al. reported that the NDSII index produces the same results as NDSI (Hall et al., 1998). The NDSII was developed in 2001 as a mapping index of snow and ice cover for the VGT sensor of the SPOT-4 satellite (Xiao et al., 2001). It has four spectral bands (blue, red, near-infrared, and shortwave infrared), and its spectral range is similar to that of the Sentinel-2 MSI. The NDSII recognizes that the expressions of snow reflectivity differ in the red and SWIR ranges. The DSI and RSI, developed by (Lin et al., 2012), respectively, imitate the difference vegetation index and ratio vegetation index with particular modifications in the spectral bands. In addition, as the snow reflectance in the SWIR-1 (1.610 μm) and SWIR-2 (2.190 μm) spectral bands are very similar, another set of snow indices was generated by changing B11 of the Sentinel 2 MSI to B12.

Table 3.3. Snow indices and their definitions

Snow Index	For Sentinel 2 MSI	For Landsat 8 OLI
NDSI ₁	$\text{Green}_{B03} - \text{SWIR}_{B11} / \text{Green}_{B03} + \text{SWIR}_{B11}$	$\text{Green}_{B03} - \text{SWIR}_{B06} / \text{Green}_{B03} + \text{SWIR}_{B06}$
NDSI ₂	$\text{Green}_{B03} - \text{SWIR}_{B12} / \text{Green}_{B03} + \text{SWIR}_{B12}$	$\text{Green}_{B03} - \text{SWIR}_{B07} / \text{Green}_{B03} + \text{SWIR}_{B07}$
NDSII ₁	$\text{Red}_{B04} - \text{SWIR}_{B11} / \text{Red}_{B04} + \text{SWIR}_{B11}$	$\text{Red}_{B04} - \text{SWIR}_{B06} / \text{Red}_{B04} + \text{SWIR}_{B06}$
NDSII ₂	$\text{Red}_{B04} - \text{SWIR}_{B12} / \text{Red}_{B04} + \text{SWIR}_{B12}$	$\text{Red}_{B04} - \text{SWIR}_{B07} / \text{Red}_{B04} + \text{SWIR}_{B07}$
DSI ₁	$\text{Green}_{B03} - \text{SWIR}_{B11}$	$\text{Green}_{B03} - \text{SWIR}_{B06}$
DSI ₂	$\text{Green}_{B03} - \text{SWIR}_{B12}$	$\text{Green}_{B03} - \text{SWIR}_{B07}$
RSI ₁	$\text{Green}_{B03} / \text{SWIR}_{B11}$	$\text{Green}_{B03} / \text{SWIR}_{B06}$
RSI ₂	$\text{Green}_{B03} / \text{SWIR}_{B12}$	$\text{Green}_{B03} / \text{SWIR}_{B07}$

3.2.3.2. Calculation of SCF

The SCF defines the share of snow-covered surfaces within each pixel and is the most crucial parameter for estimating snow depth. The SCF varies between 0 and 1 (0-100%). Thus, a pixel value of 0.91 means that 91% of the pixel area is covered with snow. The literature provides both direct and indirect SCF calculation methods. Indirect methods are based on the correlations between snow indices and SCF, whereas direct methods employ visual analysis of high- and medium-resolution images. As the NDSI is highly correlated with SCF, many authors develop their own analysis approaches. For instance, Salomonson and Appel proposed the following linear function (Salomonson & Appel, 2004):

$$SCF = a + b \times NDSI \quad (2)$$

where a and b are constants equal to 0.06 and 1.21, respectively. Barton et al. proposed the quadratic function (Barton et al., 2000):

$$SCF = a + b \times NDSI + c \times NDSI^2 \quad (3)$$

where a, b, and c are constants optimized at 0.180, 0.371, and 0.255, respectively. Lin et al. proposed the exponential function (Lin et al., 2012):

$$SCF = a + b \times e^{c \times NDSI} \quad (4)$$

where a, b, and c are equal to -0.41, 0.571, and 1.068, respectively. As direct methods are more accurate than indirect methods for estimating snow cover, we here compared the performances of four existing snow indices using a mixed linear method with two variables representing the reflectivity of an entirely snow-covered surface and a bare surface. For this purpose, we adopted the formula developed by Romanov & Tarpley (2004):

$$SCF = \frac{R-Land}{Snow-Land} \quad (5)$$

where R is the observed visible reflectance of the scene, and Land and Snow are the reflectivity of land and snow, respectively. The error in the SCF estimation was 10–13% depending on the SCF value (Romanov, 2003). In this study, we used the SCF maps of the three different soil zones in North Kazakhstan, along with the four snow indices from Sentinel-2 MSI.

3.2.3.3. Estimation of Snow Depth and SWE

Romanov et al. found a high positive correlation between the SCF and SD. They proposed the following equation:

$$SD = e^{aSCF} - 1 \quad (6)$$

where a is a constant equal to 0.33. The projections of low-level plants through the snow cover dominantly affect the dependency of snow depth on SCF. Once the snowpack completely covers the greenery, the SCF no longer responds to additional increases in snow depth. Romanov and Appel reported that the snow cover given by Equation (6) reaches 100% at a snow depth of around 27 cm (Romanov & Tarpley, 2004).

The SWE integrally characterizes the thickness and density of the snow cover. This indicator, which most fully characterizes the snow reserves in a particular area, can also clarify the water regime of rivers and lakes and the activation of erosion processes. In the current work, the SWE was simply determined as:

$$SWE = \rho \times SD \quad (7)$$

where *SWE* is in kg/m², ρ is in kg/m³, and *SD* is in m.

3.3. Results

As many maps were generated, we considered it prudent to limit our discussion to the “North Kazakhstan Agricultural Experimental Station”. The maps from A.I. Barayev “Research and Production Center for Grain Farming” and “Naidorovskoe” are displayed in Appendix A.

3.3.1. Calculation of the Snow Spectral Indices

As mentioned above, we analyzed Sentinel-2 MSI images using two variations of four spectral snow indices. Figure 3.5 displays the snow indices at the “North Kazakhstan Agricultural Experimental Station” (the spectral indices at A.I. Barayev “Research and Production Center for Grain Farming” and “Naidorovskoe” are presented in Figure A1 and Figure A2, respectively, of Appendix A).

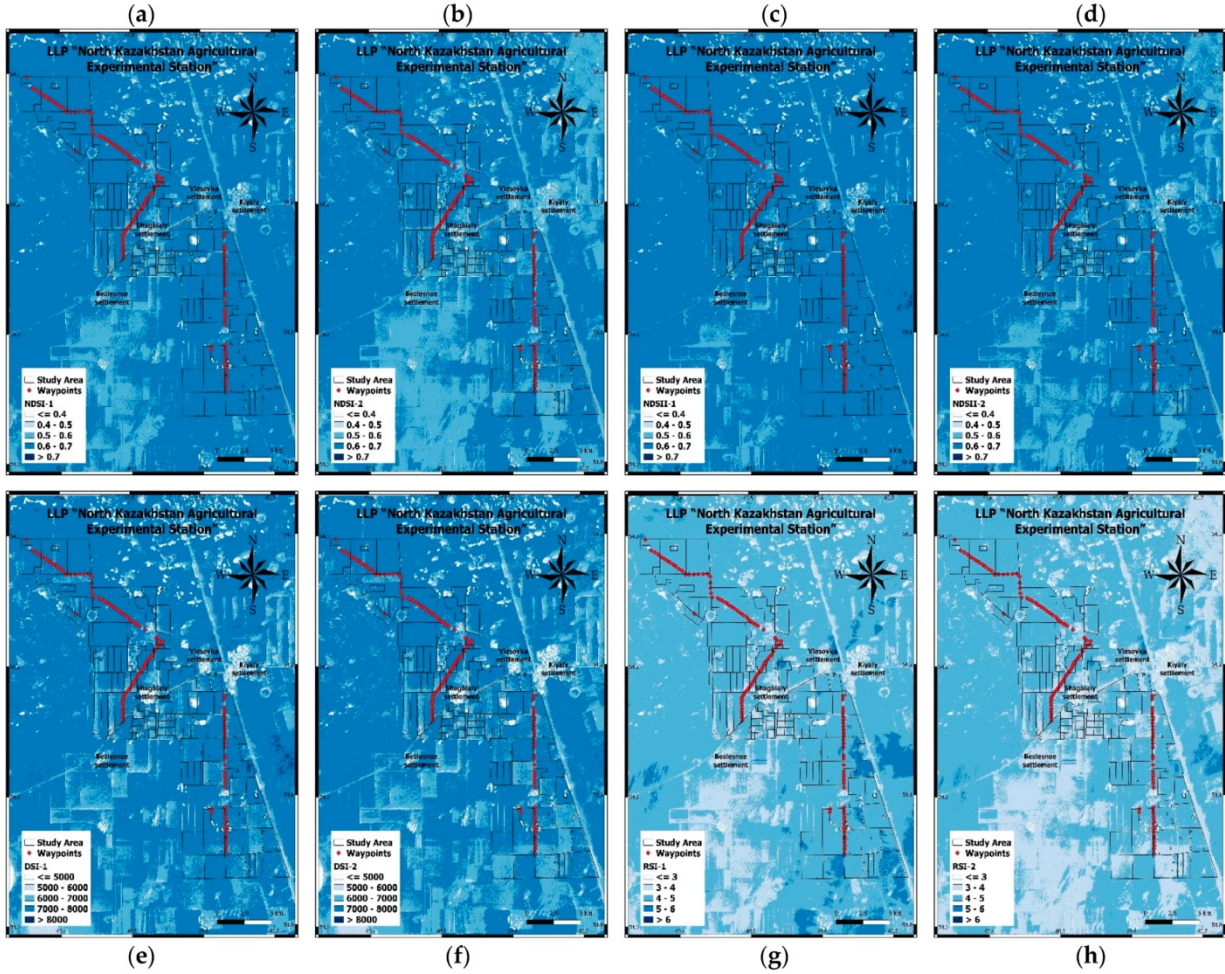


Figure 3.5. Spectral snow indices at “North Kazakhstan Agricultural Experimental Station”: (a) normalized-difference snow index [NDSI]-1, (b) NDSI-2, (c) normalized-difference snow and ice index [NDSII]-1, (d) NDSII-2, (e) difference snow index [DSI]-1, (f) DSI-2,

All spectral indices except the RSI (misclassified area: 6241 ha or 4.8%) accurately classified the snow-covered territories. The RSI-1 and RSI-2 maps displayed many large and small spots, respectively, with larger values in the northeastern part of the study area. Such patterns cannot reflect the actual intensity of the snow cover in the three agricultural enterprises. To distinguish dry snow from snow crust formed by the thawing and subsequent freezing of snow or by wind compaction (wind crust), we employed the NDSI and NDSII indices. The significant density difference between dry snow and snow/wind crust will likely affect the SWE calculation. However, consistent with Hall et al. (Hall et al., 1995), the NDSI and NDSII gave the same results and did not distinguish between snow and crust (Figure 3.5), although they classified the snow-covered territories with satisfactory accuracy. Despite the blurry class outlines, both difference snow indices detected the precise contours of the areas completely covered with snow (untouched agricultural fields), snow-free areas (settlements), and areas partially covered with snow (agricultural fields after snow retention). Snow retention is the agricultural practice of retaining and accumulating snow on arable land, mainly in the fields of steppe and forest-steppe zones

(Figure 3.6). This technique is designed to prevent freezing of the soil and wintering plants and increase soil moisture reserves.



Figure 3.6. Agricultural field at the “North Kazakhstan Agricultural Experimental Station” after applying the snow retention technique. Source: Captured by the authors during the field-snow survey

3.3.2. Estimation of SCF

Figure 3.7 shows the SCF maps at the “North Kazakhstan Agricultural Experimental Station” generated by inserting each snow index into the formula mentioned above (5). Equivalent maps at the A.I. Barayev “Research and Production Center for Grain Farming” and “Naidorovskoe” are displayed in Figure A3 and Figure A4 of Appendix A, respectively. As the SCF quantifies the share of a snow-covered area in each pixel, we calculated a single SCF value over the entire study area based on the pixel data. The SCF maps generated from the NDSII and RSI performed equally well and classified 94.3–94.5% of the land as totally snow-covered. At the “North Kazakhstan Agricultural Experimental Station”, the NDSI gave the highest snow coverage (96–96.2%), while DSI-1 and DSI-2 gave the smallest coverages (90.6% and 92.5%, respectively). It should also be noted that DSI most accurately classified non-snow areas as forest plantations, settlements, and strongly blown uplands. In the second study area located at A.I. Barayev “Research and Production Center for Grain Farming”, the NDSI and NDSII again obtained the highest proportion of snowed area (82–85.5%), followed by RSI (72.7–77.2%) and DSI (67–69.5%). In contrast, the “Naidorovskoe” territory was consistently classified as snow-covered (98.8–99.3%), although the DSI yielded the smallest share of snow-bound area (98.1–98.2%).

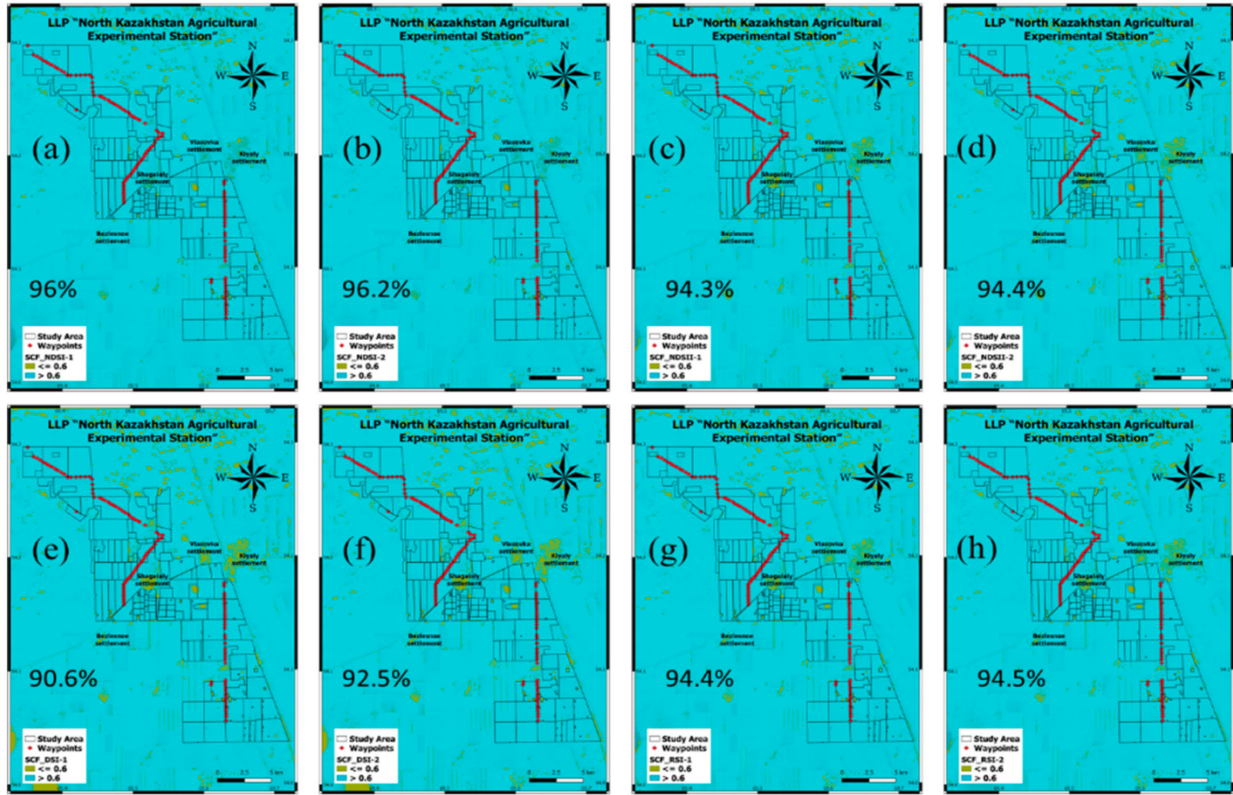


Figure 3.7. Snow cover fraction (SCF) maps at the “North Kazakhstan Agricultural Experimental Station” generated from different snow cover indices: (a) NDSI-1, (b) NDSI-2, (c) NDSII-1, (d) NDSII-2, (e) DSI-1, (f) DSI-2, (g) RSI-1, and (h) RSI-2

3.3.3. Snow Depth Modeling

Next, the snow depth maps were generated from each SCF map derived from the Sentinel-2 MSI data using Equation (6). Figure 3.8 displays the snow depth maps at the “North Kazakhstan Agricultural Experimental Station” (equivalent maps at A.I. Barayev “Research and Production Center for Grain Farming” and “Naidorovskoe” are presented in Figure A5 and Figure A6 of Appendix A, respectively). The height values in the snow depth map generated from NDSI and NDSII were similar between the variations, although NDSI-1 classified a larger snowy territory (depth > 30 cm) than NDSI-2 in the southeast part of “North Kazakhstan Agricultural Experimental Station”. The same behaviors were observed in A.I. Barayev “Research and Production Center for Grain Farming”, but in the “Naidorovskoe” territory, NDSI-2 classified the pixels more accurately than the other indices. In all three soil zones, the NDSI and NDSII obtained a blurry snow depth classification and failed to clarify the contours of the agricultural fields with and without snow retention. Meanwhile, both variations of RSI performed equally well in estimating SD in the three soil zones, and the pixel values were highly correlated with those in the snow depth maps derived from NDSII-1 and NDSII-2. The SD maps generated from DSI-1 showed the lowest depth values (0–10 cm) in the chernozem soil zone covering almost 80% of the study area, intermediate values in the chestnut soil zone (15–20 cm), and the highest value (51.4 cm) in

the dark-chestnut soil zone. The most outstanding snow depth results, with clear object patterns in all three study areas, were obtained from DSI-2. No generalization of the pixel values was observed over the entire area, and fields with recently applied snow retention were easily distinguished as regions of partially visible snow–soil mixture (southern part of the study area; see Figure 3.8f). The DSI-2-derived map showed a larger area of 10–20-cm deep snow cover (>80%) than the other maps, while only specific fields (after recent snow retention), settlements, and hills were snow-free or thinly covered (0–10 cm).

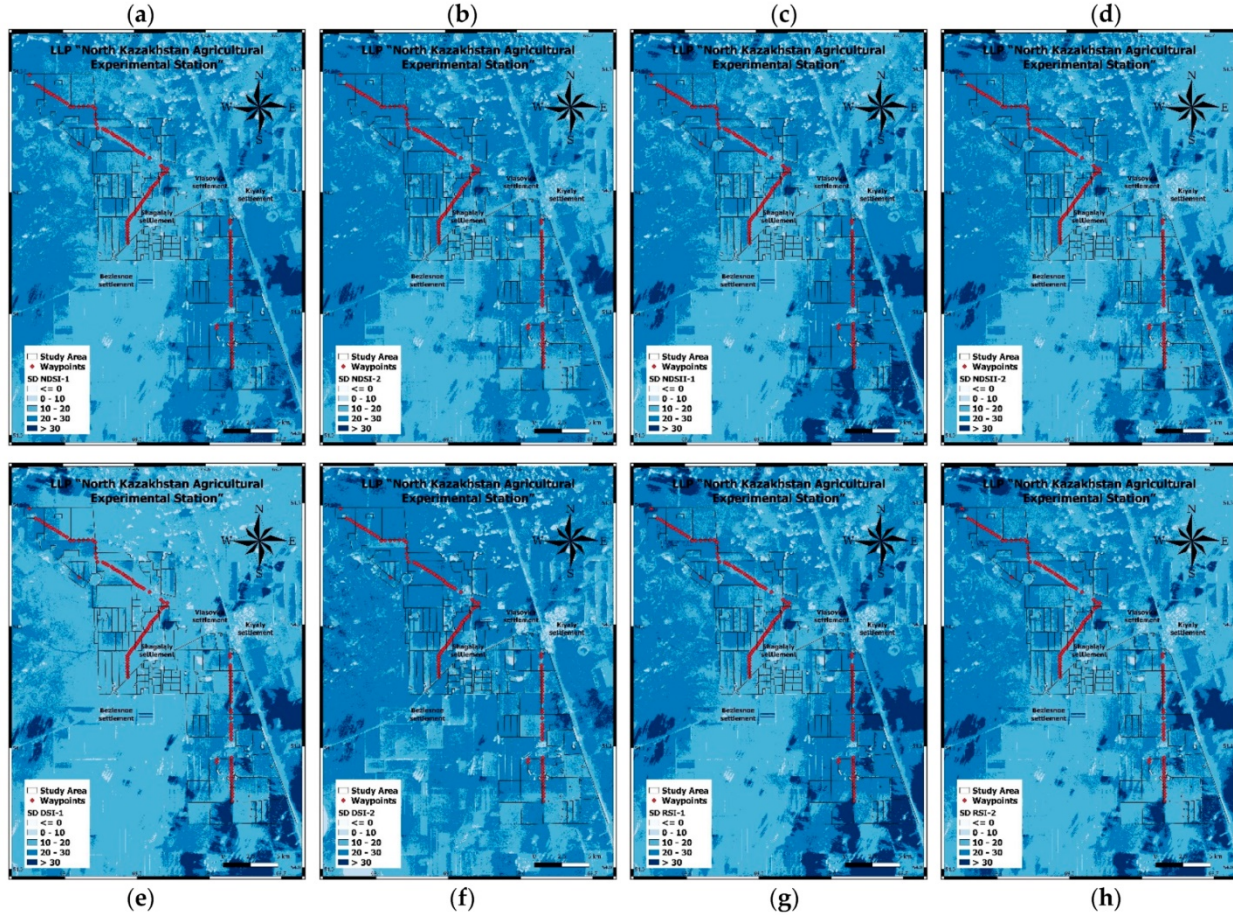


Figure 3.8. Snow depth maps at “North Kazakhstan Agricultural Experimental Station” generated from the SCFs of (a) NDSI-1, (b) NDSI-2, (c) NDSII-1, (d) NDSII-2, (e) DSI-1, (f) DSI-2, (g) RSI-1, and (h) RSI-2

The performances of the SCF maps generated from both variations of the four indices were compared in terms of the RMSEs and correlation coefficients (R) between the snow depths simulated using Equations (5) and (6) and the snow survey data collected in the field (Table 3.4). The RMSE decreased from the chernozem to the chestnut soil zones and varied from 5.62 (DSI-2) to 6.85 (NDSII-2) in the “North Kazakhstan Agricultural Experimental Station”, from 3.46 (DSI-2) to 4.86 (RSI-1) in the A.I. Barayev “Research and Production Center for Grain Farming”, and from 2.86 (DSI-2) to 3.53 (NDSII-1) in “Naidorovskoe”. The results of the DSI-2 model were most strongly correlated with the ground-truth snow depths in all three agricultural enterprises,

with R values of 0.78, 0.69, and 0.80 in “North Kazakhstan Agricultural Experimental Station”, A.I. Barayev “Research and Production Center for Grain Farming”, and “Naidorovskoe”, respectively. At the latter two enterprises, the simulated snow depth from DSI-1 was the second-best match to the ground truth, but at the “North Kazakhstan Agricultural Experimental Station”, the snow depth was better modeled by RSI-2 (0.55) and NDSI-2 (0.53) than by DSI-1.

Table 3.4. Modeled snow depth error assessments

Study Area	Error	NDSII-2	NDSII-1	NDSI-2	NDSI-1	RSI-2	RSI-1	DSI-2	DSI-1
LLP “North Kazakhstan Agricultural Experimental Station”	R	0.45	0.2	0.53	0.24	0.55	0.25	0.78	0.51
	RMSE	6.85	7.45	6.44	7.02	6.16	6.66	5.62	7.29
LLP A.I. Barayev “Research and Production Center for Grain Farming”	R	−0.07	−0.01	−0.06	0	−0.06	0	0.69	0.5
	RMSE	4.75	4.69	4.84	4.67	4.85	4.86	3.46	4.1
LLP “Naidorovskoe”	R	0.26	0.18	0.44	0.41	0.44	0.4	0.80	0.51
	RMSE	3.47	3.53	3.4	3.5	3.27	3.35	2.86	3.17

3.3.4. SWE Calculation

The SWE was calculated from each snow depth map using Equation (7). The SWE maps of the “North Kazakhstan Agricultural Experimental Station” generated from the snow depth maps of NDSI, NDSII, RSI, and DSI are displayed in Figure 3.9 (those of the A.I. Barayev “Research and Production Center for Grain Farming” and “Naidorovskoe” are displayed in Figure A7 and Figure A8 of Appendix A, respectively). Accurate SWE calculations require the snow densities in the steppe zone, which were averaged from our own data in each study area rather than extracted from the literature. The average snow density was 300 kg/m³ at “North Kazakhstan Agricultural Experimental Station” and 220 kg/m³ at A.I. Barayev “Research and Production Center for Grain Farming” and “Naidorovskoe”. This difference can be explained from a geographical viewpoint. The first study area is located in the forest-steppe zone, whereas the second is located in the steppe, and the third occupies the border between the steppe and the semi-desert zone. Comparing the SWE maps, all indices except DSI-2 underestimated the amount of snowpack water in all three soil zones. The SWE from DSI-2 exceeded 50 kg/m² over a large proportion of the “North Kazakhstan Agricultural Experimental Station”. In fields with recent snow retention, the SWE reduced to 20–40 kg/m², and in settlements and heavily blown hills, it varied between 0 and 20 kg/m².

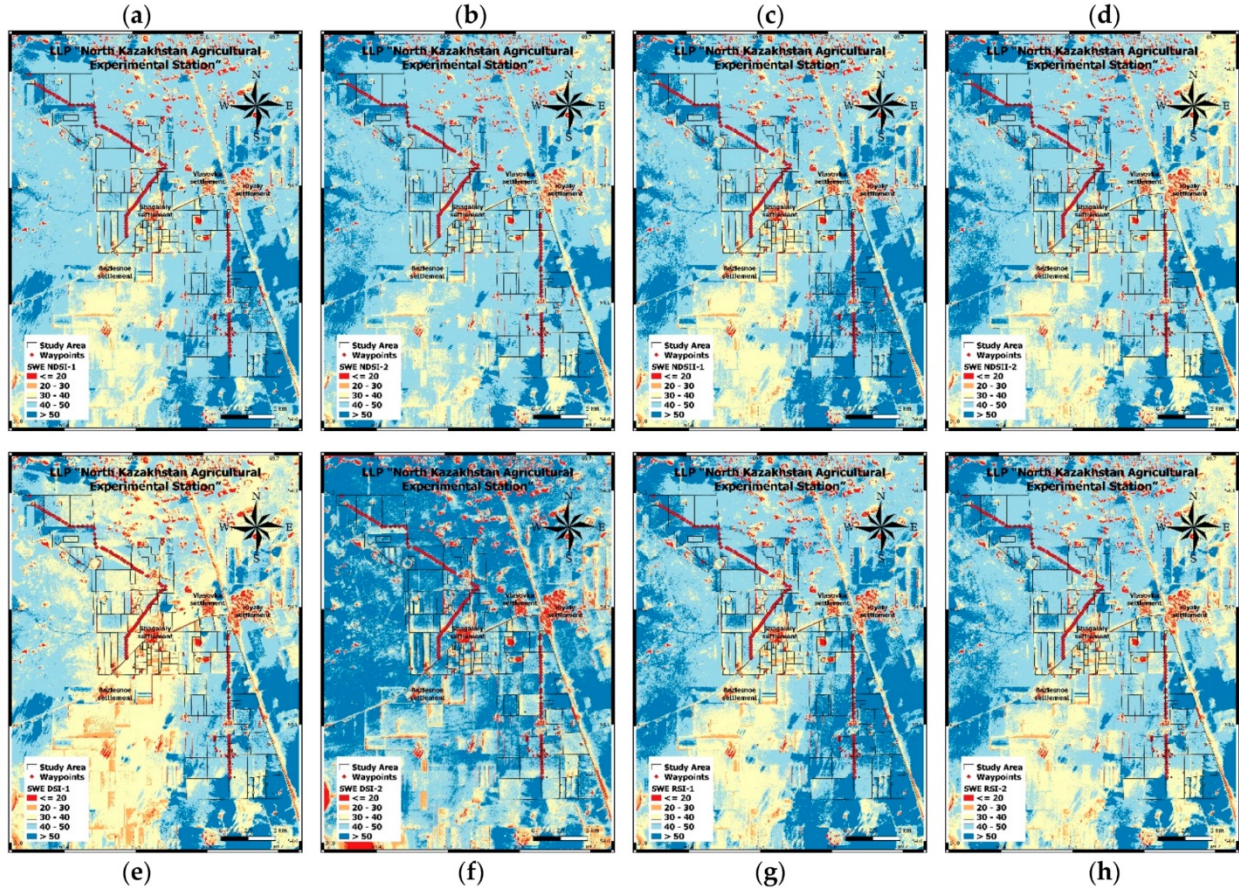


Figure 3.9. Snow water equivalent (kg/m²) maps of the “North Kazakhstan Agricultural Experimental Station” generated from the SDs of (a) NDSI-1, (b) NDSI-2, (c) NDSII-1, (d) NDSII-2, (e) DSI-1, (f) DSI-2, (g) RSI-1, and (h) RSI-2

In general, the liquid water contained in snowpacks at all three enterprises is available in surplus for potential agricultural reservation and rational use during the dry season. Moreover, the retained water could flood nearby communities and damage their infrastructures during a sudden spring thaw.

3.4. Discussions

The above results indicate that snow depths can be more accurately estimated using spectral snow indices from SCF maps than from previously proposed SCFs and snow depth estimation techniques. As mentioned, the SCF can be calculated either directly or indirectly. Barton et al. (2000), Lin et al. (2012), Salomonson & Appel (2004) proposed different regression functions based on NDSI. However, as direct methods are more accurate than indirect methods, we here compared the performances of four snow indices (NDSI, NDSII, DSI, and RSI) using two variables representing the reflectivities of an entirely snow-covered surface and a bare soil surface. In the NoSREx of Lemmetyinen et al. (2016), the snow depth, snow density, and SWE NoSREx were automatically measured in real-time using a gamma water instrument at intensively observed points, but this work only characterized the snow cover at one or a few points. Although the study

delivered the highest accuracy, its spatiality was very low. Furthermore, spatial interpolation will decrease the overall accuracy of the snow cover characteristics measured by NoSREx. Gan et al. (2021) compared two passive microwave-obtained snow depths with SWE retrievals, but only achieved high accuracy for snow depths below 20 cm. Our present method increases this limit to 27 cm. Analogous work was performed by Jenssen & Jacobsen (2021) in Norway. They measured the snow depth, snow density, and SWE using a UAV-mounted ultra-wide-band (0.7–4.5 GHz) radar. They found that pseudo-noise radar can measure the snow depth up to 5.5 m with high precision ($R > 0.92$). However, this method requires constantly repeated flights, which consumes time and resources; moreover, UAV flights are limited to smaller areas than those of our study ($>10,000$ ha). Regarding the work of Dixit et al. (2019), a comparative analysis of NDSI, NDSII, and S3 performance in assessing the snow cover in India was carried out, and the SWI index was proposed. Since SWI prevents the snow-water mixing and S3 averts the snow-vegetation mixing, they were excluded in the current study since this problem is not relevant in the steppe zone. Nevertheless, if the results of the snow cover assessment using NDSI and NDSII by Indian colleagues showed high accuracy, in our case, we observed an overestimation of these indices compared to DSI and RIS. Thus, according to the averaged Snow Cover Fraction data, NDSI classified 93% of the study area as snow-covered, and NDSII classified 92%. In comparison, DSI and RIS labeled only 86% and 89% of the area, respectively. Considering that DSI-2 showed the highest accuracy in snow depth estimation, we believe that NDSI and NDSII are less effective in assessing snow cover in Northern Kazakhstan. The approach we propose to use DSI-2 for snow cover depth estimation and further calculating the SWE can be used over a vast territory, with optimal temporal resolution (revisit time of Sentinel-2 is five days) and without field snow surveys.

Considering the advantages and limitations of estimating snow depths and SWE, we expect that our approach will be helpful for sustainable water management, the reservation and rational use of meltwater in agriculture during the dry season, and as an early warning system for spring floods.

3.5. Conclusions

All spectral indices except the RIS classified snow-covered territories with satisfactory performance. The NDSI and NDSII obtained the same results and did not distinguish between snow and crust. Both difference snow indices performed very well and clarified the completely snow-covered contours (untouched agricultural fields), snow-free areas (settlements, hills), and partially snow-covered areas (agricultural fields after snow retention) in the territory.

The SCF maps generated from NDSI and NDSII classified the highest proportion of the study area as snow-covered, whereas the maps generated from DSI-1 and DSI-2 identified the smallest share of snow-covered land. The SCF generated from DSI most accurately classified non-snow areas into forest plantations, settlements, and strongly blown uplands.

The RMSE between the simulated and surveyed snow depths decreased as the soil zone changed from chernozem to dark-chestnut. The snow depth maps generated from DSI-2 showed clear patterns of objects in all three study areas, and fields in which snow retention had been recently applied were easily identified as partially visible snow–soil mixtures. At the “North

Kazakhstan Agricultural Experimental Station”, the A.I. Barayev “Research and Production Center for Grain Farming”, and “Naidorovskoe” areas, the RMSE varied from 5.62 (DSI-2) to 6.85 (NDSII-2), from 3.46 (DSI-2) to 4.86 (RSI-1), and from 2.86 (DSI-2) to 3.53 (NDSII-1), respectively, with DSI-2 yielding the highest correlation coefficients between the modeled and ground-truth data (0.78, 0.69, and 0.80, respectively).

The average snow density was 300 kg/m^3 at “North Kazakhstan Agricultural Experimental Station” and A.I. Barayev “Research and Production Center for Grain Farming” and 220 kg/m^3 at “Naidorovskoe”. The SWE maps generated from all indices except DSI-2 underestimated the amount of water in a snowpack. In general, the snowpacks in the study area contain surplus water that can be harnessed for reservation and rational use in agriculture during the dry season. Utilizing this water could also prevent flooding and damage to nearby communities during a sudden spring thaw.

The current study was limited to three agricultural enterprises in the North Kazakhstan, Aqmola, and Qaragandy regions and did not attempt a thorough investigation of all snow-covered regions in Kazakhstan. Further work will include a relief analysis and a methodology for choosing the best places for reserving melt and flood water in the northern regions of the Republic of Kazakhstan.

3.6. Appendix A

This appendix contains figures for the other two agricultural enterprises.

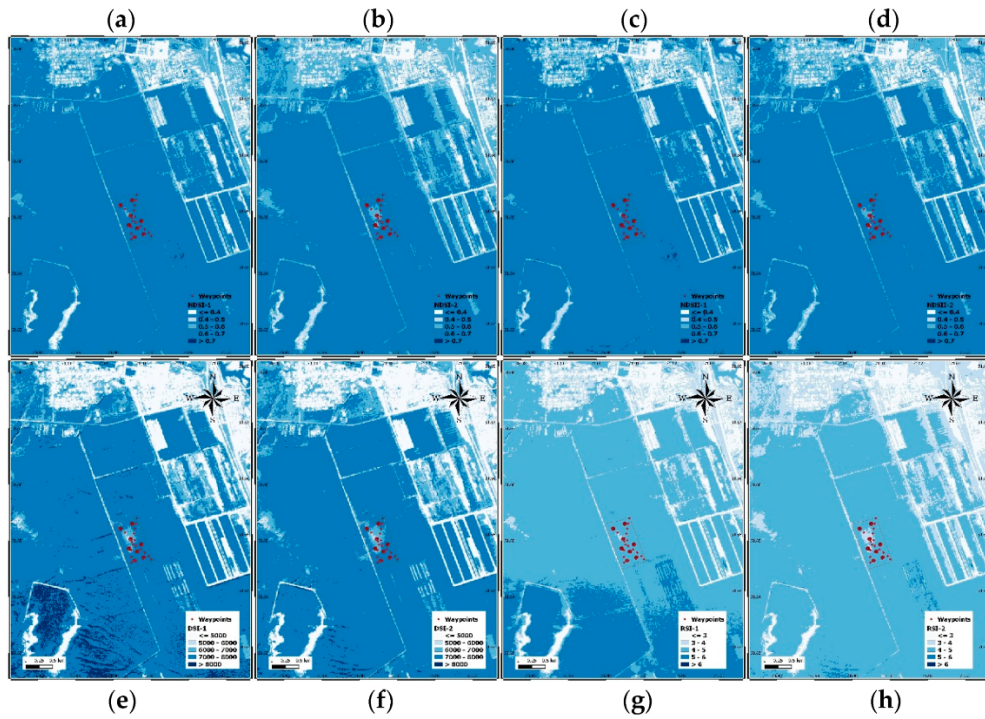


Figure A1. Spectral snow indices at A.I. Barayev "Research and Production Center for Grain Farming": (a) normalized-difference snow index [NDSI]-1, (b) NDSI-2, (c) normalized-difference snow and ice index [NDSII]-1, (d) NDSII-2, (e) difference snow index [DSI]-1, (f) DSI-2, (g) ratio snow index [RSI]-1, and (h) RSI-2.

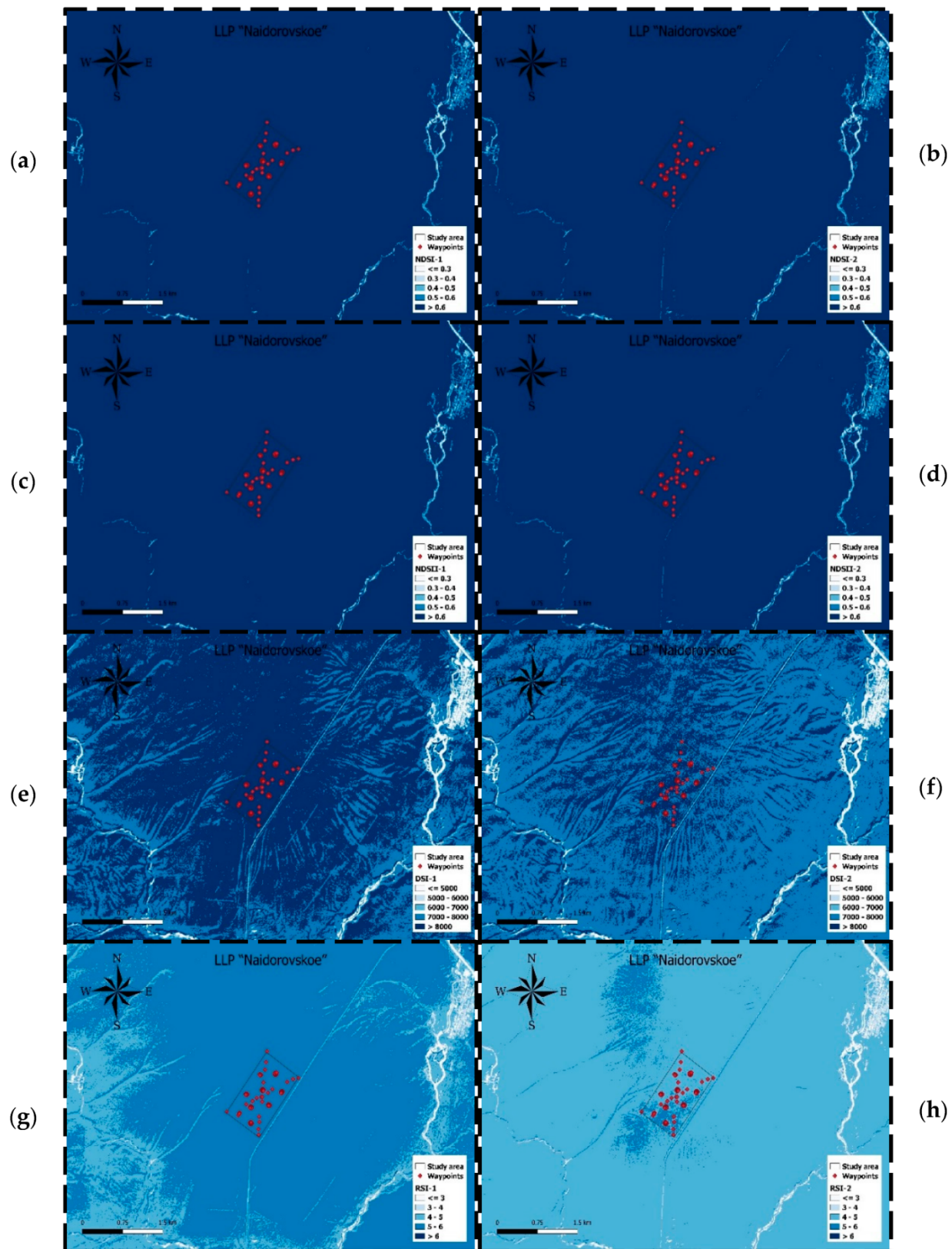


Figure A2. Spectral snow indices at "Naidorovskoe": (a) NDSI-1, (b) NDSI-2, (c) NDSII-1, (d) NDSII-2, (e) DSI-1, (f) DSI-2, (g) RSI-1, and (h) RSI-2.

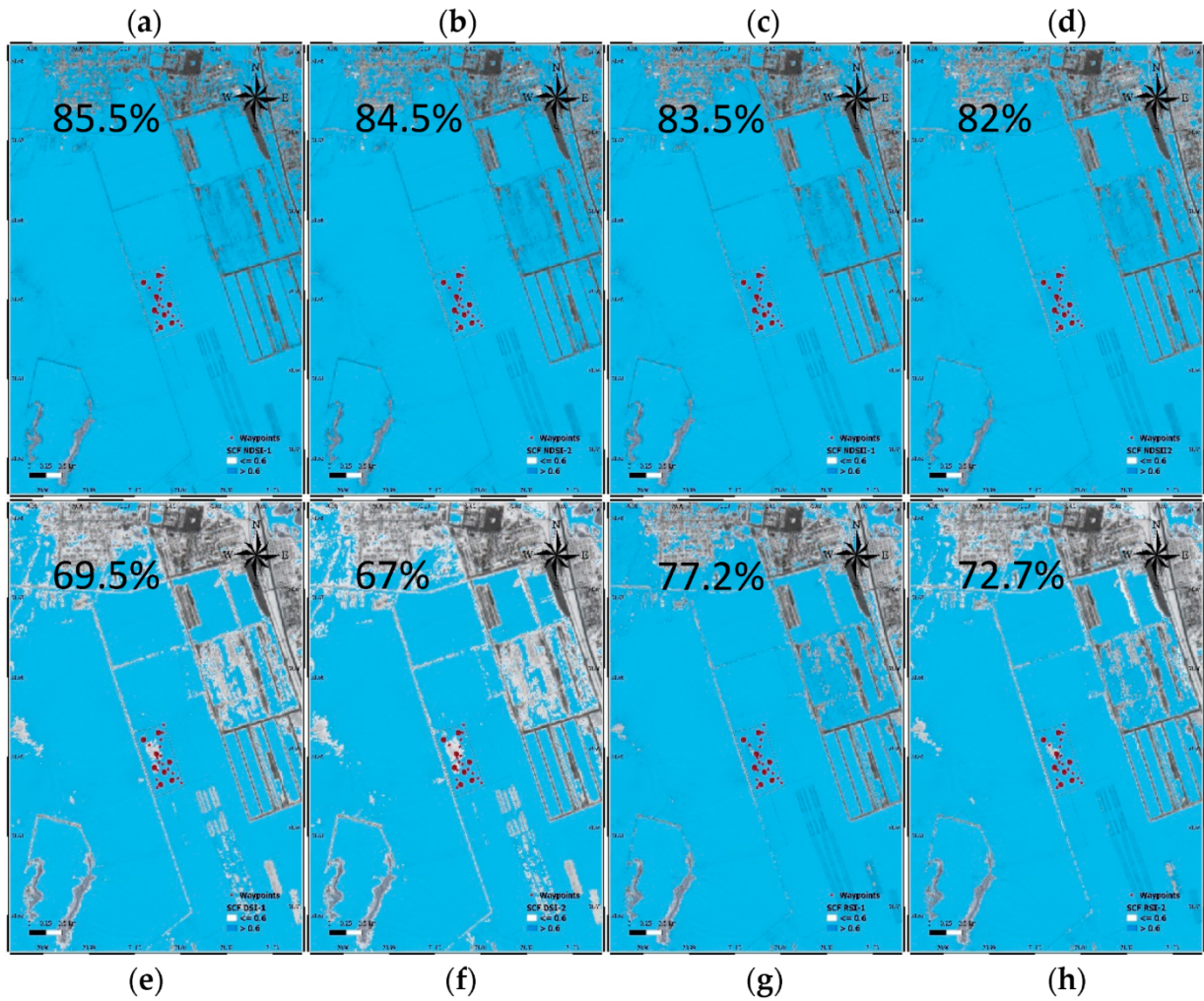


Figure A3. Snow cover fraction (SCF) maps at A.I. Barayev “Research and Production Center for Grain Farming” generated from (a) NDSI-1, (b) NDSI-2, (c) NDSII-1, (d) NDSII-2, (e) DSI-1, (f) DSI-2, (g) RSI-1, and (h) RSI-2.

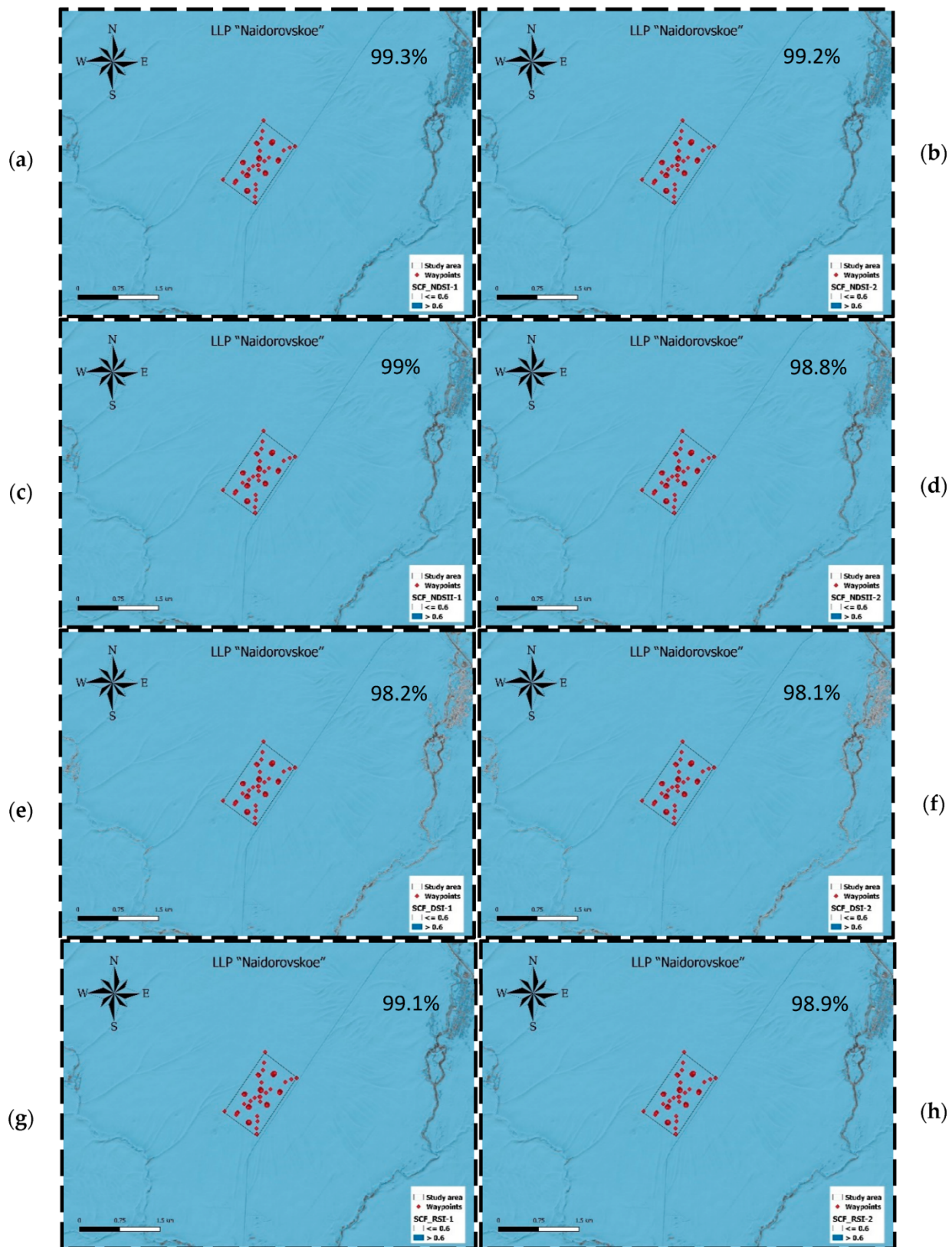


Figure A4. SCF maps at "Naidorovskoe" generated from (a) NDSI-1, (b) NDSI-2, (c) NDSII-1, (d) NDSII-2, (e) DSI-1, (f) DSI-2, (g) RSI-1, and (h) RSI-2.

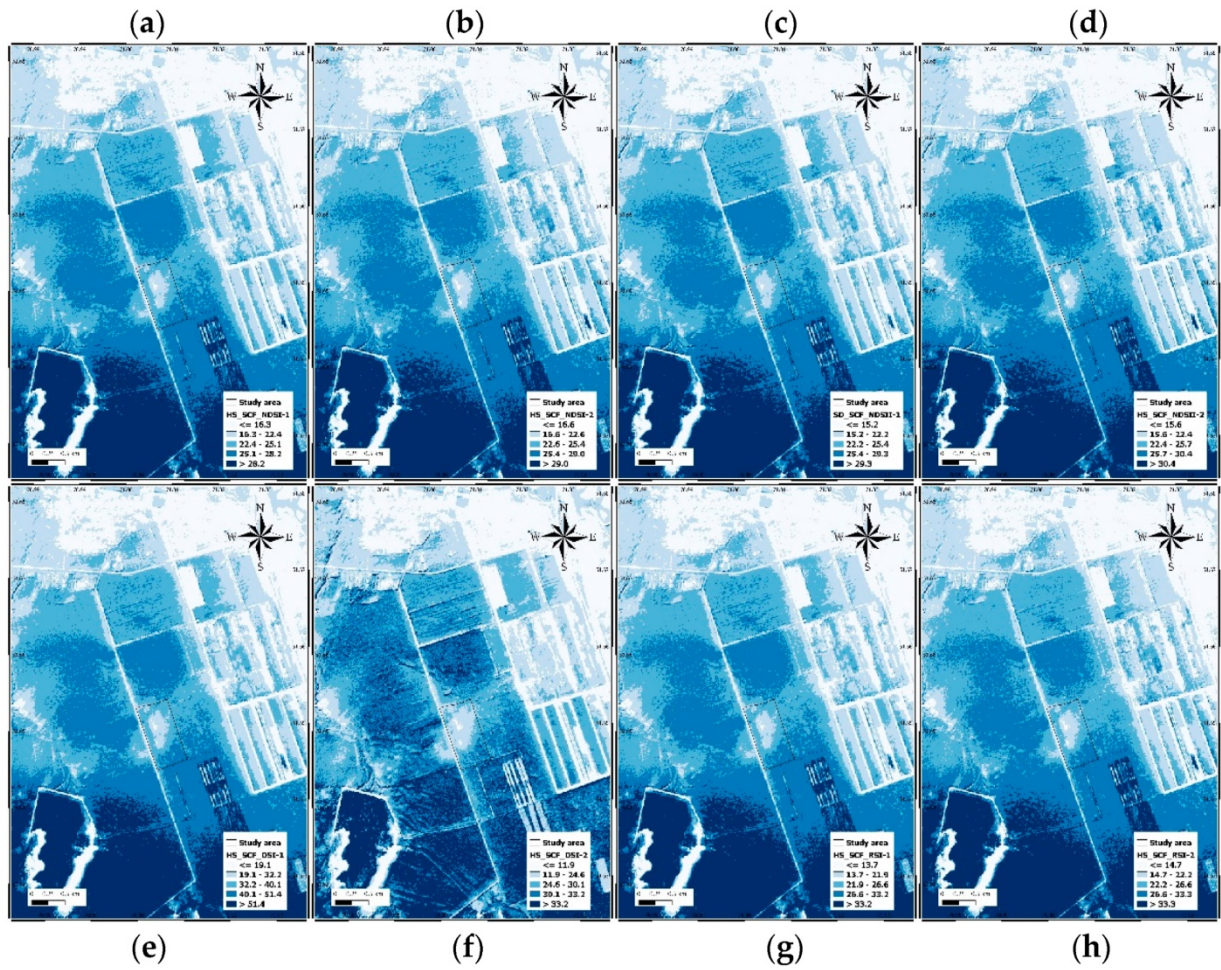


Figure A5. Snow depth maps at A.I. Barayev "Research and Production Center for Grain Farming" generated from the SCFs of (a) NDSI-1, (b) NDSI-2, (c) NDSII-1, (d) NDSII-2, (e) DSI-1, (f) DSI-2, (g) RSI-1, and (h) RSI-2.

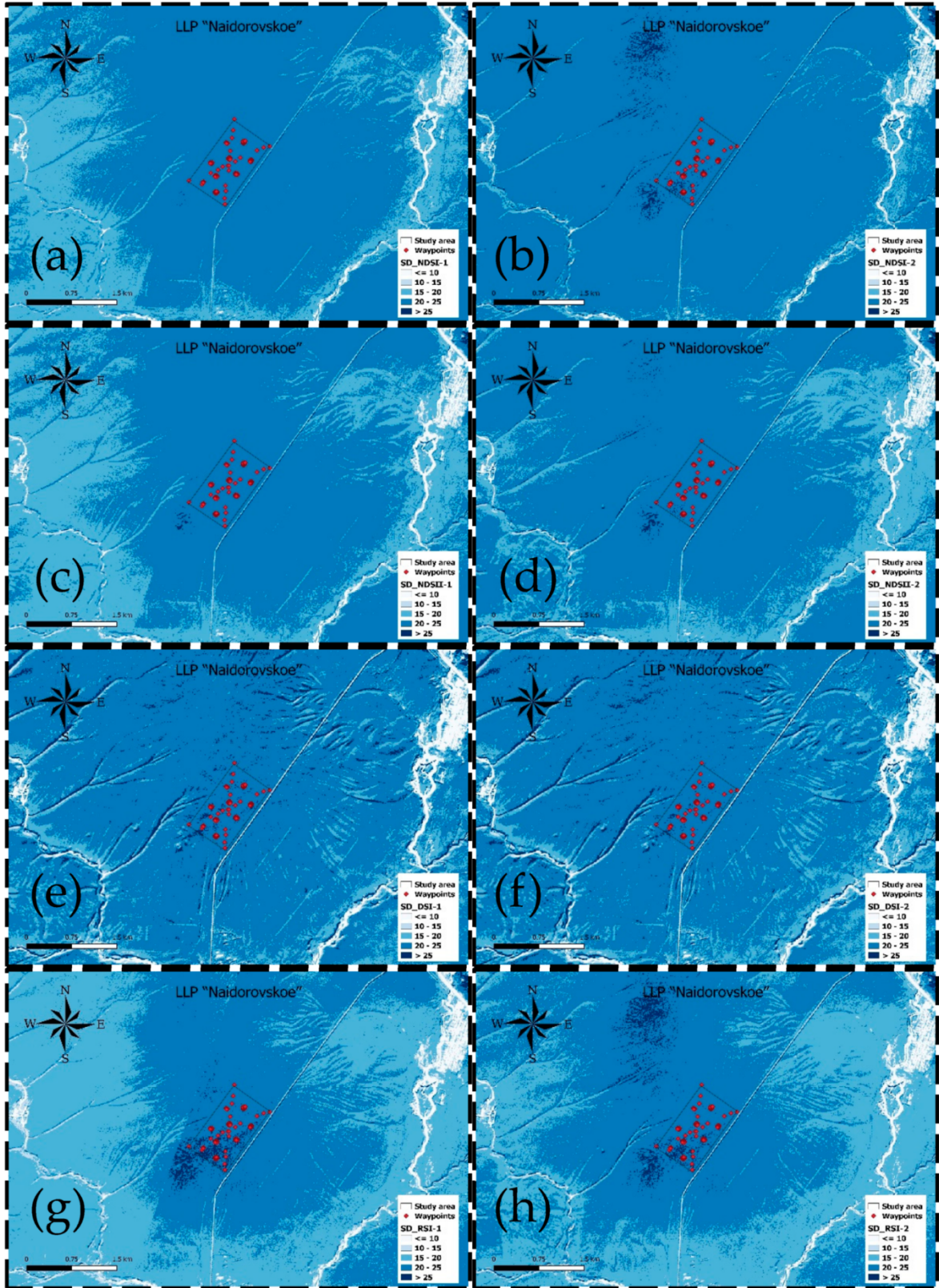


Figure A6. Snow depth maps at “Naidorovskoe” generated from the SCFs of (a) NDSI-1, (b) NDSI-2, (c) NDSII-1, (d) NDSII-2, (e) DSI-1, (f) DSI-2, (g) RSI-1, and (h) RSI-2.

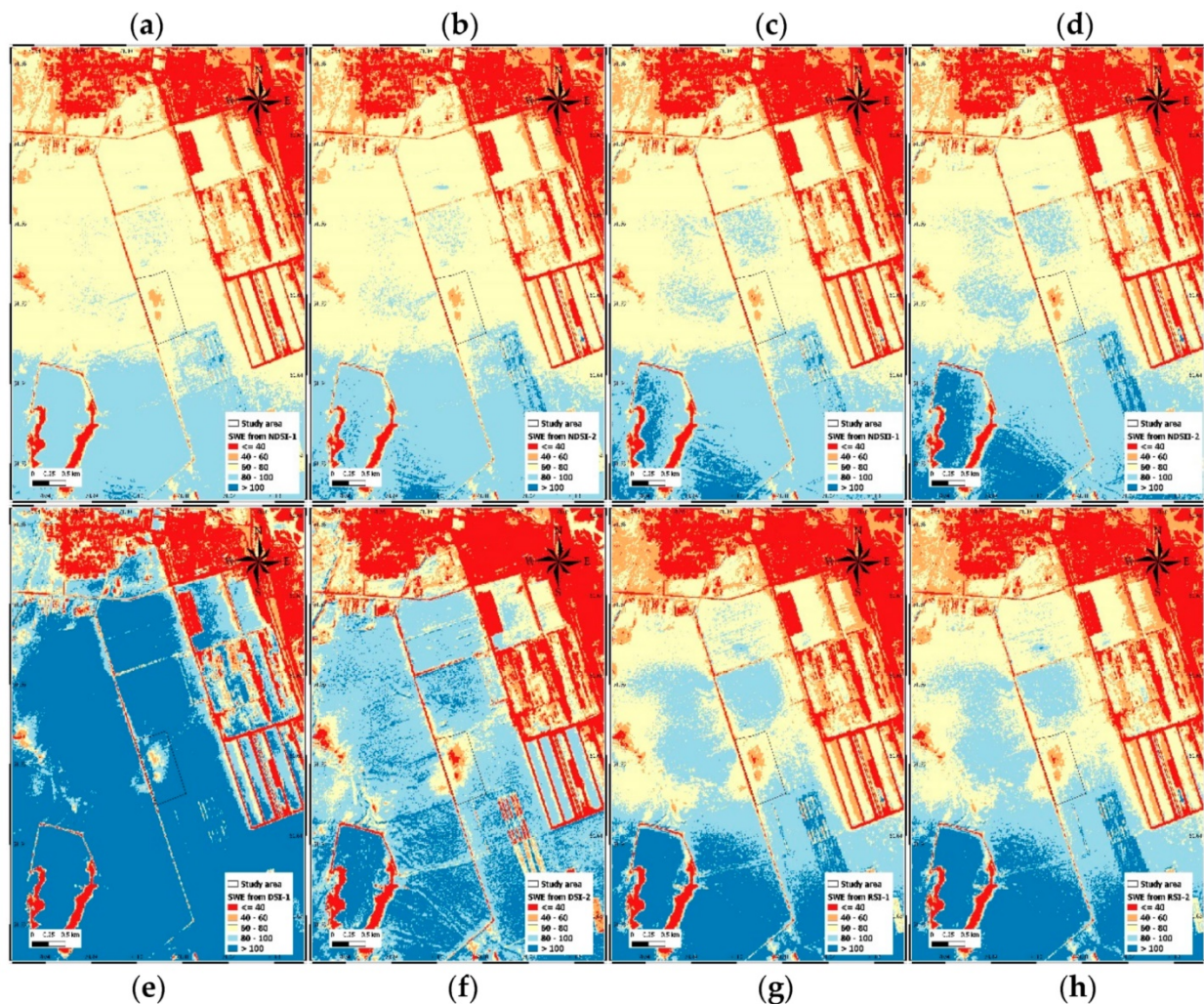


Figure A7. Snow water equivalent maps at A.I. Barayev “Research and Production Center for Grain Farming” generated from the SDs of (a) NDSI-1, (b) NDSI-2, (c) NDSII-1, (d) NDSII-2, (e) DSI-1, (f) DSI-2, (g) RSI-1, and (h) RSI-2.

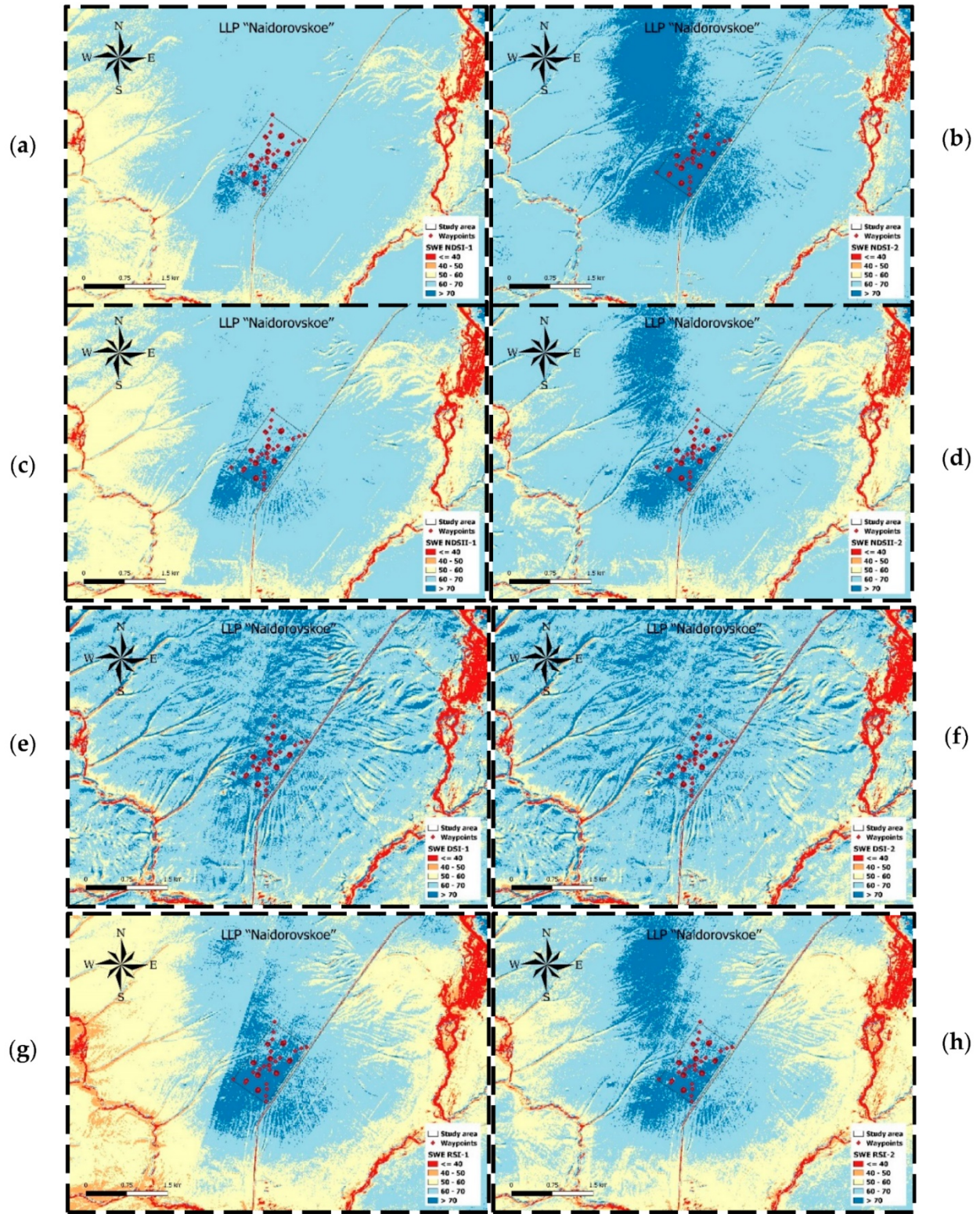


Figure A8. Snow water equivalent maps at "Naidorovskoe" generated from the SDs of (a) NDSI-1, (b) NDSI-2, (c) NDSII-1, (d) NDSII-2, (e) DSI-1, (f) DSI-2, (g) RSI-1, and (h) RSI-2

4. Identification of Potential Farm Pond Sites for Spring Surface Runoff Harvesting Using an Integrated Analytical Hierarchy Process in a GIS Environment in Northern Kazakhstan

This article is published in Water journal as: **Zhanassyl Teleubay**, Farabi Yermekov, Ismail Tokbergenov, Zhanat Toleubekova, Aigerim Assylkhanova, Nurlan Balgabayev and Zoltan Kovacs. 2022



Identification of Potential Farm Pond Sites for Spring Surface Runoff Harvesting Using an Integrated Analytical Hierarchy Process in a GIS Environment in Northern Kazakhstan

Water Volume 15, June 2023, 2258

<https://doi.org/10.3390/w15122258>




Journal CiteScore (Scopus): 6.0

Author Contributions: Z.T. (Zhanassyl Teleubay) analyzed the data and drafted the manuscript; F.Y., I.T., Z.T. (Zhanat Toleubekova) and N.B. completed the manuscript and made major revisions; A.A. searched for references; Z.K. revised and proofread the manuscript.



Article

Identification of Potential Farm Pond Sites for Spring Surface Runoff Harvesting Using an Integrated Analytical Hierarchy Process in a GIS Environment in Northern Kazakhstan

Zhanassyl Teleubay ^{1,2,*} , Farabi Yermekov ¹, Ismail Tokbergenov ¹ , Zhanat Toleubekova ¹, Aigerim Assylkhanova ², Nurlan Balgabayev ³ and Zoltán Kovács ^{2,4} 

¹ Center for Technological Competence in the Field of Digitalization of the Agro-Industrial Complex, S.Seifullin Kazakh AgroTechnical Research University, Astana 010000, Kazakhstan; f.yermekov@gmail.com (F.Y.); titssp@mail.ru (I.T.); zh.toleubekova@kazatu.kz (Z.T.)


² Department of Economic and Social Geography, University of Szeged, 6720 Szeged, Hungary; aigerim.assylkhanova@gmail.com (A.A.); zkovacs@iif.hu (Z.K.)

³ Kazakh Research Institute of Water Management, Taraz 080000, Kazakhstan; nurlan.balgabayev1958@gmail.com

⁴ Research Centre for Astronomy and Earth Sciences, Geographical Institute, 1112 Budapest, Hungary

* Correspondence: zhanassyl.kz@gmail.com; Tel.: +7-(775)-860-06-80

Abstract: People living in arid and semi-arid areas with highly variable rainfall often face droughts and floods that affect water availability. Surface runoff harvesting is a historical water delivery system utilized in times of water scarcity to fulfill the ever-increasing demand for water, address climate change, and prevent desertification. However, the study of snowmelt and flood water harvesting in steppe areas with cold and semi-arid climates are understudied in the international literature. This paper, combining remote sensing (RS) and a geographic information systems (GIS)-based analytical hierarchy process (AHP), provides a cost-efficient and reliable tool for assessing potential farm pond sites in the steppe region of Northern Kazakhstan. The research is based on six weighted thematic layers: hydrogeology (5%), slope (10%), drainage density (25.5%), land use/land cover (25.5%), soil (5%), and snow water equivalent (29%), which mainly influence the availability, runoff, infiltration, and accumulation of snowmelt and flood water, in order to identify potential farm pond sites in the Akkayin district (North Kazakhstan). As a result, 3.3% of the study area had a very high potential, 35.5% high, 56.5% medium, 4.6% low, and only 0.1% was recognized as the least preferred. The most suitable sites had medium drainage density, low slope, high snow water equivalent, and were located on flooded vegetation. The accuracy of our model was assessed using the existing farm pond sites from the Soviet era, which showed 82% coincidence. Furthermore, by collecting meltwater from 30% of the study area (135,000 ha), one-fourth of the cultivated land in the Akkayin district (i.e., 54,000 ha)

**check for updates**

Citation: Teleubay, Z.; Yermekov, F.; Tokbergenov, I.; Toleubekova, Z.; Assylkhanova, A.; Balgabayev, N.; Kovács, Z. Identification of Potential Farm Pond Sites for Spring Surface Runoff Harvesting Using an Integrated Analytical Hierarchy Process in a GIS Environment in

Abstract: People living in arid and semi-arid areas with highly variable rainfall often face droughts and floods that affect water availability. Surface runoff harvesting is a historical water delivery system utilized in times of water scarcity to fulfill the ever-increasing demand for water, address climate change, and prevent desertification. However, the study of snowmelt and flood water harvesting in steppe areas with cold and semi-arid climates are understudied in the international literature. This paper, combining remote sensing (RS) and a geographic information systems (GIS)-based analytical hierarchy process (AHP), provides a cost-efficient and reliable tool for assessing potential farm pond sites in the steppe region of Northern Kazakhstan. The research is based on six weighted thematic layers: hydrogeology (5%), slope (10%), drainage density (25.5%), land use/land cover (25.5%), soil (5%), and snow water equivalent (29%), which mainly influence the availability, runoff, infiltration, and accumulation of snowmelt and flood water, in order to identify potential farm pond sites in the Akkayin district (North Kazakhstan). As a result, 3.3% of the study area had a very high potential, 35.5% high, 56.5% medium, 4.6% low, and only 0.1% was recognized as the least preferred. The most suitable sites had medium drainage density, low slope, high snow water equivalent, and were located on flooded vegetation. The accuracy of our model was assessed using the existing farm pond sites from the Soviet era, which showed 82% coincidence. Furthermore, by collecting meltwater from 30% of the study area (135,000 ha), one-fourth of the cultivated land in the Akkayin district (i.e., 54,000 ha) could be transferred to deficit irrigation. This would reduce floods, stabilize farmers' income in dry years, and open up the possibility of cultivating other highly profitable crops. Overall, the study provides evidence of the great potential of the Akkayin district in snow meltwater harvesting in farm ponds as a response to agricultural drought and spring floods.

Keywords: snow meltwater harvesting; irrigation; climate resilience; multi-criteria decision analysis

4.1. Introduction

Owing to intensifying climate change and shifting seasons, the northern grain-growing regions of the Republic of Kazakhstan suffer from regular droughts in the warm season and floods in the spring (Dubovyk et al., 2019; Patrick, 2017). According to the agricultural drought-monitoring data of the CACILM-2 project of the FAO UN, in the period from 2001 to 2022, Akkaiyn district was not affected by droughts only for 8 years, which mainly occurred at the beginning of the millennium (2001–2007), and after 2016, the severity of drought increased on an annual basis (with the exception of 2018). Owing to the absence of major rivers in the North Kazakhstan Region, most agricultural production focuses on rain-fed crops (i.e., crops without irrigation); drought is a major threat to crop failure (Suleimenov et al., 2012). There are three major crop types cultivated in the study area: cereals (wheat, barley, and oat), legumes (lentils, clover, alfalfa, and peas), and oilseeds (safflower, sunflower, rapeseed, and flax). The sowing campaign typically begins in mid-May and ends in October. According to a United Nations Development Programme report (Strategic Measures to Combat Desertification in the Republic of Kazakhstan Until 2025), drought is causing Kazakhstan to lose around 200 million euros annually

(Zhumabayev, 2023). At the same time, there is heavy precipitation in the solid form (snow) during the winter, which is accompanied by excess liquid precipitation in spring, resulting in devastating floods (Ongdas et al., 2020). Hence, a record high water over the past half a century was recorded in 2017, which forced 4000 people to leave their homes and 15 flooded settlements (Berezhnaya, 2020). In this regard, collecting snow melt and flood water in farm ponds could solve the abovementioned challenges caused by regular droughts and floods in the region (Al-Abadi et al., 2014; Rahman, 2017). This was practiced during Soviet times in the 1970s and 1980s, when thousands of farm ponds were created, most of which were for agricultural purposes. However, after the collapse of the Soviet Union in 1991, many farm ponds were abandoned, which led to an increase in the salinity of stagnant water. It must be noted that, when planning these ponds, the factors of climate change and increased spring floods were not taken into account. Thus, they were not aimed at solving flood problems in the region.

Spring surface runoff harvesting in farm ponds is “the management and collection of surface runoff to increase the availability of water for agriculture and domestic needs and to maintain the ecosystem” (Mekdaschi Studer & Liniger, 2013). This is a historical water delivery system utilized in times of water scarcity to fulfill the ever-increasing demand for water, combat climate change and unpredictability, and prevent desertification. Spring surface runoff harvesting in farm ponds prevents erosion and flooding, and reduces water pollution at the same time (Alwan et al., 2020). This method has several advantages, such as regulating surface runoff during the spring flood season, providing water for irrigation, and mitigating water shortages during droughts using excess water. People living in arid and semi-arid areas with highly variable rainfall often face droughts or floods that affect water availability. The success of the spring surface runoff harvesting technique principally depends on the selection of a suitable location. Combining remote sensing (RS) and a geographic information systems (GIS)-based analytical hierarchy process (AHP) would be a cost-effective and reliable tool to assess potential farm pond sites. RS technology can gather, process, and manage vast amounts of data, allowing researchers to effectively investigate, analyze, and manage water resources. The GIS-driven AHP method, being the most preferred multi-criteria decision analysis (MCDA) tool in engineering, allows us to find the degree of superiority of one alternative over another according to specified criteria (Ayan et al., 2023). Despite the novel MCDA methods, such as CILOS, SAPEVO-M, MEREC, etc., proposed in the last decade, it is important to remember that no single method is perfect or suitable for application in all decision-making circumstances (Guitouni & Martel, 1998). In this work, we have given preference to the traditional AHP method of the American School of Decision Support Systems (Karthikeyan et al., 2019). This was justified by the fact that the AHP incorporates such qualities as an effortlessly reasonable system, the ability to disentangle a troublesome issue by dividing it into smaller steps, and the unnecessary of authentic information sets. Furthermore, recent works on the identification of potential surface runoff (rainwater) harvesting using the AHP method proved the effectiveness of this approach, with an accuracy of 70 to 92% (Alwan et al., 2020; Balkhair & Ur Rahman, 2021; Chowdhury & Paul, 2021; Sayl et al., 2020; Wu et al., 2018). Table 4.1 provides a quick summary of recent studies on potential rainwater harvesting

using MCDA methods. Nevertheless, the AHP model has a disadvantage in the limited number of pairwise comparisons. If the model contains a large number of criteria as well as alternatives, the decision-making process can take a long time, and over time, matrix inconsistencies can begin to increase due to loss of attention and lack of concentration on the subject. In our case, this problem was not material. Previously, several researchers utilized the above-mentioned approach with different parameters to assess groundwater potential (Aouragh et al., 2015; Arulbalaji et al., 2019; Berhanu & Hatiye, 2020; Doke et al., 2021; Lentswe & Molwalefhe, 2020; Melese & Belay, 2022; Murmu et al., 2019; Şener et al., 2018; Subbarayan et al., 2020; Upwanshi et al., 2023), land suitability for solar farms (Elboshy et al., 2022; Mehdaoui et al., 2022; Noorollahi et al., 2016; Sindhu et al., 2017; Uyan, 2013), urban flood vulnerability (Gigović et al., 2017; Ouma & Tateishi, 2014; Vojtek & Vojteková, 2019), dam site selection along rivers (Esavi et al., 2012; Jozaghi et al., 2018; Yasser et al., 2013), and rainwater harvesting (Alwan et al., 2020; Balkhair & Ur Rahman, 2021; Chou et al., 2014; Chowdhury & Paul, 2021; Kadam et al., 2012; Maina & Raude, 2016; Sayl et al., 2020; Wu et al., 2018). However, there is an immense gap in the study of spring melt and flood water harvesting in snowy, steppe areas with cold and semi-arid climates, as most similar works were carried out in tropical or desert areas, with no winter (Guatemala, Saudi Arabia, Taiwan, Iraq, India, Kenya, etc.) (Alwan et al., 2020; Balkhair & Ur Rahman, 2021; Chou et al., 2014; Chowdhury & Paul, 2021; Kadam et al., 2012; Maina & Raude, 2016; Sayl et al., 2020; Wu et al., 2018). This is reflected in the input parameters and criteria chosen by the authors for the AHP model. For instance, Maina and Raude (Maina & Raude, 2016) used rainfall, slope, soil, land use/land cover, and distance from settlements and roads, Wu et al. (2018) used the same parameters, but replaced rainfall with runoff, and Kadam et al. (2012) included catchment size in this list. In general, about 75% of the list of parameters remained unchanged. It should also be noted that none of the previous works considered the snow cover factor, as this was not possible for their study areas.

Table 4.1. A quick summary of recent studies on identification of potential rainwater harvesting sites

Reference	Year	Country	Applied method
Kadam et al.	2012	India	Self-weighting
Chou et al.	2014	Taiwan	Analytical Hierarchy Process
Maina and Raude	2016	Kenya	Self-weighting
Wu et al.	2018	Guatemala	Analytical Hierarchy Process
Alwan et al.	2020	Iraq	Analytical Hierarchy Process
Sayl et al.	2020	Iraq	Analytical Hierarchy Process
Balkhair and Ur Rahman	2021	Saudi Arabia	Analytical Hierarchy Process

Reference	Year	Country	Applied method
Chowdhury and Paul	2021	India	Analytical Hierarchy Process

In contrast, in our research in the northern part of the Republic of Kazakhstan, snow cover is the most influential input parameter, as we assess the possibility of reserving snow meltwater in farm ponds for further agricultural use. This approach contributes to increasing water productivity in agriculture, which is very critical for arid and semi-arid areas. Water in farm ponds can be used for deficit irrigation; thus, farmers will not focus on achieving the maximum yield during dry periods, but will increase their economic benefits and income stability (English, 1990). Nevertheless, experiments with deficit irrigation in Turkey that lasted for four years found that the wheat yield increased by 65% and the water productivity doubled compared with rainfed agriculture (Ilbeyi et al., 2006). This fact has also been confirmed by studies in China (Kang et al., 2002; Zhang et al., 2004), Syria (Zhang & Oweis, 1999), and Bangladesh (Ali et al., 2007).

Although there are many approaches to identifying potential rainwater harvesting sites worldwide using AHP methods, there is a great need for more advanced, new approaches adapted to cold, semi-arid, and steppe conditions. Thus, the main objective of this study is to evaluate the potential of the Akkayin district in snow meltwater harvesting in farm ponds for agricultural needs as a response to agricultural drought and spring floods. To achieve this, within the framework of this study, we set the goals to (1) develop an approach that can assess farm pond sites for snow meltwater harvesting in the cold, semi-arid steppe zone with high accuracy (>80%), (2) identify limiting factors, and (3) exclude field studies in the future that require a lot of time and resources. During the research, six parameters were considered to assess the potential zones of farm ponds: hydrogeology, slope, drainage density, land use/land cover, soil, and snow water equivalent, which mainly influence the availability, runoff, infiltration, and accumulation of snow melt and flood water in the Akkayin district, North Kazakhstan region. The use of these particular input parameters is based both on the existing literature and the opinion of three experts (two academic: Zhanat Toleubekova and Nurlan Balgabayev, and one industrial: Askar Abirov). It should also be noted that the snow water equivalent map was compiled based on the methodology developed by the authors earlier (Teleubay et al., 2022). After assigning the weights to each factor using the AHP method, a map showing potential areas with low, medium, high, and very high snowmelt and floodwater storage potential for agriculture was prepared. Actual data from existing farm ponds in the study area were collected to assess the accuracy of the final result. The outcomes of the study can provide a basis for early warning of floods, mitigation of agricultural drought, and, most importantly, socio-economic advancement in the region. Moreover, under the CC BY license, field snow survey data have been published for independent testing and comparative research by the international research community, and a freely accessible geoportal containing all research results has been created (see Data Accessibility Statement).

This work is organized as follows: (1) the materials and methods for selecting suitable sites for meltwater collection are thoroughly explained, (2) technical, economic, and environmental

limiting factors are identified, (3) the results of the GIS-driven AHP implementation are discussed, and (4) conclusions and recommendations for future research are provided.

4.2. Materials and Methods

4.2.1. Study Area

The study area (see Figure 4.1) is one of the largest grain-sowing regions of Kazakhstan, the Akkayin district, which is located in the North Kazakhstan region. The area experiences a sharply continental climate characterized by a large amplitude of annual temperatures and dryness. Most of the region is located on the West Siberian lowland. The main feature of the relief is characterized by many closed basins with groups of lakes and single lakes. The distribution of precipitation over the years has been highly uneven. The average annual rainfall is typically between 225 and 335 mm. However, there have been years when the total annual precipitation rose above 600 mm or dropped to 204 mm. The coldest month is January, with an average mean temperature of -18.5 – -18.7 °C. The hottest month is July, when the average mean temperature is $+18.5$ – $+18.7$ °C. The average precipitation in winter varies between 22 and 42 mm. The snow cover in the area is unevenly distributed due to strong winds blowing away snow in open areas. During the summer, dry winds cause the soil to dry out quickly. The soils in the region are zonally distributed, so that ordinary loamy chernozems occur in the northern part, and to the south, they turn into southern chernozems with a lighter composition.

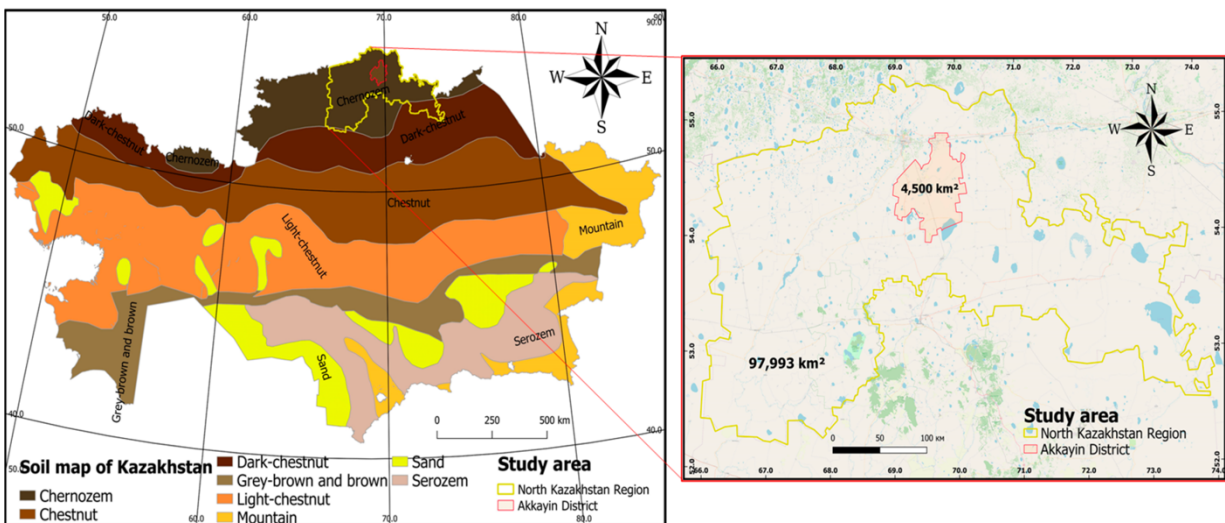


Figure 4.1. Study area and the soil map of the Republic of Kazakhstan

4.2.2. Data Sources

4.2.2.1. In Situ Surveying

A field snow survey in key areas was carried out on two dates, in the middle (from 25 to 27 January 2023) and at the end (from 25 to 27 February 2023) of the winter season (Figure

4.2). In total, the depth of the snow cover was measured at 312 points, and the density at 65 points in the Akkayin district, North Kazakhstan region (see Table 4.2).

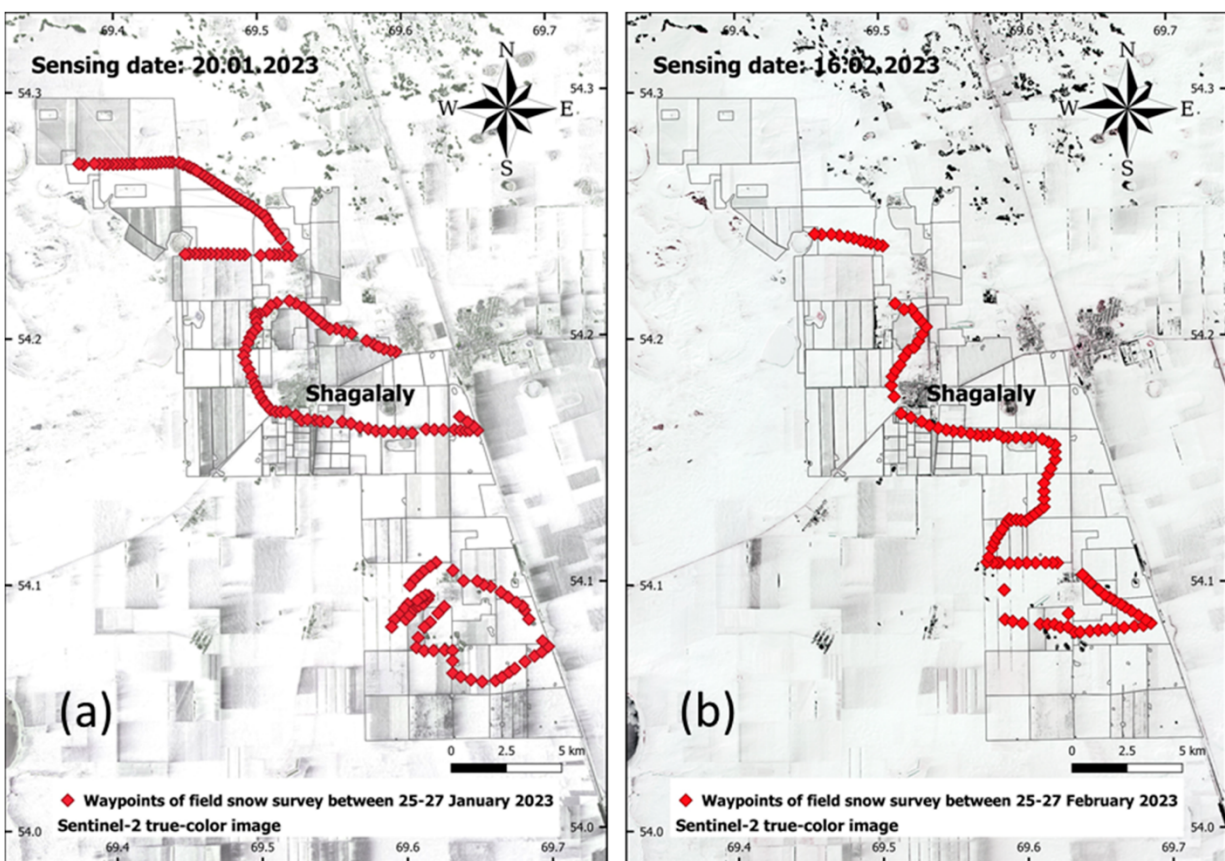


Figure 4.2. Waypoints of snow survey over the territory of Akkayin district, North Kazakhstan Region (a) between 25 and 27 January 2023 and (b) between 25 and 27 February 2023

Table 4.2. Snow survey dates and number of measured points in the study area

Snow Survey Dates and Number of Points	25–27 January 2023		25–27 February 2023	
	Depth	Density	Depth	Density
Territory of Akkayin District	197	39	115	26

A wooden snow gauge M-103 II (LLP “Seaguard-Group”, Almaty, Kazakhstan) with a division of 1 mm was used to measure the snow cover depth, and for snow density, a snow weight gauge VS-43M (LLP “Seaguard-Group”, Almaty, Kazakhstan) was utilized. The following equation was used to calculate the actual snow density:

$$\rho = \frac{m}{SD \times S}$$

where ρ is the density of snow in g/cm³, m is the mass of snow in g, SD is the snow depth in cm, and S is the area of the snow weight gauge VS-43M in cm².

Owing to the difficulty of movement in the study area, most of which is occupied by snow-covered agricultural fields, an RM Vector 551i snowmobile (JSC “Russkaya mekhanika”, Ryabinsk, Russia) was used for fast movement (see Figure B1 of Appendix B). The accurate geopositioning of snow survey points was carried out using a Garmin Montana 610 system. All the gathered field snow survey data are available under the CC BY license in FigShare (see Data Availability Statement).

Moreover, a UAV survey was conducted between 16 and 21 August 2021 to build a detailed digital surface model (DSM) for further hydrological analysis. For this purpose, a fixed-wing UAV Supercam S350 (Unmanned Systems Group, Izhevsk, Russia) with a Sony A6000 (Sony Group Corporation, Minato, Japan) payload was used (see Figure B2 of Appendix B). The flight was carried out at a height of 1 km with a longitudinal overlap of 80% and a transverse overlap of 60%. Thus, 4368 images were received within six days, covering an area of around 45,000 ha. Ground control points (GCP) were not used due to the vastness of the territory during the UAV survey. Nevertheless, the post-processing of the central points of all images was performed using data from the onboard dual-frequency GPS and Stonex S900 and S10 base stations.

4.2.2.2. Thematic Layers and Digital Satellite Image Datasets

Six thematic layers (hydrogeology, slope, drainage density, land use/land cover, soil, and snow water equivalent) essentially controlling melt and flood water availability were prepared based on the expert’s opinion and the available literature. Hydrogeological maps on a scale of 1:200,000 compiled by the Kazakh Hydrological Department were digitized and used as input parameters. The slope and drainage density were mapped using a digital elevation model, while the land-use map was generated using high-resolution (10 m) satellite imagery (Sentinel-1 and Sentinel-2) and a knowledge-based classification method. The FAO-UNESCO Soil Map of the World database was used to prepare the soil map of the study area. Field snow survey data and Sentinel-2 MSI images with the nearest dates to the survey were utilized to prepare the most critical parameter, the snow water equivalent. The details of digital satellite image specification are provided in Table 4.3. Satellite images were downloaded from the Google Earth Engine (GEE) multi-petabyte catalog.

Table 4.3. Specifications of the Sentinel-2 multispectral instrument

Sensor	Acquisition Date	Cloud Cover	Spectral Band with Wavelet (μm)
Sentinel-2	20 January 2023, 42UWE	1.13%	Coastal aerosol (0.443)
			Blue (0.490)

Sensor	Acquisition Date	Cloud Cover	Spectral Band with Wavelet (μm)
	20 January 2023, 42UWF	11.99%	Green (0.560)
			Red (0.665)
	16 February 2023, 42UWE	0%	Vegetation red edge (0.705)
			Vegetation red edge (0.740)
	16 February 2023, 42UWF	0%	Vegetation red edge (0.783)
			Near-infrared (0.842)
			Vegetation red edge (0.865)
			SWIR-Cirrus (1.375)
			SWIR-1 (1.610)
			SWIR-2 (2.190)

4.2.3. Methodology

The potential zones for snowmelt and flood water reservations were determined by overlaying all thematic layers in a weighted linear combination method using the spatial analysis tool in ArcGIS Pro 2.8 software. The relative weights of thematic layers and subgroups were determined using the analytical hierarchy process method. The conceptual model of the proposed framework is shown in Figure 4.3. The weights were set considering the opinion of a team of experts, which included one industrial and two academic experts. In addition, to identify unsuitable zones, a vector layer of agricultural land in the Akkayin district with a buffer zone of 1 km was used to identify productive zones for reserving melt and flood waters for agriculture. We considered collecting and reserving meltwater at a distance of more than 1 km from agricultural land inefficient.

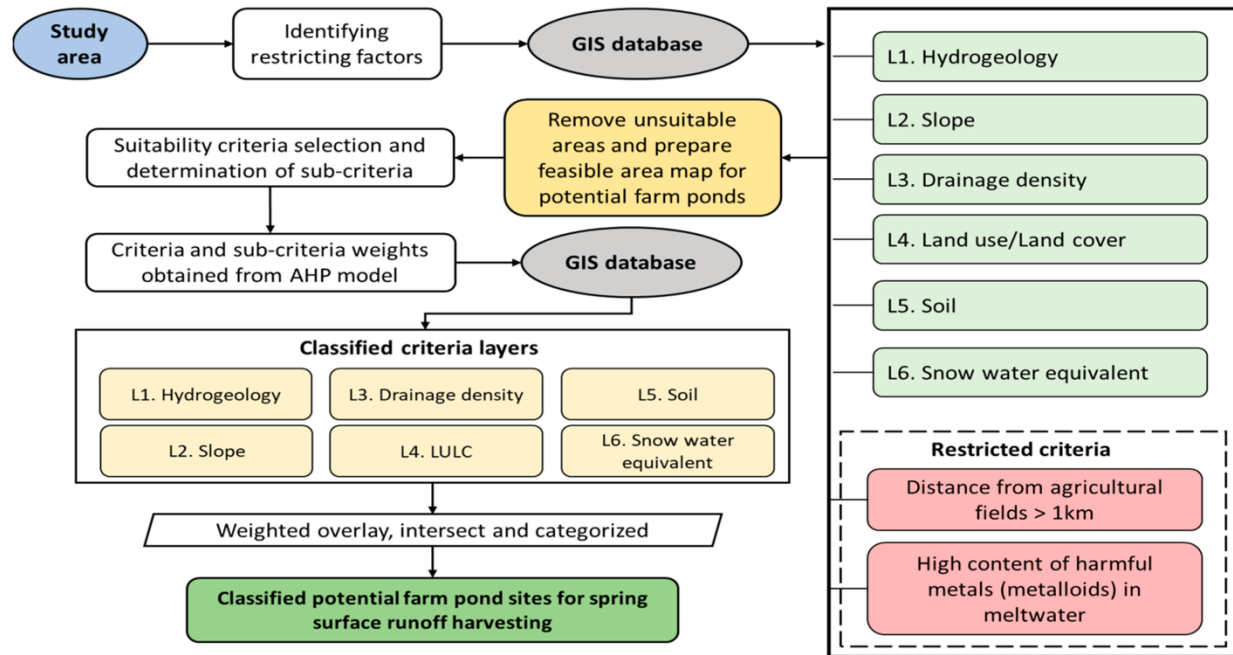


Figure 4.3. The conceptual framework of the research

4.2.3.1. Identification of Unsuitable Zones to Reserve Melt and Flood Water

At this stage of research, a feasibility study was carried out regarding the potential to reserve melt and flood water in the Akkayin district. During the designation of potential areas for reserving melt and flood water for agricultural use, it is necessary to consider some technical, economic, and environmental factors. From a technical point of view, it is not justifiable to reserve meltwater in remote places and extend miles of pipes to agricultural fields. From an economic point of view, agricultural enterprises would need to purchase a large number of necessary goods, such as pipes, and maintain them, which requires enormous financial and labor resources. From an environmental point of view, we excluded areas with a high content of harmful metals (metalloids) in water, such as manganese and arsenic, which is unacceptable for agricultural use. For this purpose, six meltwater samples were taken at key points to conduct chemical water analysis in May 2022. Detailed results of the chemical analysis of meltwater are provided in the test report (see Figure B3 of Appendix B). For example, the analysis recorded an excess of the maximum allowable norm of arsenic by three times (the norm is 0.05 mg/dm^3 , and the measured value was 0.16 mg/dm^3). In addition, to create a buffer zone of 1 km, the boundaries of agricultural land in the study area were digitized in the .shp format (Figure 4.4).

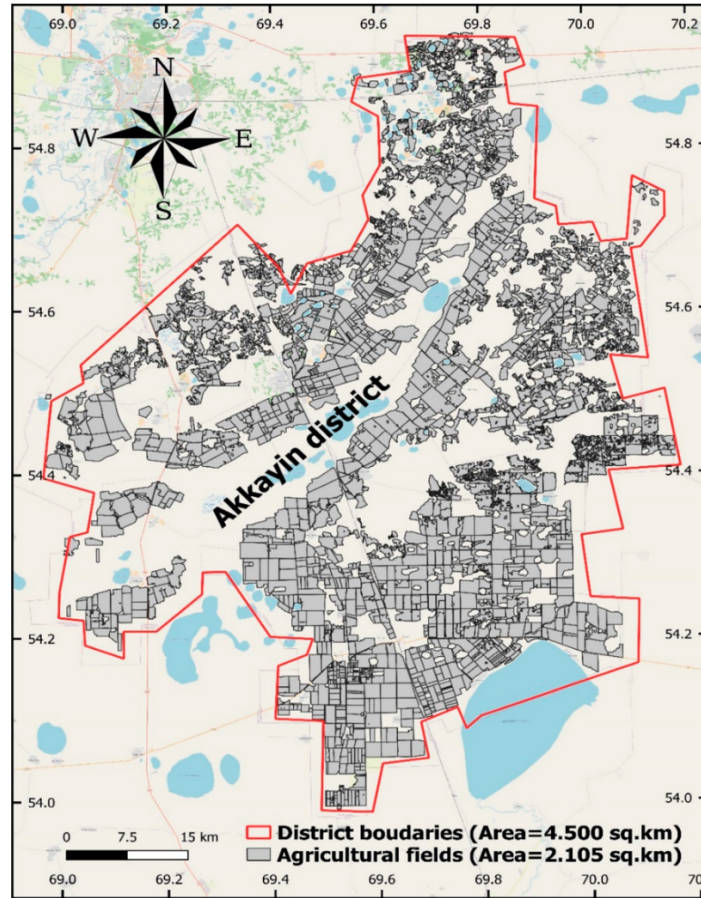


Figure 4.4. Digitized boundaries of agricultural fields in the study area

4.2.3.2.Preparation of Thematic Layers

On the basis of the existing literature and expert opinions, eight thematic layers were created. To avoid unnecessary complications, experts removed two thematic layers, and the remaining six layers were weighted based on the AHP method (see Figure B4 of Appendix B). Further, explanations are provided regarding specific thematic layers.

Hydrogeology

The hydrogeological map displays the conditions of the occurrence, distribution patterns, and formation of groundwater (Ravier & Buoncristiani, 2018; Smith, 2015). As these maps are based on the results of hydrogeological surveys, considering geological and tectonic maps, parameters such as the lithological composition of aquifers and mineralization were important in this study. A hydrogeological map of the study area was digitized using ArcGIS Pro 2.8 software.

Slope

The slope gradient, which depicts the steepness of the Earth's surface, is a crucial relief component. According to Melese & Belay (2022), a moderate slope has the maximum potential for infiltration, whereas a steeper slope produces more runoff. The slope is one of the more important parameters when choosing zones for reserving melt and flood waters, the average value

of which in the Akkayin district is about 2%. In our case, sites with a slope of more than 5% had lower potential as surface runoff increased. The slope gradient map was created from the digital elevation model using the spatial analyst toolbox in ArcGIS Pro 2.8 software, which utilized the following formula:

$$S = \sqrt{\left(\frac{dZ}{dx}\right)^2 + \left(\frac{dZ}{dy}\right)^2}$$

where S is a slope in 3D, dZ/dx is the horizontal difference in height divided by the distance between pixels, and dZ/dy is the vertical difference in height divided by the distance between pixels.

Drainage Density

Another factor that affects the evaluation of locations for snowmelt and floodwater storage in farm ponds is drainage density. According to several researchers (Murmu et al., 2019; Thomas et al., 2016; Yifru et al., 2021), locations with high drainage density inevitably have high runoff, which, in turn, suggests poor infiltration rates and reserve potential. In this paper, we consider that the most preferable areas for farm ponds should be downstream, but below the highest drainage density value. To create a drainage density map of the study area, we performed multiple geoprocessing operations, such as stream ordering to identify and classify streams from the digital elevation model based on the number of tributaries and creating a grid index. Finally, the drainage density was calculated by the following equation using the Line Density tool in ArcGIS Pro 2.8 software:

$$DD = \frac{\sum_1^n L}{A}$$

where DD is the drainage density, L is the stream length, and A is the basin area.

Land Use/Land Cover

Land use and land cover significantly influence surface runoff, the infiltration rate, water consumption, and snow accumulation (Yifru et al., 2021). Accordingly, strongly snow-blown bare ground, built-up areas, and water bodies were classified as the least-preferable areas for snowmelt and flood water storage, while flooded vegetation, grasslands, and shrubs were the top-three areas with a favorable environment for constructing farm ponds. The land use/land cover map of the study area was created using high-resolution Sentinel-1 and Sentinel-2 imagery, and a knowledge-based classification method was obtained from the ESRI LULC 2021.

Soil

According to Anbazhagan & Ramasamy (2006) and Etikala et al. (2019), soil cover influenced surface water runoff and infiltration rate, which, in turn, affected the availability of melt and flood water for the reservation. The soil's physical characteristics, including grain size and pore space, could also strongly impact groundwater recharge (Gomboš et al., 2019; Musa et al., 2017). In comparison with fine-grained soils, coarse-grained soils are known to have a high infiltration rate and cause a larger loss of surface runoff in reserving snow meltwater in farm ponds

(Nolan et al., 2006). However, due to global climate change, snow cover is melting faster than usual when the ground is still frozen to a depth of 1 to 1.5 m. According to the permafrost-measuring device (merzlometr) installed in the regional center of the Akkayin district, the depth of soil freezing varied from 45 cm to 197 cm between October 2022 and April 2023. Thus, in the early spring, regardless of the soil type, meltwater does not infiltrate the soil and, in turn, causes destructive floods. In this study, a soil map of the study area was obtained from the FAO/UNESCO Soil Map of the World portal.

Snow Water Equivalent

The snow water equivalent was the most important parameter in this study, as it integrally characterized the depth and density of snow cover that was theoretically planned to be reserved in the farm ponds. Additionally, this parameter fully described the snow reserves in a particular area and could clarify the water regime of rivers and lakes (Teleubay et al., 2022). A high-resolution (10 m) snow water equivalent map of the study area was prepared using the authors' previously developed and validated methodology for assessing the depth of snow cover and snow water equivalent using remote sensing data and GIS technologies. The main approaches and methods for calculating the snow water equivalent are shown in Figure 4.5. All calculations were carried out on the Google Earth Engine multi-petabyte cloud platform, and the source codes are available at the following link (Teleubay, 2023).

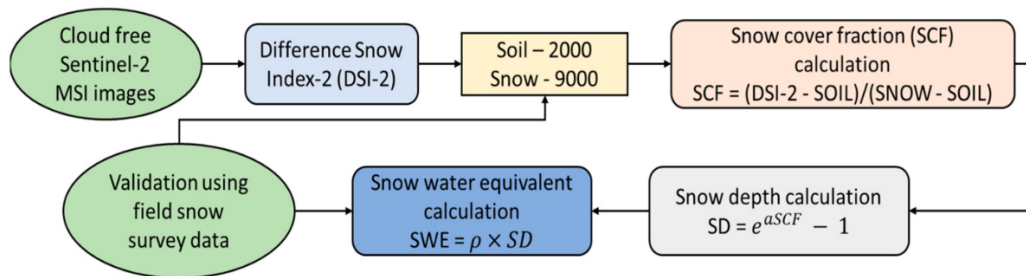


Figure 4.5. Flow chart of the methodology for calculating the snow water equivalent

4.2.3.3. Assigning Relative Weights

Each thematic layer has a distinct effect on the runoff, infiltration, and accumulation of melt and flood waters on the Earth's surface (Yeh et al., 2016). The relative weight of the input parameters was determined by using the AHP method and was based on the degree of influence of layers on the occurrence and dynamics of surface waters (Saaty, 2008). As the hierarchy-based structure of the decision issue was essential to the AHP method, determining the primary criteria, sub-criteria, alternatives, and hierarchy structure was a significant component of the decision process. The hierarchical structure of this process is illustrated in Figure 4.6.

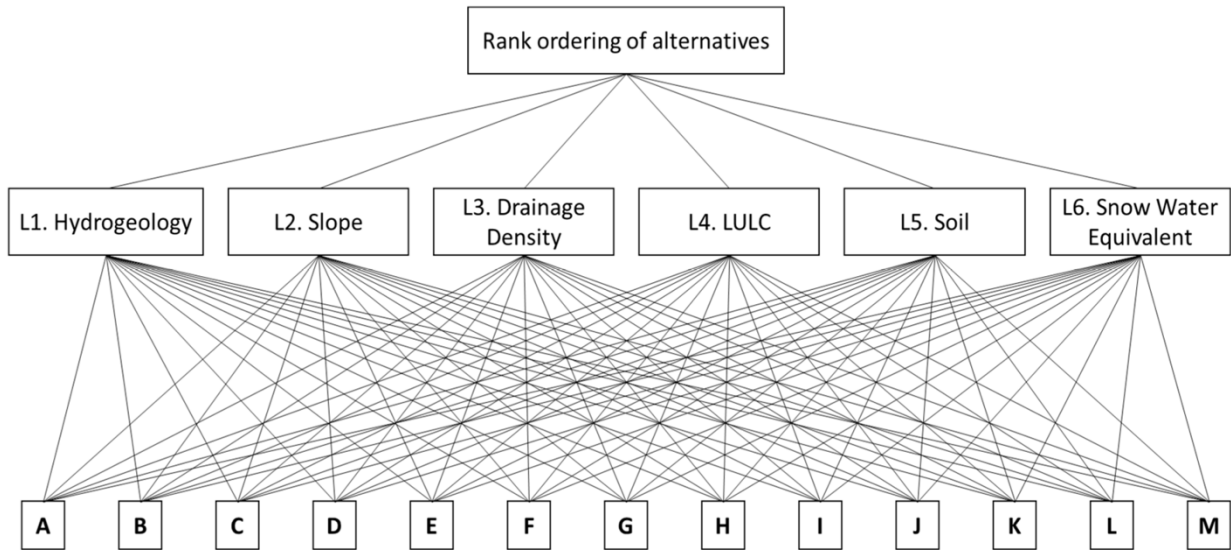


Figure 4.6. Hierarchy structure of the identification of potential farm pond sites

This model has been frequently employed as a decision-making tool in issues requiring intricate parameters and domains with constrained data, both in terms of variety and reliability (Asadabadi et al., 2019; T. Saaty & Vargas, 2001). In the current research, expert judgment and an eigenvector were applied to assign weight and order to the input layers, while the principal eigenvalue was used to rank the factors (Carver, 1991; Hajkowicz & Higgins, 2008; Malczewski, 2006). To define the relative significance of indicators based on Saaty scale values (T. Saaty, 2008), a hydrogeologist with industrial experience was recruited from the Kazakh Research Institute of Water Management, and two academic experts were involved from the local university (Table 4.4).

Table 4.4. Analytical hierarchy process significance scale by Saati

Scale	1	2	3	4	5	6	7	8	9
Importance	Equal	Weak	Moderate	Moderate plus	Strong	Strong plus	Very strong	Highly strong	Extreme

By dividing the column values by the column grand total, the eigenvector—representing each indicator’s relative weight (Brunelli, 2015)—was created, as illustrated in Table 4.5. The consistency of the matrix was measured by the sum of the eigenvalues (principal eigenvalue λ_{\max}), and a pairwise comparison matrix (6×6) was created using the input factors. Each entry describes how the relative row has an impact on the column factor. By contrasting the λ_{\max} values of the pairwise comparison matrix with different thematic layers present, the validity of the matrix was evaluated. It is important to note that the total number of parameters was less than λ_{\max} . When indications are solved in pairs, a certain degree of consistency may develop. Therefore, verifying the given weight’s correctness in a pairwise comparison is crucial.

Table 4.5. Relative weights of input layers compiled with expert judgment

Layers	SWE	Hydrogeology	Slope	Drainage Density	LULC	Soil
SWE	1	5	5	1	1	5
Hydrogeology	1/5	1	1/3	1/3	1/5	1
Slope	1/5	3	1	1/3	1/3	3
Drainage Density	1	5	3	1	1	5
LULC	1	5	3	1	1	5
Soil	1/5	1	1/3	1/5	1/5	1
Sum (col)	3.6	20.0	12.7	3.9	3.7	20.0

Given that the discrepancy of the matrix grew with the number of comparisons, the AHP technique incorporated a consistency index to track variance. A consistency ratio lower than 10% was required to determine the weight; otherwise, the relative weights of each indicator should have been changed to mitigate the disparity (Saaty, 1986). The consistency index, as illustrated in the formula, was the ratio of the difference between λ_{max} and the total amount of input layers used.

$$CI = \frac{\lambda_{max} - n}{n - 1}$$

$$CR = \frac{CI}{RI}$$

where CI is the consistency index, λ_{max} is the principal eigenvalue, n is the number of layers, CR is the consistency ratio, and RI is a random index.

Table 4.6 shows that the principal eigenvalue for this research was 6.15, which was higher than the total number of input layers, and that the consistency ratio of 2% was also within the tolerance limit (10%), showing that both the given weighting and consistency in pairs were appropriate.

Table 4.6. Evaluation of pairwise matrix consistency

Layers	Column Sum (1)	Principal Eigenvector (2)	Rank (1 × 2)
SWE	3.60	0.290	1.045
Hydrogeology	20.00	0.047	0.943
Slope	12.67	0.100	1.268

Layers	Column Sum (1)	Principal Eigenvector (2)	Rank (1 × 2)
Drainage Density	3.87	0.258	0.996
LULC	3.73	0.258	0.962
Soil	20.00	0.047	0.943
λ_{\max}			6.158

Moreover, each input layer was reclassified into a common ratio scale and combined to produce a map of potential farm pond sites (PFPSs) to store melt and flood water. All reclassified rasterized maps were overlaid using the Weighted Overlay analysis tool. Finally, the weighted values of each raster layer were multiplied by the cell score of each input raster. In addition, potential farm pond sites were classified based on the potential farm pond site index value. The PFPS index was a dimensionless value calculated from the weights of each thematic layer and its characteristics. The PFPS index was calculated using the following formula:

$$PFPS_i = \sum_{i=1}^n w_i x_i$$

where PFPS_i is the potential farm pond sites index, n is the number of layers, W is the normalized weighting of the layer, and x_i is a relative score of the ith layer at the tth pixel.

4.2.3.4. Validation of Farm Pond Sites

Regarding the scientific relevance of this study, model validation is essential to assess the reliability of the results (Chung & Fabbri, 2003). In this work, the identified potential areas of farm ponds for snowmelt and flood water storage were tested using existing farm ponds, or rather, their digitized vector layers (see Figure B5 of Appendix B). In the literature, other researchers also used ground data to cross-check the developed model for identifying potential zones (Jha et al., 2010; Magesh et al., 2012; Sarwar et al., 2021). The observed data on existing farm ponds were digitized, geo-positioned, and overlaid on a delineated map of potential farm pond areas for melt and flood water storage in a GIS environment. Thus, the share of existing farm ponds located in zones with low, medium, high, and very high potentials was calculated.

4.3. Results

In this research, six parameters (hydrogeology, slope, drainage density, land use/land cover, soil, and snow water equivalent) that mainly influence the runoff, infiltration, and accumulation of surface melt and flood water were carefully considered in the study area to assess the potential zones for the location of farm ponds. After assigning weights to each factor using the AHP method, a map of potential areas with low, medium, high, and very high snowmelt and floodwater storage potential for agriculture was compiled.

4.3.1. Hydrogeology

As the hydrogeological map combined both hydrological and geological characteristics of the area, parameters such as the infiltration rate, runoff, mineralization, and lithological composition of the aquifer were considered essential. The study area was classified into three classes: Pliocene–Quaternary aquifer, Quaternary lacustrine–alluvial aquifer, and Neogene aquifer, and their areas accounted for 323,700 ha (70.4%), 88,600 ha (19.3%), and 47,500 ha (10.3%), respectively (Figure 4.7). In this study, the Neogene aquifer had low potential for farm pond construction sites, because most of its territory was already occupied by salty lakes unsuitable for agriculture. The quaternary lacustrine–alluvial aquifer was assigned medium potential, because it has a low infiltration rate and higher runoff. However, this class tends to be very well sorted with highly laminar clays and sometimes carbonates that do not allow common crops of the region to be cultivated. The Pliocene–Quaternary aquifer, with lower mineralization but a high infiltration rate occupying almost three-quarters of the Akkayin district, was the most suitable for reserving melt and flood water for agriculture.

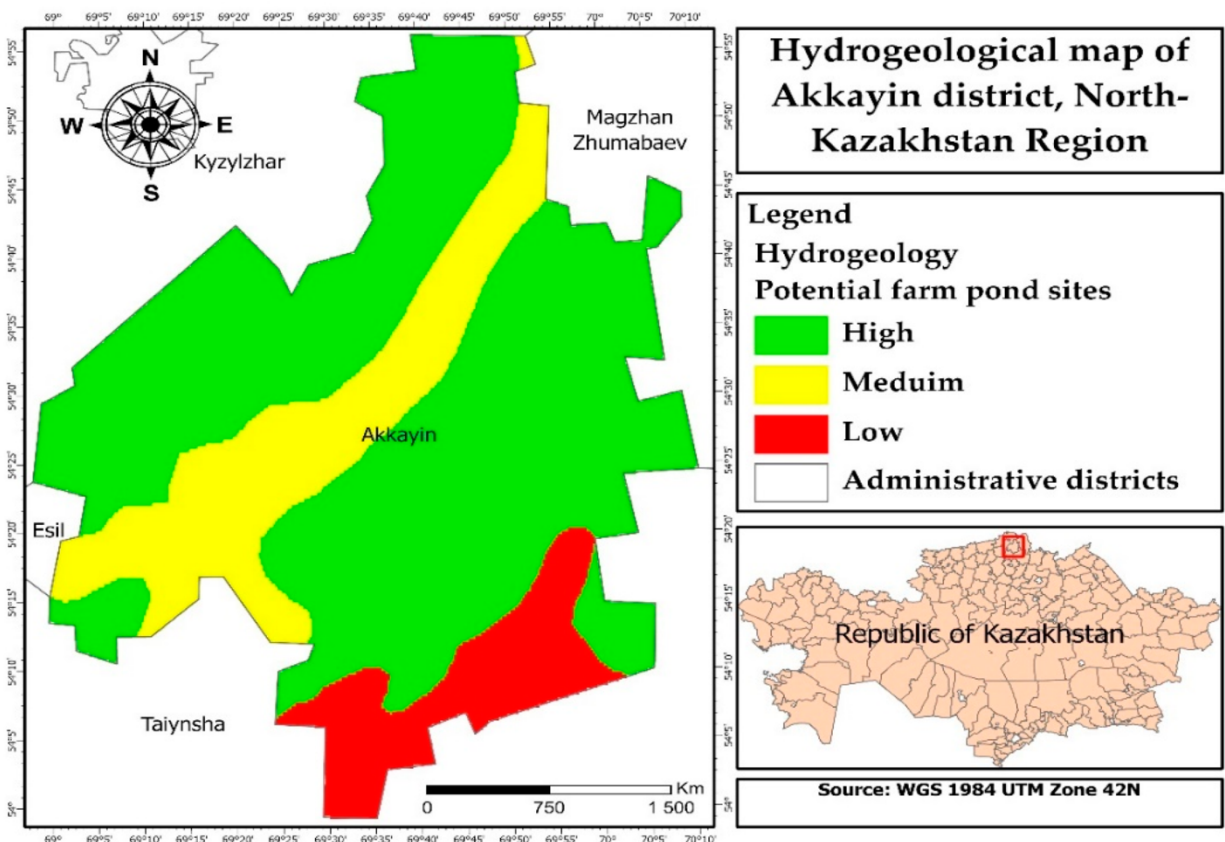


Figure 4.7. Reclassified hydrogeological map of Akkayin district

4.3.2. Slope

Slope is an important parameter when it comes to selecting zones for reserving melt and flood waters, the average value of which is about 2% in the Akkayin district. Generally, the steeper the slope, the greater the runoff, and conversely, a moderate slope provides more potential for surface water infiltration. The slope map of the study area was classified into five classes, namely very high (0–1%), high (1–2%), medium (2–3%), low (3–4%), and very low (>4%) potential areas (Figure 4.8). The results showed that more than 80% of the Akkayin district is suitable for farm pond construction in terms of surface relief, as 42% of the territory had a score of very high potential and 40.5% had high potential. Nevertheless, 64,153 ha (14%) was found to have medium, 12,074 ha (2.6%) low, and 4287 ha (0.9%) very low potential to reserve spring surface runoff.

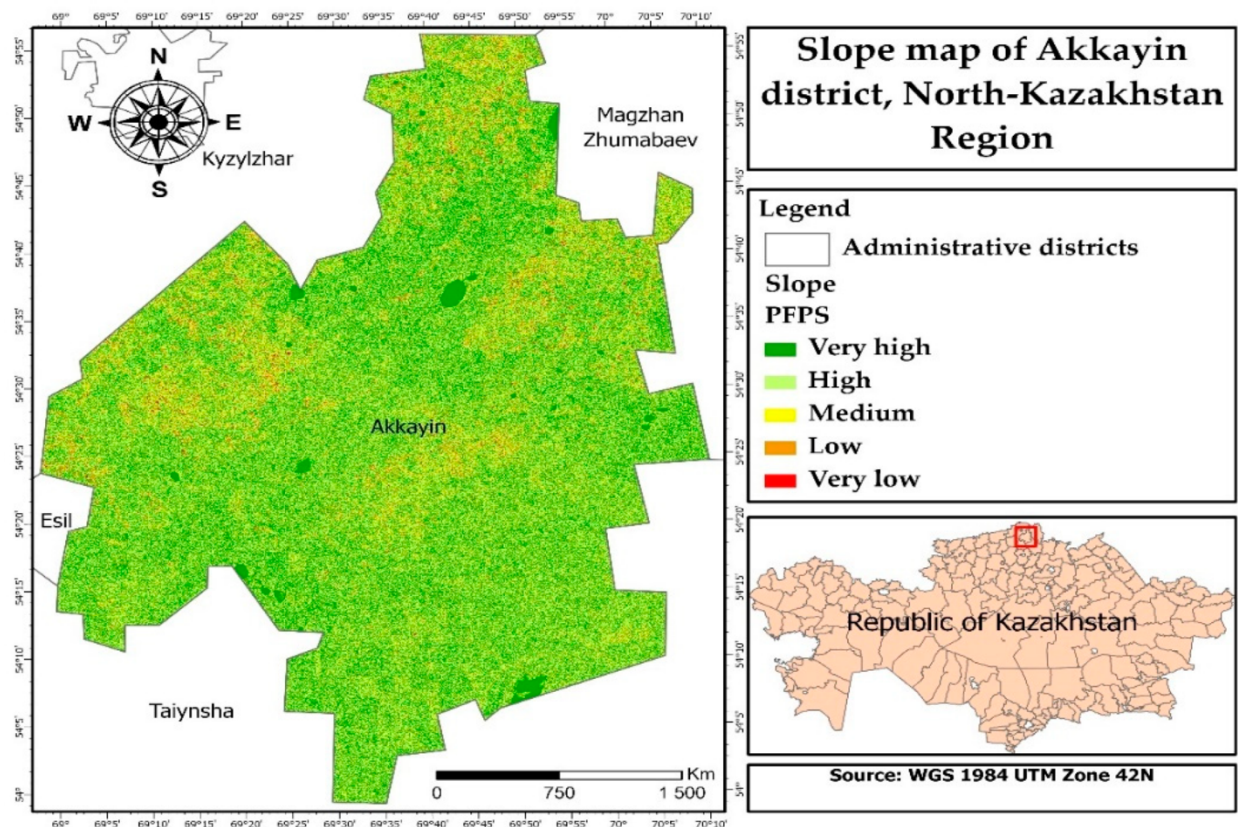


Figure 4.8. Reclassified slope map of Akkayin district

4.3.3. Drainage Density

Drainage density was the second most important parameter after the snow water equivalent in this study. Commonly, locations with high drainage density inevitably have high runoff, which, in turn, suggests poor infiltration rates and reserve potential. The drainage density map of the Akkayin district had five similar classes to the slope map. During classification, we granted more preference to drainage density values higher than zero but below the maximum. Thus, the areas with very high drainage density had very low potential (1.3%), high drainage density areas had

low potential (8.5%), and very low drainage density areas had medium potential (29%) for snow meltwater reservation. Very high potential was found in areas with low drainage density (34.5%), and areas with an average drainage density had high potential (26.7%) (Figure 4.9). To sum up, more than 60% of the study area was found to be suitable for farm ponds in terms of drainage density.

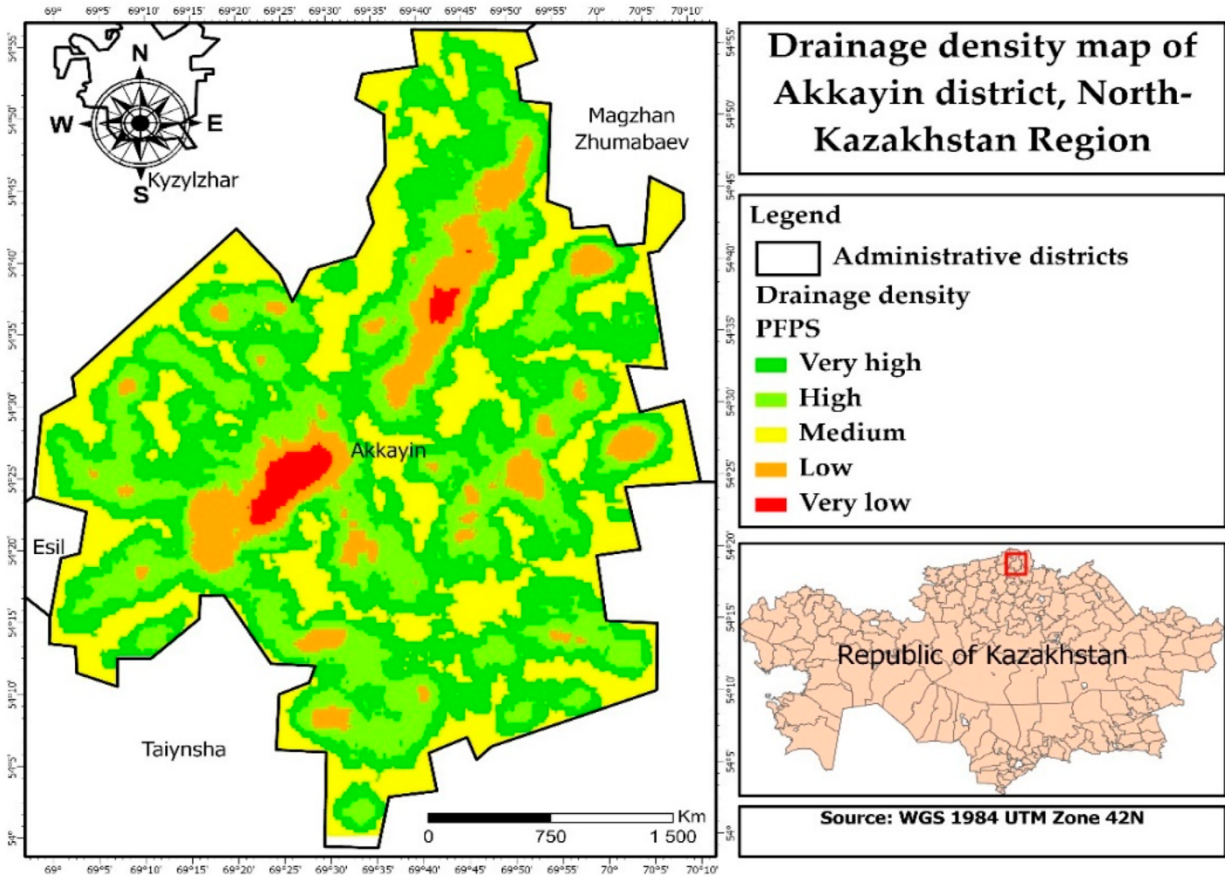


Figure 4.9. Reclassified drainage density map of Akkayin district

4.3.4. Land Use/Land Cover

The third most important parameter, the land use/land cover map, originally had eight classes, but was reclassified into five, similar to the previous maps' classes (Figure 4.10). As built-up areas are unsuitable for agriculture and bare ground surfaces are useless for snow meltwater reservation, they were amalgamated into one class with very low potential for farm pond site construction (0.9%). Low potential was also afforded to water bodies (2%), because most of them had high mineralization and were located relatively far from agricultural fields. Trees and crops were also grouped together and classified as areas with medium potential (59.1%), while shrubs were considered more suitable for farm pond sites and ranked as surfaces with high potential (24.1%). According to the opinion of experts, grass and flooded vegetation surfaces were the most appropriate fields for snow meltwater reservation, occupying only 13.9% of the study area.

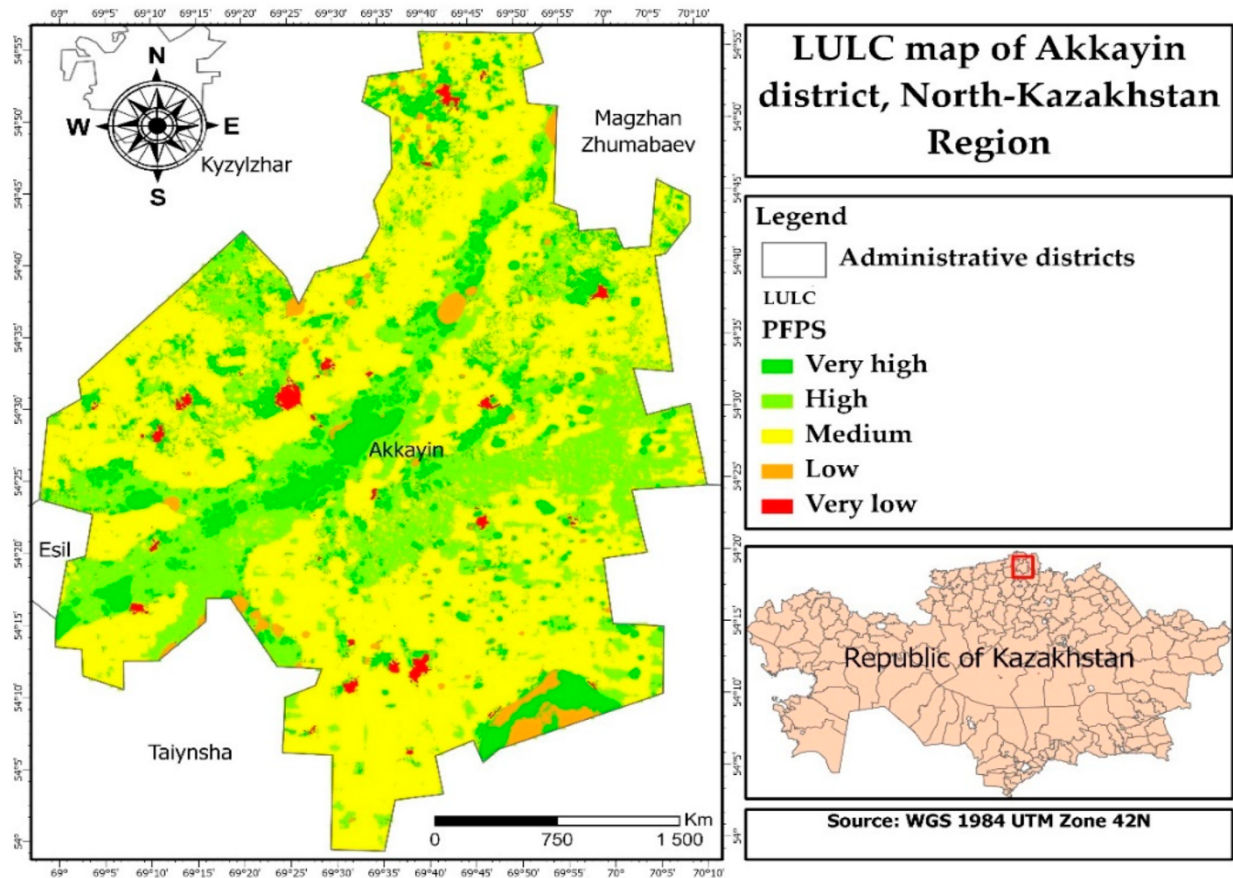


Figure 4.10. Reclassified land use/land cover map of Akkayin district

4.3.5. Soil

The soil map of the study area consisted of four classes: ordinary chernozems, ordinary carbonate chernozems, ordinary solonetz chernozems, and solonetz (Figure 4.11). Based on its physicochemical characteristics, solonetz with excessive alkalinity, which is harmful to many crops, was classified as an area with very low (4%) potential for farm ponds. Further, depending on the degree of salinity, ordinary solonetz chernozem had medium potential (27.2%), ordinary carbonate chernozem high (7.2%), and ordinary chernozem had very high (61.6%) potential for reserving melt and spring water for agriculture. Considering that the infiltration and water-holding capacity of the watershed depended on the structure, mechanical composition, and soil type, these properties were not considered when ranking the classes, as the type (chernozem) and subtype (ordinary) of soil were the same throughout the Akkaiyn region.

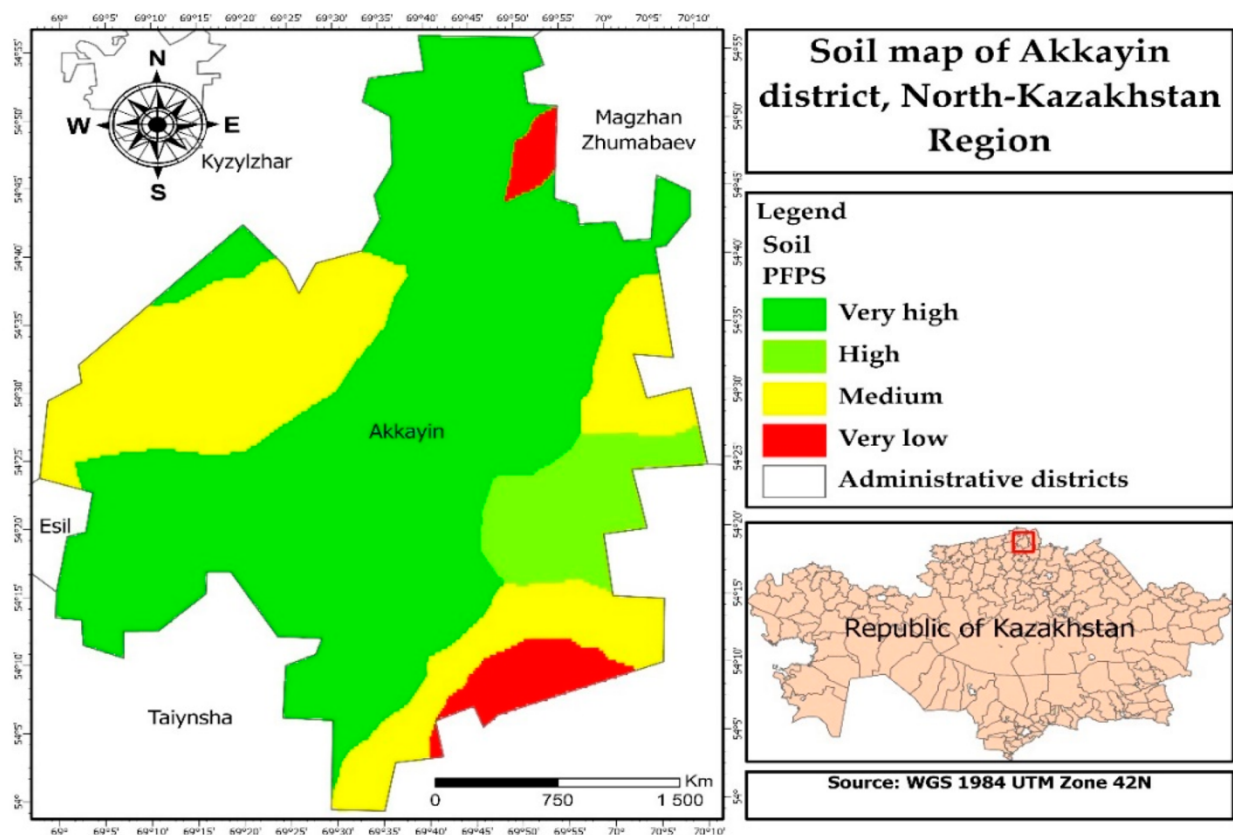


Figure 4.11. Reclassified soil map of Akkayin district

4.3.6. Snow Water Equivalent

A high-resolution snow water equivalent map of the study area was prepared using the earlier methodology of the authors (Teleubay et al., 2022). After all, in the framework of this study, it was planned to assess the snow cover and the possibility of its reservation in the spring for agricultural needs. Thus, the snow water equivalent map was the most crucial parameter in the hierarchy structure. The final map was reclassified into five classes, and the ranking was based on the rule that the more snow, the better (Figure 4.12). According to the map, zones with very low potential occupied 5.9% of the study area ($SWE \leq 10 \text{ kg/m}^2$), zones with low potential covered 6.9% ($SWE \leq 20 \text{ kg/m}^2$), and the area of the medium-potential zone accounted for 8.6% ($SWE \leq 30 \text{ kg/m}^2$). Such a small share of unsuitable territories indicates that the region receives an enormous amount of precipitation during the winter, affording good potential for snow meltwater reservation in spring. Accordingly, territories with a snow water equivalent between 30 and 40 kg/m^2 and more than 50 kg/m^2 were classified as zones with high (19.8%) and very high (58.8%) potential for farm pond sites, respectively.

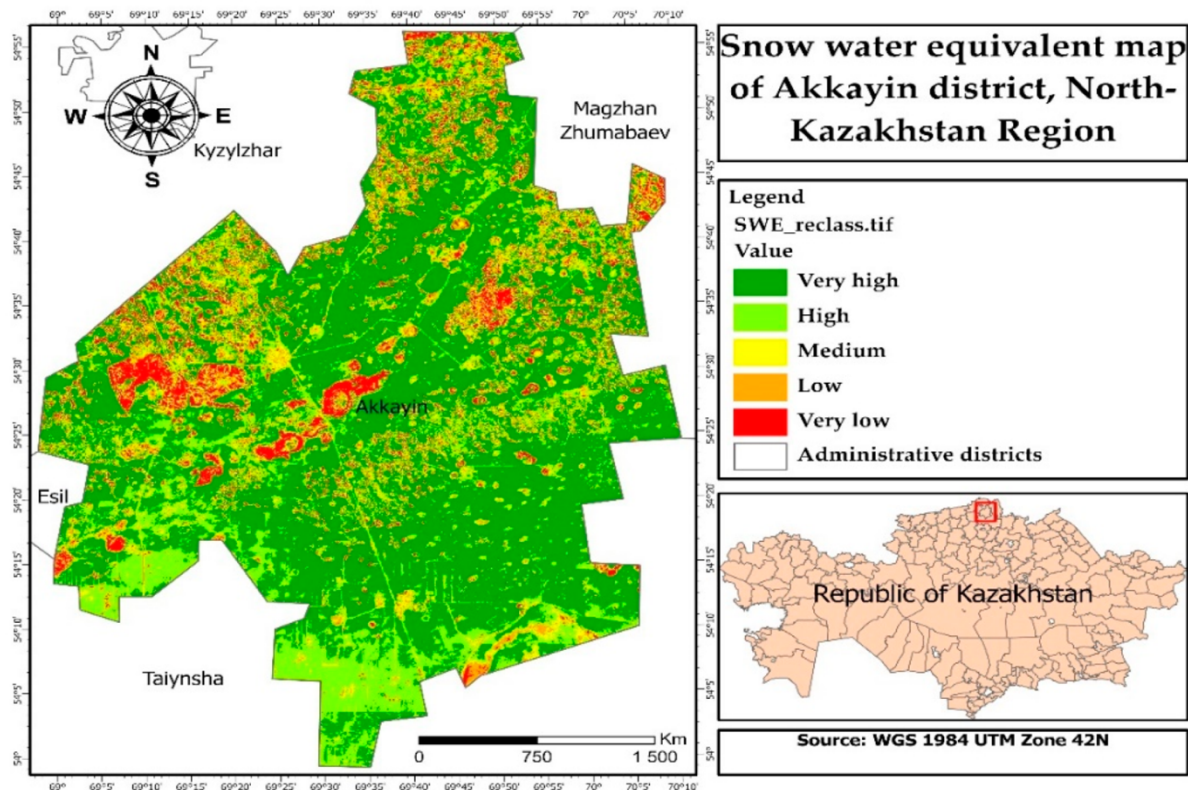


Figure 4.12. Reclassified snow water equivalent map of Akkayin district

4.3.7. Overall Assessment of Potential Farm Pond Sites

Weights were assigned to each input parameter using the experts' opinions and the AHP methodology described in Section 2.3.3. As a result, the snow water equivalent map had the most significant weight (29%), drainage density and land use/land cover maps had the same weight, which was equal to 25.5%, slope was assigned a less significant weight (10%), and hydrogeology and soil cover maps equally had the smallest share in the weighting, accounting only for 5% (Figure 4.13). According to our understanding, this is the most appropriate weight distribution for the northern steppe regions of the Republic of Kazakhstan and regions with similar soil and climatic conditions.

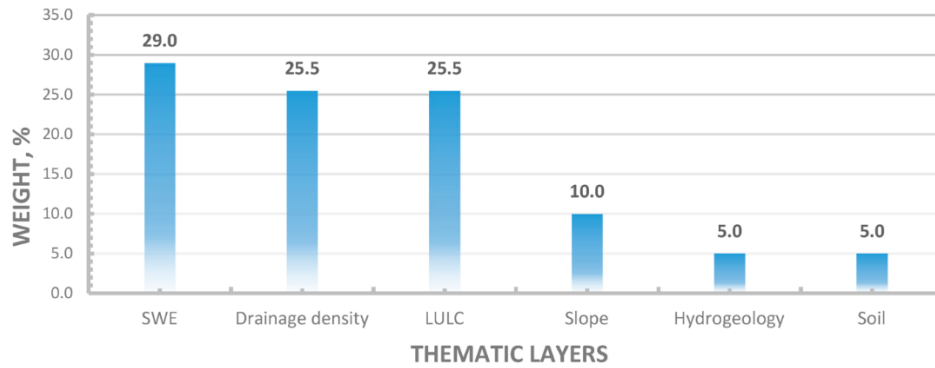


Figure 4.13. The relative weights of the potential farm pond site indicators

Furthermore, using the Weighted Overlay tool in ArcGIS Pro 2.8 software, weights and ranks were assigned to each input parameter and their classes in the GIS environment. Thus, after reclassifying and layering maps of unsuitable zones (1 km buffer zone from agricultural land and the results of the chemical analysis of water), a final map of potential farm pond sites for spring surface runoff harvesting was obtained (Figure 4.14). As in the previous cases, the map with potential zones was classified into five categories: very high (3.3%), high (35.5%), medium (56.5%), low (4.6%), and very low (0.1%) potential. When unsuitable areas were skipped, the 450,000-hectare surface of the study area decreased to 370,000 ha. In the remaining territory, the area of the most reasonable sites for reservation of snow meltwater was 12,224 ha, while the territory with high potential occupied 131,502 ha. Shrubs and flooded vegetation with medium drainage density and high snow water equivalent occupied a major part of the most suitable territories for farm ponds. The largest part of the Akkayin district, accounting for almost 210,000 ha, fell into zones with medium potential. According to our results, the greater share of agricultural fields had medium potential for snowmelt reservation in the study area. On the other hand, water bodies, built-up areas, and territories with high slope and drainage density were classified as zones with low (17,039 ha) and very low (370 ha) potential. The results illustrate that they formed a relatively smaller proportion of the study area, but, in fact, many unsuitable zones (e.g., saline and clayey soils, high drainage density, and low snow water equivalent) coincided with the clipped areas with a buffer zone of 1 km from agricultural fields. Overall, almost 145,000 ha of productive land was found to be suitable for harvesting spring surface runoff in small farm ponds in the Akkayin district.

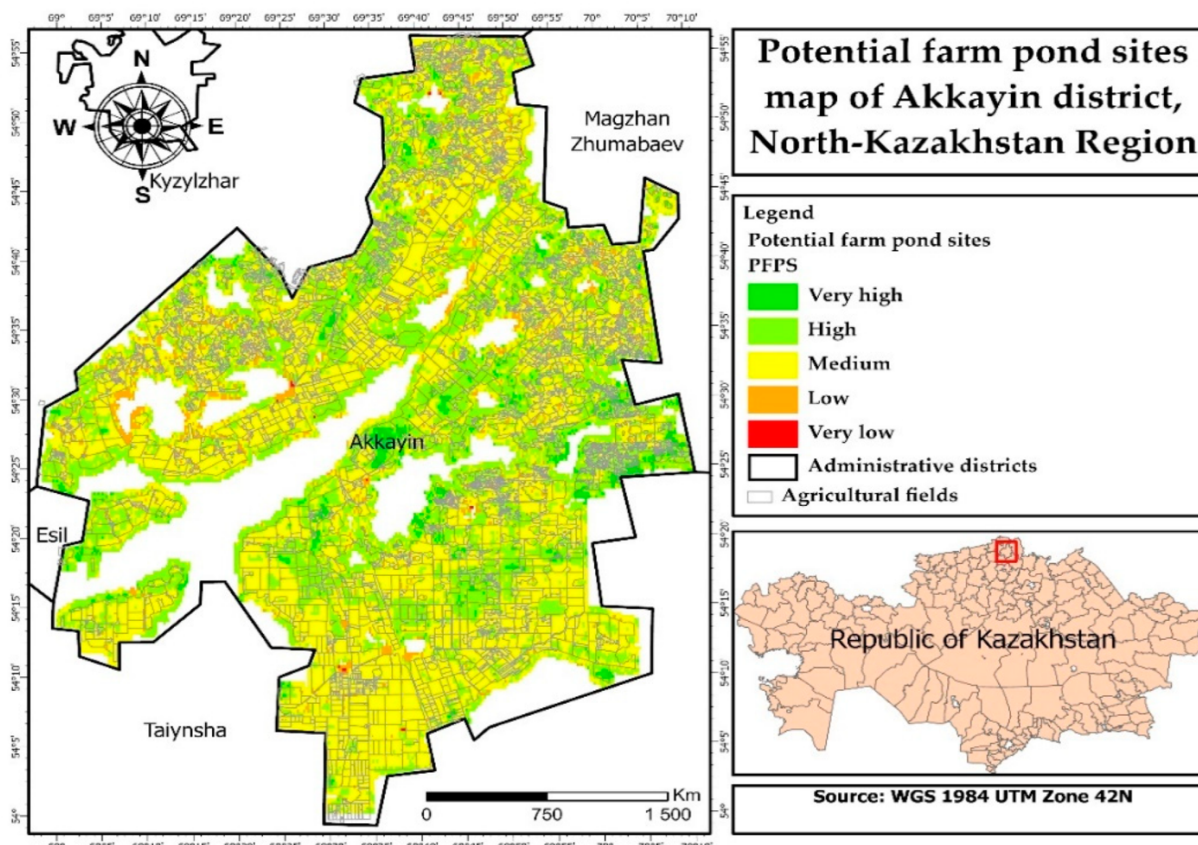


Figure 4.14. Overall potential farm pond sites for melt and flood water reservation map of Akkayin district, North Kazakhstan region, overlaid on agricultural fields

4.3.8. Validation of Potential Farm Pond Sites Map

To validate the final results for potential farm pond sites for spring surface runoff harvesting, existing farm ponds from the Soviet era in the Akkayin district were digitized (see Figure B5 of Appendix B). These farm ponds were created in the 1970s and 1980s with bulldozer technology; some of them are funnels that were deliberately blown up with explosives. Given that the topographic and geodetic works were carried out during the planning stages of these massive farm ponds, we believe that the most suitable places from a geographical point of view were chosen. Thus, we overlaid a vector file with 121 existing farm ponds on the final map showing potential zones. We found that not a single Soviet-type farm pond was located in a low-potential zone (0%), while 18% of them were constructed on a territory with medium potential (see Figure B6 of Appendix B). This is because some farm ponds were also supplied with groundwater using drilled wells, thus being located close to existing settlements and also serving livestock. However, 79% of the Soviet farm ponds (95) were located in a high-potential zone, and 3% in a zone with very high potential. On average, the qualitative assessment of potential melt and flood water reservation areas matched more than 80% of the ground data of existing farm ponds. This means that our data highly correlate with the areas of existing sites using the analytical hierarchy process in the GIS environment.

4.4. Discussions

Our results indicate that the GIS-driven AHP method performed well in identifying potential farm pond sites for snow meltwater harvesting in the study area. The results also show that the Akkayin district has a great potential to utilize excess surface runoff in agriculture, which creates opportunities for sustainable agriculture in the future amidst climate change. Previous studies showed that, by using the AHP methodology, it is possible to determine potential groundwater zones (Andualem & Demeke, 2019; Doke et al., 2021; Melese & Belay, 2022) and flood-vulnerable areas (Ouma & Tateishi, 2014; Vojtek & Vojteková, 2019) with an accuracy of 70 to 92%, while the current work achieved a precision of 82%, which was in line with the average accuracy range of earlier works. Compared with similar studies related to the identification of potential rainwater harvesting sites (Alwan et al., 2020; Balkhair & Ur Rahman, 2021; Chowdhury & Paul, 2021; Kadam et al., 2012; Maina & Raude, 2016; Sayl et al., 2020; Wu et al., 2018), this study used a snow parameter that was not previously taken into account. We found that snow was a major cause of spring floods and was also a possible solution to drought in the region. It all depends on the planning and management of natural resources. According to long-term data from field snow surveys in the Akkayin district, the territory is annually covered with 20 cm of snow, and the average snow density reaches 300 kg/m³. This means that one square meter of land contains about 60 L of snow water, or 600 m³ per hectare. Suppose we assume that water losses through evaporation and infiltration are 15%. In this case, the meltwater collected from the territory of 5 hectares will be enough for 1 ha of wheat under fully fledged irrigation or 2 ha under deficit irrigation (Geerts & Raes, 2009). Considering this proportion, it is easy to calculate that, theoretically, by collecting meltwater from 30% of the study area (135,000 ha), one-fourth of the cultivated land in the Akkayin district, which accounts for 54,000 ha, can be transferred to deficit irrigation. This would not only reduce floods and stabilize farmers' income in dry years, but would also open up the possibility of cultivating other highly profitable crops. Accordingly, local municipalities would receive more taxes, and they would spend less money to restore infrastructure after devastating floods. This would lead to more sustainable development in the region, increase economic growth and social responsibility, and maintain ecological balance.

Nevertheless, during this research, we also found that using the AHP method in a GIS environment for the delimitation of potential zones had several limitations: (1) the results obtained were partially subjective, as they partly depended on the opinion of experts, (2) although the primary approach remained unchanged, the weighting of input parameters and sub-criteria were strongly tied to a particular geographic area and could not be scaled, and (3) adding/removing alternatives to/from the existing model led to a change in the preferential order of other alternatives without alternating the values of pairwise comparisons concerning individual criteria. Considering the advantages and limitations of the identification of potential farm pond sites for spring surface runoff harvesting using an integrated AHP in a GIS environment, we expect that our approach will be helpful for sustainable water management, improving the socio-economic conditions of the population, and the development of irrigated agriculture in the Akkayin district, North Kazakhstan.

Overall, the potential of the Akkayin district in snow meltwater harvesting in farm ponds for agricultural needs as a response to agricultural drought and spring floods was found to be great. This is because the region receives a huge amount of precipitation in the winter and spring every year, and the snow melts very quickly due to climate change. Even though the territory of the Akkayin district is covered with highly water-holding capacity chernozem, the snow meltwater does not infiltrate the soil, as it remains frozen to a depth of 1–1.5 m until April. This creates destructive floods, high surface runoff, soil erosion, and the possibility of excess water retention in farm ponds.

4.5. Conclusions

In this study, the identification of potential farm pond sites for surface runoff harvesting in the Akkayin district, North Kazakhstan region, was carried out using a GIS-driven AHP method and six input parameters: hydrogeology, slope, drainage density, land use/land cover, soil, and snow water equivalent, which mainly influence the availability, runoff, infiltration, and accumulation of snowmelt and flood water. As a result, 3.3% of the study area was recognized as a very-high-potential zone, 35.5% high, 56.5% medium, 4.6% low, and 0.1% as a very-low-potential zone. The most suitable territories were found to have medium drainage density, low slope, high snow water equivalent, and be located on flooded vegetation and shrubs. Moreover, the majority of cultivated agricultural land was classified to have medium potential, despite the significant amount of snow water stored and moderate slope. On the other hand, the less preferred zones formed a relatively smaller proportion of the study area, but the larger part of them coincided with the clipped areas with a buffer zone of 1 km from agricultural fields. As a result, using ground-based surveys, remote sensing, and AHP in a GIS environment, potential zones for farm ponds were obtained with an accuracy of 82%. The model accuracy was assessed by using the locations of existing farm ponds. Furthermore, limiting factors, such as the high content of harmful metals in meltwater and the optimal distance of farm ponds from agricultural fields, were also identified. The use of the model allows us to avoid field studies that require a lot of time and resources in further research. We think that our approach can be suitable for regions with similar soil and climatic conditions to Northern Kazakhstan to address drought and spring flood challenges through sustainable management and increasing water productivity. Further work is planned to evaluate the possible socio-economic effects of introducing sustainable water management by snowmelt and flood water harvesting in farm ponds and increasing water productivity in irrigation.

4.6. Appendix B



Figure B1. The process of measuring the snow height and density.



Figure B2. The process of conducting a field UAV survey in the study area



Агроэкологический испытательный центр (лаборатория) при
 НАО «Казакский агроэкологический университет имени С. Сейфуллина»
 г. Нур-Султан, ул. Агымсарина, 2 (2-й корпус КАТУ), лаб.2208, 2218,
 2206

Стр.1 из 1

ПРОТОКОЛ № 1В

от 19-го мая 2022 г.

- Наименование и характеристика испытываемого объекта: вода природная (талая)
- Наименование и адрес заказчика: Физ. лицо
- Вид испытаний: контрольное
- Основание для выполнения испытаний: по заявке
- Нормативный документ на объект испытаний: СП №209 от 16.03.2015 г.
- Количество (объем) образцов, поступивших на испытание: 1 образец, 1000 мл.
- Номер пробы: 1
- Дата поступления проб: 16.05.2022 г.
- Дата начала и конца проведения испытаний: 16.05.2022-19.05.2022 г.
- Общие условия испытаний: температура + 21,3-22,0°С, относительная влажность – 59,4-62,9%.

11. Результаты испытаний:

№ п/п	Наименование показателей, единица измерения	Нормативный документ (НД) на метод испытаний	Норма по НД (предельно-допустимая концентрация и т.п.)	Фактические результаты испытаний, единица измерения
1	2	3	4	5
1	pH	ГОСТ 26449.1-85	6-9	8,05
2	Жесткость общая, мг/дм³	ГОСТ 26449.1-85	7,0 мг-экв/дм³	9,0 мг-экв/дм³
3	Кальций, мг/дм³	ГОСТ 31869-2012	-	65,0 мг/дм³
4	Магний, мг/дм³	ГОСТ 31869-2012	-	15,0 мг/дм³
5	Калий, мг/дм³	ГОСТ 31869-2012	-	71,72 мг/дм³
6	Натрий, мг/дм³	ГОСТ 31869-2012	200,0 мг/дм³	49,59 мг/дм³
7	Аммоний, мг/дм³	ГОСТ 31869-2012	2,0 мг/дм³	2,58 мг/дм³
8	Хлориды, мг/дм³	ГОСТ 31869-2012	350,0 мг/дм³	140,0 мг/дм³
9	Нитраты, мг/дм³	ГОСТ 31869-2012	45,0 мг/дм³	4,92 мг/дм³
10	Нитриты, мг/дм³	ГОСТ 31869-2012	3,0 мг/дм³	0,36 мг/дм³
11	Фосфаты, мг/дм³	ГОСТ 18309-2014 п. 4	3,5 мг/л	0,045 мг/дм³
12	Фосфор, мг/дм³	ГОСТ 26449.1-85 п. 14	-	0,03 мг/дм³
13	Сульфаты, мг/дм³	ГОСТ 31867-2012	500,0 мг/дм³	41,55 мг/дм³

Испытания провели:

Научный сотрудник

Инженер (менеджер по качеству)

Зав. Агроэкологического испытательного центра (лаборатории)

Назарова А.Ж.

Майсет Ж.

Каспихан А.

Данный протокол оформлен в 2-х экземплярах.

АИЦ

Агроэкологический испытательный центр (лаборатория) при
 НАО «Казакский агроэкологический университет имени С. Сейфуллина»
 г. Нур-Султан, ул. Агымсарина, 2 (2-й корпус КАТУ), лаб.2208, 2218,
 2206

Стр.1 из 1

ПРОТОКОЛ № 2

от 19-го мая 2022 г.

- Наименование и характеристика испытываемого объекта: вода природная (талая)
- Наименование и адрес заказчика: Физ. лицо
- Вид испытаний: контрольное
- Основание для выполнения испытаний: по заявке
- Нормативный документ на объект испытаний: СП №209 от 16.03.2015 г.
- Количество (объем) образцов, поступивших на испытание: 1 образец, 1000 мл.
- Номер пробы: 1
- Дата поступления проб: 16.05.2022 г.
- Дата начала и конца проведения испытаний: 16.05.2022-19.05.2022 г.
- Общие условия испытаний: температура + 21,3-22,0°С, относительная влажность – 59,4-62,9%.

11. Результаты испытаний:

№ п/п	Наименование показателей, единица измерения	Нормативный документ (НД) на метод испытаний	Норма по НД (предельно-допустимая концентрация и т.п.)	Фактические результаты испытаний, единица измерения
1	2	3	4	5
1	Сухой остаток, мг/дм³	ГОСТ 26449.1-85	1000,0 мг/дм³	352,0 мг/дм³
2	Карбонаты, мг/дм³	ГОСТ 26449.1-85	-	не обнаружено
3	Гидрокарбонаты, мг/дм³	ГОСТ 26449.1-85	-	не обнаружено
4	Железо, мг/дм³	ГОСТ Р 57165-2016	0,3 мг/дм³	0,52 мг/дм³
5	Цинк, мг/дм³	ГОСТ Р 57165-2016	5,0 мг/дм³	0,17 мг/дм³
6	Кадмий, мг/дм³	ГОСТ Р 57165-2016	0,001 мг/дм³	не обнаружено
7	Медь, мг/дм³	ГОСТ Р 57165-2016	1,0 мг/дм³	0,07 мг/дм³
8	Никель, мг/дм³	ГОСТ Р 57165-2016	0,1 мг/дм³	не обнаружено
9	Свинец, мг/дм³	ГОСТ Р 57165-2016	0,03 мг/дм³	не обнаружено
10	Хром, мг/дм³	ГОСТ Р 57165-2016	0,5 мг/дм³	0,03 мг/дм³
11	Кобальт, мг/дм³	ГОСТ Р 57165-2016	0,1 мг/дм³	0,04 мг/дм³
12	Марганец, мг/дм³	ГОСТ Р 57165-2016	0,1 мг/дм³	0,27 мг/дм³
13	Молибден, мг/дм³	ГОСТ Р 57165-2016	0,25 мг/дм³	не обнаружено
14	Ртуть, мг/дм³	ГОСТ Р 57165-2016	0,0005 мг/дм³	не обнаружено
15	Мышьяк, мг/дм³	ГОСТ Р 57165-2016	0,05 мг/дм³	0,16 мг/дм³

Испытания провели:

Научный сотрудник

Инженер (менеджер по качеству)

Зав. Агроэкологического испытательного центра (лаборатории)

Назарова А.Ж.

Майсет Ж.

Каспихан А.

Данный протокол оформлен в 2-х экземплярах.

АИЦ

Selection date: 13.05.2022			
Name and characteristics of the tested object: melt water			
Place of sampling: LLP "North-Kazakhstan Agricultural Experimental Station"			
Date of analysis: 15-19.05.2022			
№	Indicators	Results	Norm*
1.	pH	8.05	6-9
2.	Hardness total, mmol/dm³	9 mg-eq/ dm³	7 mg-eq/ dm³
3.	Dry residue, mg/dm³	352.0 mg/l	100-1500 mg/l
4.	Chlorides, mg/dm³	140.0 mg/l	350.0 mg/l
5.	Nitrates, mg/dm³	4.92 mg/l	45.0 mg/l
6.	Ammonium nitrogen, mg/dm³	2.58 mg/l	2.0 mg/l
7.	Nitrites, mg/dm³	0.36 mg/l	3.0 mg/l
8.	Sulphates, mg/dm³	41.55 mg/l	500.0 mg/l
9.	Phosphates, mg/dm³	0.045 mg/l	3.5 mg/l
10.	Phosphorus, mg/dm³	0.03 mg/l	-
11.	Carbonates, mg/dm³	not detected	-
12.	Bicarbonates, mg/dm³	not detected	-
13.	Calcium, mg/dm³	65.0 mg/l	-
14.	Magnesium, mg/dm³	15.0 mg/l	-
15.	Potassium, mg/dm³	71.72 mg/l	-
16.	Sodium, mg/dm³	49.59 mg/l	200.0 mg/l
17.	Iron, mg/dm³	0.52 mg/l	0.3 mg/l
18.	Zinc, mg/l	0.17 mg/l	5.0 mg/l
19.	Cadmium, mg/l	not detected	0.001 mg/l
20.	Copper, mg/l	0.07 mg/l	1.0 mg/l
21.	Nickel, mg/l	not detected	0.1 mg/l
22.	Lead, mg/l	not detected	0.03 mg/l
23.	Chromium, mg/l	0.03 mg/l	0.5 mg/l
24.	Cobalt, mg/l	0.04 mg/l	0.1 mg/l
25.	Manganese, mg/l	0.27 mg/l	0.1 mg/l
26.	Molybdenum, mg/l	not detected	0.25 mg/l
27.	Mercury, mg/l	not detected	0.0005 mg/l
28.	Arsenic, mg/l	0.16 mg/l	0.05 mg/l

* Sanitary rules "Sanitary and epidemiological requirements for water sources, places of water intake for domestic and drinking purposes, domestic and drinking water supply and places of cultural and domestic water use and safety of water bodies"

* mg/dm³ = mg/l

Figure B3. Results (protocol) of the chemical analysis of meltwater at critical points of Akkayin district, North Kazakhstan region, and its English translation

86

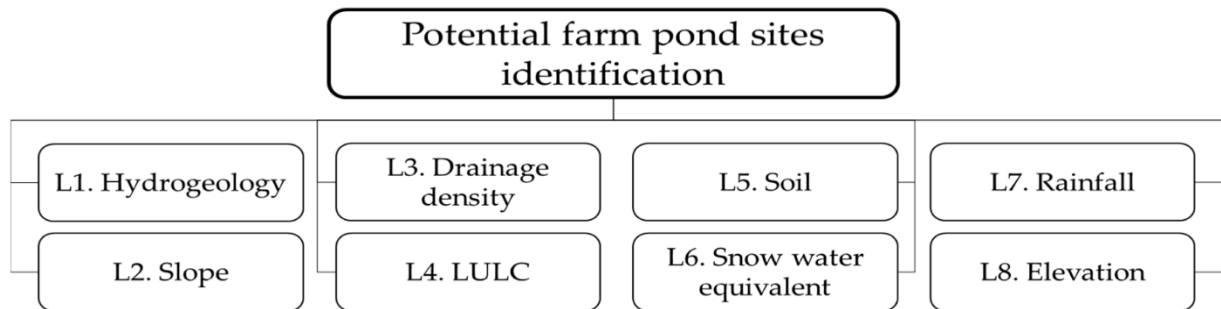


Figure B4. Input thematic layers for potential farm pond site identification

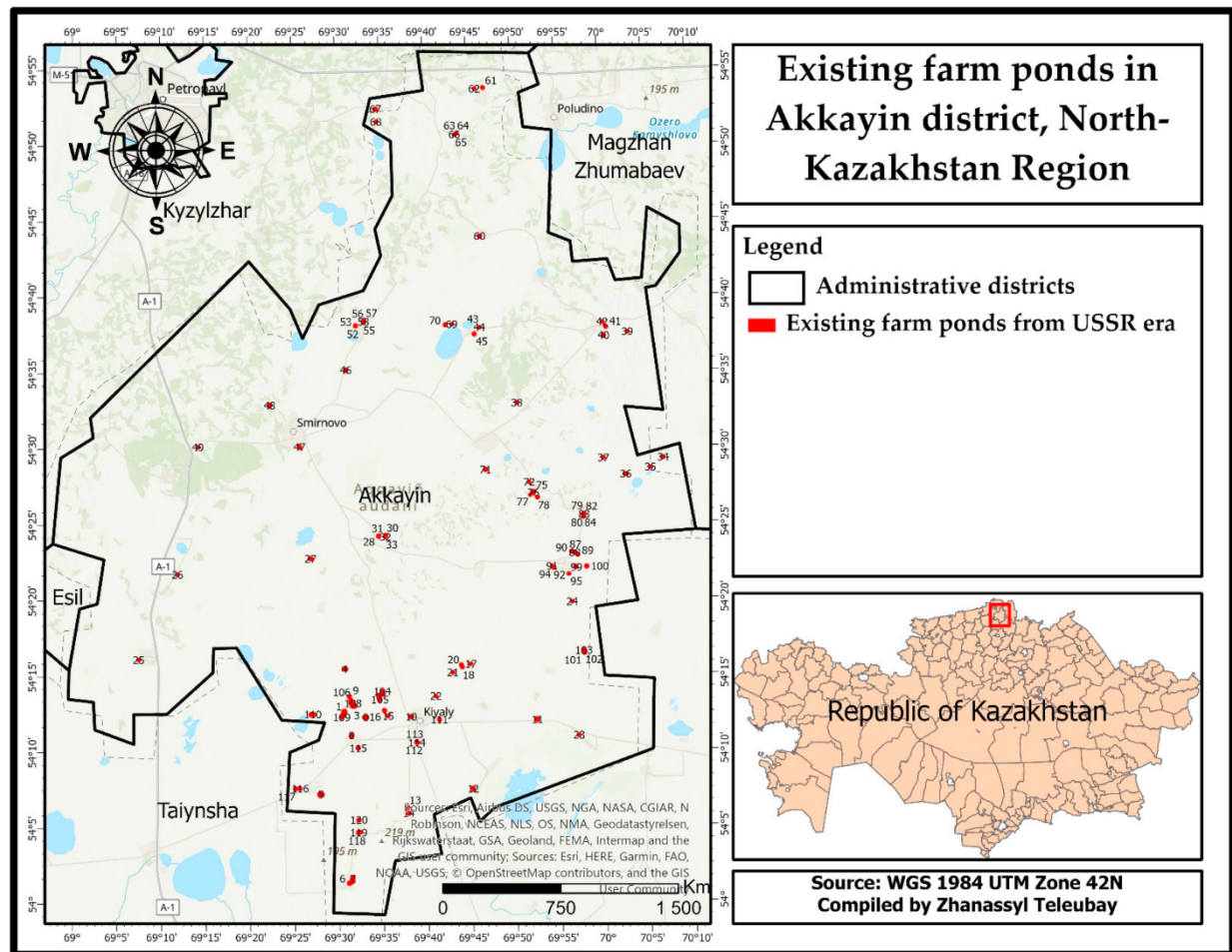
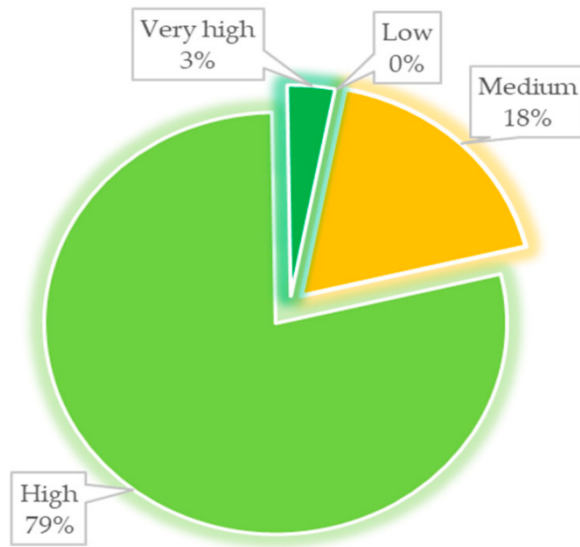


Figure B5. Existing farm ponds from the USSR era in Akkayin district, North Kazakhstan region



■ Low ■ Medium ■ High ■ Very high

Figure B6. Share of existing farm ponds in the developed map of potential zones

5. Conclusions

5.1. Summary of Key Findings

This dissertation examined the intersection of climate change, snowmelt water management, and agricultural adaptation in Northern Kazakhstan, utilizing remote sensing, crop modeling, and spatial decision analysis. The following key findings were derived from the research:

Thesis 1: Climate change is expected to significantly reduce wheat yields across North Kazakhstan. This underscores the urgent need for adaptation strategies. Given the region's climatic duality, springtime water surplus due to snowmelt and severe summer droughts, snowmelt harvesting emerges as a promising and practical solution for mitigating water stress in agriculture.

Thesis 2: Model simulations under RCPs indicate that, under the high-emissions RCP 8.5 scenario, wheat yield losses could exceed 10% in the arid steppe zone, 7.6% in the small hilly zone, 7.5% in the forest steppe, and 6% in the colo steppe. Overall, the region may experience average yield declines of 25.2 kg/ha (RCP 2.6–4.5), 59.5 kg/ha (RCP 4.5–8.5), and 84.7 kg/ha (RCP 2.6–8.5). Such declines pose a serious threat to food security across Central Asia.

Thesis 3: Remote sensing analysis showed that snow-covered areas could be effectively delineated using most tested indices, with the DSI and DSI-2 performing best. DSI-2 consistently produced snow depth estimates with the highest correlation to ground truth data ($R = 0.78\text{--}0.80$) and the lowest RMSE values (2.86–5.62 cm), proving its utility for snow monitoring and water resource assessment in agricultural zones.

Thesis 4: A GIS-based AHP framework using six weighted parameters, SWE (29%), LULC (25.5%), drainage density (25.5%), slope (10%), soil (5%), and hydrogeology (5%), was developed to identify optimal sites for snowmelt harvesting ponds. The analysis revealed that 3.3% of the Akkayin district had very high suitability, 35.5% high, and 56.5% moderate. Validation

against Soviet-era farm pond locations showed 82% spatial overlap. If meltwater from just 30% of the district (135,000 ha) were captured, deficit irrigation could be applied to one-fourth of cultivated land (54,000 ha), reducing flood damage, stabilizing yields during dry years, and enabling the cultivation of higher-value crops.

5.2. Implications

This research makes significant contributions to the growing body of work on climate resilience, agro-hydrological modeling, and sustainable land and water management in cold semi-arid regions. The study's integrated framework, linking crop modeling, snow remote sensing, and spatial decision support, serves not only as a diagnostic tool for assessing climate impacts but also as a prescriptive model for targeted adaptation planning.

The dissertation advances the methodological toolkit for climate change impact assessment by combining high-resolution remote sensing data (Sentinel-2), robust crop simulation models (DSSAT), and multi-criteria spatial analysis (GIS-AHP). This multidisciplinary approach enhances the understanding of how snow-derived water resources can be quantified, spatially prioritized, and operationalized for agricultural benefit. It fills a critical research gap by adapting runoff harvesting techniques to snow-dominated agroecosystems, a domain historically underrepresented in the literature, which has largely focused on tropical and arid climates. The successful validation of snow indices for snow depth estimation (notably DSI-2) contributes to the global discourse on remote sensing applications in water resource monitoring, especially in data-scarce regions.

The study reveals that snowmelt, an often-overlooked water source in the region, can be strategically harvested to support agriculture during peak drought periods. By identifying that 54,000 hectares, approximately one-fourth of the cultivated land in the Akkayin district, could benefit from deficit irrigation if meltwater is stored from just 30% of the area, this research offers a scalable pathway to stabilize yields, reduce vulnerability to summer droughts, and diversify cropping systems. It also promotes a shift from traditional yield-maximization approaches toward income-stabilization strategies rooted in climate-smart resource management. Moreover, snowmelt harvesting could mitigate spring flood risks, reducing damage to infrastructure and enhancing overall land resilience.

From a development perspective, the findings support rural economic resilience by promoting water storage systems that are low-cost, locally feasible, and scalable. Improved water availability during critical crop growth stages could reduce yield volatility, encourage diversification into higher-value crops, and enhance household food and income security. For farming communities in Kazakhstan, where access to large-scale irrigation is limited and often unaffordable, the proposed snowmelt harvesting strategy offers a decentralized and farmer-driven solution.

At the policy level, the study's outputs, particularly the suitability maps for pond construction and the quantified impact of climate change on wheat yield, can inform national and regional adaptation plans. By providing spatially explicit evidence, this work helps prioritize infrastructure investments and guides the rehabilitation or construction of farm ponds. The

research also aligns with Kazakhstan's broader climate adaptation and food security goals, as well as international frameworks like the UN Sustainable Development Goals (SDGs), particularly SDG 2 (Zero Hunger), SDG 6 (Clean Water and Sanitation), and SDG 13 (Climate Action).

Furthermore, the framework developed in this study can be adapted for use in policy decision-making platforms, offering local governments and environmental agencies a replicable tool for agricultural planning. The integration of SWE, land use, drainage, and soil parameters into a transparent AHP model supports evidence-based prioritization of water harvesting sites, fostering better intersectoral coordination between agriculture and water ministries.

Beyond Kazakhstan, this research is highly transferable to other snow-dominated regions with similar hydroclimatic profiles, such as parts of Mongolia, Central Asia, Eastern Europe, and western China, where snowmelt-induced floods and summer droughts co-occur. The methodological framework, data processing pipeline, and validation procedures outlined in the dissertation provide a replicable model that can be customized to local conditions. In this way, the study contributes to global efforts to leverage remote sensing for sustainable water management in the face of accelerating climate variability.

5.3. Limitations, Recommendations, and Future Research

While this dissertation offers a comprehensive and interdisciplinary approach to addressing climate-induced water scarcity in Northern Kazakhstan, it is important to acknowledge the limitations that emerged throughout the research process. These constraints, stemming from data availability, methodological assumptions, and the inherent complexity of environmental systems, provide valuable context for interpreting the findings and identifying avenues for future investigation.

One of the most significant limitations of the study is the reliance on temporally limited satellite imagery for snow monitoring. Although Sentinel-2 data proved valuable for assessing snow cover and estimating snow depth, the analysis was based primarily on a narrow time window during the spring months. This temporal constraint limits the capacity to capture the full dynamics of snow accumulation and melt processes, particularly in years with atypical weather patterns or delayed snowfall. A more robust time-series analysis using imagery across multiple snow seasons would improve the temporal resolution and allow for the development of early-warning systems based on snowpack trends.

Furthermore, the estimation of SWE was conducted using empirical models that rely on assumed average snow densities. While practical for large-area mapping, this approach does not account for spatial and temporal variability in snowpack properties, such as changes in density caused by wind redistribution, freeze-thaw cycles, or snow aging processes. The accuracy of SWE estimation could be improved by integrating passive microwave data or LiDAR-based snow profiling, which offer more physically grounded representations of snow structure. Similarly, incorporating surface temperature and albedo data may further refine snowmelt timing models.

Another limitation relates to the spatial resolution and availability of ground truth data. Field validation of snow depth and SWE was based on a limited number of sampling sites concentrated in specific areas of the Akkayin district. Although the study demonstrated strong

statistical agreement between modeled and observed values, a more spatially diverse set of validation points, collected over multiple years and covering different landscape types, would enhance the reliability and generalizability of the results. Expanding snow surveys to include areas with contrasting topographic and land cover conditions would also strengthen the calibration of regression models used for snow index validation.

With regard to crop modeling, DSSAT simulations were conducted under static management and planting assumptions, which may not reflect the diversity of real-world farming practices in the region. In particular, the use of a fixed sowing date across all zones does not account for interannual variation in rainfall or farmer decision-making based on local conditions. Although the model offered valuable projections of wheat yield decline under various RCP scenarios, the absence of adaptive agronomic strategies, such as cultivar selection, flexible planting dates, or variable fertilization rates, underestimates the adaptive capacity of farmers. Incorporating adaptive management scenarios in future simulations would better reflect on-the-ground realities and provide a more nuanced picture of yield resilience under climate stress.

Moreover, the spatial decision framework developed for identifying suitable snowmelt harvesting sites assumed uniform economic and institutional feasibility across the region. In practice, the construction of farm ponds depends on land tenure, funding availability, farmer willingness, and government support, factors not explicitly considered in the GIS-AHP model. While the physical suitability of locations was rigorously assessed, future studies should integrate socio-economic layers to better align technical recommendations with real-world implementation potential. Combining stakeholder interviews or participatory mapping with the spatial analysis could reveal additional constraints and opportunities not evident from geospatial data alone.

In terms of climate modeling, the study relied on downscaled outputs from a single Earth System Model (MPI-ESM1.2) to generate mid-century projections. While this model is widely regarded for its accuracy and high spatial resolution, climate uncertainty could be further addressed by incorporating ensemble outputs from multiple General Circulation Models (GCMs) to account for inter-model variability. This would help better quantify the range of possible yield outcomes and strengthen the robustness of policy recommendations under different emission trajectories.

Looking forward, future research should aim to build on the methodological foundation established in this dissertation by pursuing several key directions. First, there is a need to couple real-time snowmelt monitoring with dynamic irrigation scheduling systems that can inform water release decisions in near real-time. This would require integrating remote sensing platforms, meteorological stations, and decision-support tools into a unified platform accessible to both farmers and planners. Second, exploring the feasibility of integrating unmanned aerial vehicle (UAV)-based snow and soil moisture monitoring could provide high-resolution, real-time data that complements satellite-based assessments, especially in heterogeneous or cloud-prone areas.

Third, expanding the spatial scope of the study to cover other districts in Northern Kazakhstan or across Central Asia would allow for the testing of model transferability and the identification of regional adaptation corridors. Additionally, interdisciplinary collaborations that involve agronomists, hydrologists, social scientists, and local stakeholders would enrich the

scientific and practical impact of future studies. Such efforts could include cost-benefit analyses of pond construction, long-term monitoring of pond performance, and surveys to assess the socio-economic impacts of snowmelt-based irrigation on rural livelihoods.

Ultimately, the limitations identified here do not undermine the contributions of this dissertation but rather highlight the complex, multifaceted nature of climate resilience in agriculture. Addressing these challenges through continued research, innovation, and stakeholder engagement will be essential for turning the promise of snowmelt harvesting into a practical and scalable solution for climate adaptation in Kazakhstan and beyond.

Acknowledgements

I would like to express my deepest gratitude to my supervisor, Dr. Zoltán Kovács, for his invaluable guidance, unwavering support, and encouragement throughout the course of my PhD journey. His expertise, patience, and constructive feedback have been instrumental in shaping my academic development and research path. It has been a privilege to study under his supervision, and I am sincerely thankful for the opportunities and insights he has provided over these years.

I gratefully acknowledge the Hungarian government for awarding me the Stipendium Hungaricum scholarship, which made it possible for me to pursue doctoral studies in Hungary. This generous support not only enabled me to engage in meaningful research but also allowed me to grow personally and professionally while experiencing life in such a welcoming and culturally rich country.

My sincere appreciation also goes to the University of Szeged for offering a stimulating academic environment and excellent research facilities. I am thankful to all faculty members, administrative staff, and fellow doctoral candidates for their kindness, assistance, and camaraderie throughout my time in Szeged.

I extend special thanks to the Center for Technological Competence in Digitalization of the Agro-Industrial Complex at Kazakh Agrotechnical Research University. Their generous collaboration, providing access to equipment, drones, snowmobiles, and other logistical support, was critical for conducting snow surveys and generating ultra-high-resolution DEMs, which formed an essential part of this research. I am grateful for their professionalism, technical expertise, and cooperation.

Lastly, I owe profound thanks to my family, whose love and support have been my greatest source of strength. To my wife and my five-year-old son, thank you for your patience, encouragement, and unwavering belief in me, even during the most challenging times. To my parents, I am deeply grateful for everything you have done for me. Your sacrifices, values, and endless support have shaped who I am today.

This dissertation is a reflection of the collective contributions and kindness of all those mentioned above. To each of you, thank you from the bottom of my heart.

References

- Abdelhakim, L. O. A., Mendanha, T., Palma, C. F. F., Vrobel, O., Štefelová, N., Čavar Zeljković, S., Tarkowski, P., De Diego, N., Wollenweber, B., Rosenqvist, E., & Ottosen, C.-O. (2022). Elevated CO₂ Improves the Physiology but Not the Final Yield in Spring Wheat Genotypes Subjected to Heat and Drought Stress During Anthesis. *Frontiers in Plant Science*, 13. <https://www.frontiersin.org/articles/10.3389/fpls.2022.824476>
- Al-Abadi, A., Al-Shamma'a, A., & Aljabbari, M. (2014). A GIS-based DRASTIC model for assessing intrinsic groundwater vulnerability in northeastern Missan governorate, southern Iraq. *Applied Water Science*. <https://doi.org/10.1007/s13201-014-0221-7>
- Ali, M. H., Hoque, M. R., Hassan, A. A., & Khair, A. (2007). Effects of deficit irrigation on yield, water productivity, and economic returns of wheat. *Agricultural Water Management*, 92(3), 151–161. <https://doi.org/10.1016/j.agwat.2007.05.010>
- Alkolibi, F. (2002). Possible Effects of Global Warming on Agriculture and Water Resources in Saudi Arabia: Impacts and Responses. *Climatic Change*, 54, 225–245. <https://doi.org/10.1023/A:1015777403153>
- Alsafadi, K., Bi, S., Abdo, H. G., Almohamad, H., Alatrach, B., Srivastava, A. K., Al-Mutiry, M., Bal, S. K., Chandran, M. A. S., & Mohammed, S. (2023). Modeling the impacts of projected climate change on wheat crop suitability in semi-arid regions using the AHP-based weighted climatic suitability index and CMIP6. *Geoscience Letters*, 10(1), 20. <https://doi.org/10.1186/s40562-023-00273-y>
- Alwan, I. A., Aziz, N. A., & Hamoodi, M. N. (2020). Potential Water Harvesting Sites Identification Using Spatial Multi-Criteria Evaluation in Maysan Province, Iraq. *ISPRS International Journal of Geo-Information*, 9(4), Article 4. <https://doi.org/10.3390/ijgi9040235>
- Amthor, J. S. (2001). Effects of atmospheric CO₂ concentration on wheat yield: Review of results from experiments using various approaches to control CO₂ concentration. *Field Crops Research*, 73(1), 1–34. [https://doi.org/10.1016/S0378-4290\(01\)00179-4](https://doi.org/10.1016/S0378-4290(01)00179-4)
- Anbazhagan, S., & Ramasamy, S. (2006). Evaluation of Areas for Artificial Groundwater Recharge in Ayyar Basin, Tamil Nadu, India through Statistical Terrain Analysis. *Journal of Geological Society of India*. <https://www.semanticscholar.org/paper/Evaluation-of-Areas-for-Artificial-Groundwater-in-Anbazhagan-Ramasamy/f568b20629210a752a6149683c70b7dcebaae915>
- Andualem, T. G., & Demeke, G. G. (2019). Groundwater potential assessment using GIS and remote sensing: A case study of Guna tana landscape, upper blue Nile Basin, Ethiopia. *Journal of Hydrology: Regional Studies*, 24, 100610. <https://doi.org/10.1016/j.ejrh.2019.100610>
- Aouragh, M. H., ESSAHLAOUI, A., Abdelhadi, O., El Hmaidi, A., & Said, K. (2015). Using Remote Sensing and GIS-Multicriteria decision Analysis for Groundwater Potential

- Mapping in the Middle Atlas Plateaus, Morocco. *Research Journal of Recent Sciences*, 4, 1–9.
- Arisco, N. J., Sewe, M. O., Bärnighausen, T., Sié, A., Zabre, P., & Bunker, A. (2023). The effect of extreme temperature and precipitation on cause-specific deaths in rural Burkina Faso: A longitudinal study. *The Lancet Planetary Health*, 7(6), e478–e489. [https://doi.org/10.1016/S2542-5196\(23\)00027-X](https://doi.org/10.1016/S2542-5196(23)00027-X)
- Armstrong, R. L., & Brun, E. (Eds.). (2008). *Snow and climate: Physical processes, surface energy exchange and modeling*. Cambridge University Press.
- Arulbalaji, P., Padmalal, D., & Sreelash, K. (2019). GIS and AHP Techniques Based Delineation of Groundwater Potential Zones: A case study from Southern Western Ghats, India. *Scientific Reports*, 9(1), 2082. <https://doi.org/10.1038/s41598-019-38567-x>
- Asadabadi, M., Chang, E., & Saberi, M. (2019). Are MCDM methods useful? A critical review of Analytic Hierarchy Process (AHP) and Analytic Network Process (ANP). *Cogent Engineering*. <https://doi.org/10.1080/23311916.2019.1623153>
- Attia, A., El-Hendawy, S., Al-Suhaibani, N., Tahir, M. U., Mubushar, M., Vianna, M. dos S., Ullah, H., Mansour, E., & Datta, A. (2021). Sensitivity of the DSSAT model in simulating maize yield and soil carbon dynamics in arid Mediterranean climate: Effect of soil, genotype and crop management. *Field Crops Research*, 260(107981). <https://doi.org/10.1016/j.fcr.2020.107981>
- Ayan, B., Abacioğlu, S., & Basilio, M. P. (2023). A Comprehensive Review of the Novel Weighting Methods for Multi-Criteria Decision-Making. *Information*, 14(5), Article 5. <https://doi.org/10.3390/info14050285>
- Bakhshandeh, E., Zeraatpisheh, M., Soleimani, A., & Francaviglia, R. (2022). Land use conversion, climate change and soil organic carbon: Modeling a citrus garden chronosequence in Northern Iran. *Geoderma Regional*, 30, e00559. <https://doi.org/10.1016/j.geodrs.2022.e00559>
- Balkhair, K. S., & Ur Rahman, K. (2021). Development and assessment of rainwater harvesting suitability map using analytical hierarchy process, GIS and RS techniques. *Geocarto International*, 36(4), 421–448. <https://doi.org/10.1080/10106049.2019.1608591>
- Barnett, T. P., Adam, J. C., & Lettenmaier, D. P. (2005). Potential impacts of a warming climate on water availability in snow-dominated regions. *Nature*, 438(7066), Article 7066. <https://doi.org/10.1038/nature04141>
- Barton, J. S., Hall, D. K., & Riggs, G. A. (2000). Remote sensing of fractional snow cover using Moderate Resolution Imaging Spectroradiometer (MODIS) data. *Proceedings of the 57th Eastern Snow Conference*, 171–181.
- Batjes, N. H., Ribeiro, E., & van Oostrum, A. (2020). Standardised soil profile data to support global mapping and modelling (WoSIS snapshot 2019). *Earth System Science Data*, 12(1), 299–320. <https://doi.org/10.5194/essd-12-299-2020>

- Berezhnaya, Y. (2020, January 31). *Residents of Northern Kazakhstan are afraid of a repeat of the unprecedented flood*. Sputnik Kazakhstan. <https://ru.sputnik.kz/20200131/severnyi-kazakhstan-povtorenie-pavodok-12714711.html>
- Berhanu, K. G., & Hatiye, S. D. (2020). Identification of Groundwater Potential Zones Using Proxy Data: Case study of Megech Watershed, Ethiopia. *Journal of Hydrology: Regional Studies*, 28, 100676. <https://doi.org/10.1016/j.ejrh.2020.100676>
- Brisson, N., Gary, C., Justes, E., Roche, R., Mary, B., Ripoche, D., Zimmer, D., Sierra, J., Bertuzzi, P., Burger, P., Bussi re, F., Cabidoche, Y. M., Cellier, P., Debaeke, P., Gaudill re, J. P., H nault, C., Maraux, F., Seguin, B., & Sinoquet, H. (2003). An overview of the crop model stics. *European Journal of Agronomy*, 18(3), 309–332. [https://doi.org/10.1016/S1161-0301\(02\)00110-7](https://doi.org/10.1016/S1161-0301(02)00110-7)
- Broberg, M. C., H gy, P., Feng, Z., & Pleijel, H. (2019). Effects of Elevated CO₂ on Wheat Yield: Non-Linear Response and Relation to Site Productivity. *Agronomy*, 9(5), Article 5. <https://doi.org/10.3390/agronomy9050243>
- Brunelli, M. (2015). *Introduction to the Analytic Hierarchy Process*. Springer International Publishing. <https://doi.org/10.1007/978-3-319-12502-2>
- Bureau of National Statistics, Agency for Strategic Planning and Reforms of the Republic of Kazakhstan. (2023, January 31). *Gross harvest of agricultural crops in the Republic of Kazakhstan (2022)*. <https://stat.gov.kz/ru/industries/business-statistics/stat-forrest-village-hunt-fish/publications/5099/>
- Carver, S. (1991). Carver, S.J.: Integrating Multi-Criteria Evaluation with Geographical Information Systems. *International Journal of Geographic Information System* 5(3), 321–339. *International Journal of Geographical Information Science*, 5, 321–339. <https://doi.org/10.1080/02693799108927858>
- Chauhan, B., Kaur, P., Mahajan, G., Kaur, D., Singh, H., & Kang, M. (2014). Global Warming and Its Possible Impact on Agriculture in India. In *Advances in Agronomy* (Vol. 123, pp. 65–121). <https://doi.org/10.1016/B978-0-12-420225-2.00002-9>
- Chou, W.-W., Lee, S.-H., & Wu, C.-F. (2014). Evaluation of the Preservation Value and Location of Farm Ponds in Yunlin County, Taiwan. *International Journal of Environmental Research and Public Health*, 11(1), Article 1. <https://doi.org/10.3390/ijerph110100548>
- Chowdhury, M., & Paul, P. K. (2021). Identification of suitable sites for rainwater harvesting using fuzzy AHP and fuzzy gamma operator: A case study. *Arabian Journal of Geosciences*, 14(7), 585. <https://doi.org/10.1007/s12517-021-06607-4>
- Chung, C.-J., & Fabbri, A. (2003). Validation of Spatial Prediction Models for Landslide Hazard Mapping. *Natural Hazards*, 30, 451–472. <https://doi.org/10.1023/B:NHAZ.00000007172.62651.2b>
- Daloz, A. S., Rydsaa, J. H., Hodnebrog,  ., Sillmann, J., van Oort, B., Mohr, C. W., Agrawal, M., Emberson, L., Stordal, F., & Zhang, T. (2021). Direct and indirect impacts of climate

- change on wheat yield in the Indo-Gangetic plain in India. *Journal of Agriculture and Food Research*, 4, 100132. <https://doi.org/10.1016/j.jafr.2021.100132>
- de Jager, J. M., Potgieter, A. B., & van den Berg, W. J. (1998). Framework for forecasting the extent and severity of drought in maize in the Free State Province of South Africa. *Agricultural Systems*, 57(3), 351–365. [https://doi.org/10.1016/S0308-521X\(98\)00023-7](https://doi.org/10.1016/S0308-521X(98)00023-7)
- Dietz, A. J., Kuenzer, C., Gessner, U., & Dech, S. (2012). Remote sensing of snow—A review of available methods. *International Journal of Remote Sensing*, 33, 4094–4134. <https://doi.org/10.1080/01431161.2011.640964>
- Dixit, A., Goswami, A., & Jain, S. (2019). Development and Evaluation of a New “Snow Water Index (SWI)” for Accurate Snow Cover Delineation. *Remote Sensing*, 11(23), 2774. <https://doi.org/10.3390/rs11232774>
- Doke, A., Zolekar, R., Patel, H., & Das, S. (2021). Geospatial mapping of groundwater potential zones using multi-criteria decision-making AHP approach in a hardrock basaltic terrain in India. *Ecological Indicators*, 127, 107685. <https://doi.org/10.1016/j.ecolind.2021.107685>
- Donatelli, M., Cerrani, I., Fanchini, D., Fumagalli, D., & Rizzoli, A. (2012). *Enhancing Model Reuse via Component-Centered Modeling Frameworks: The Vision and Example Realizations*. <https://www.semanticscholar.org/paper/Enhancing-Model-Reuse-via-Component-Centered-the-Donatelli-Cerrani/d57b07acb7500e6d5154694a5c05297ad5ec9247>
- Dong, C. (2018). Remote sensing, hydrological modeling and in situ observations in snow cover research: A review. *Journal of Hydrology*, 561, 573–583. <https://doi.org/10.1016/j.jhydrol.2018.04.027>
- Dozier, J. (1989). Spectral signature of alpine snow cover from the landsat thematic mapper. *Remote Sensing of Environment*, 28, 9–22. [https://doi.org/10.1016/0034-4257\(89\)90101-6](https://doi.org/10.1016/0034-4257(89)90101-6)
- Duan, Y., Luo, M., Guo, X., Cai, P., & Li, F. (2021). Study on the Relationship between Snowmelt Runoff for Different Latitudes and Vegetation Growth Based on an Improved SWAT Model in Xinjiang, China. *Sustainability*, 13(3), Article 3. <https://doi.org/10.3390/su13031189>
- Dubovyk, O., Ghazaryan, G., González, J., Graw, V., Löw, F., & Schreier, J. (2019). Drought hazard in Kazakhstan in 2000–2016: A remote sensing perspective. *Environmental Monitoring and Assessment*, 191(8), 510. <https://doi.org/10.1007/s10661-019-7620-z>
- Ejaz Qureshi, M., Hanjra, M. A., & Ward, J. (2013). Impact of water scarcity in Australia on global food security in an era of climate change. *Food Policy*, 38, 136–145. <https://doi.org/10.1016/j.foodpol.2012.11.003>
- Elboshy, B., Alwetaishi, M., M. H. Aly, R., & Zalhaf, A. S. (2022). A suitability mapping for the PV solar farms in Egypt based on GIS-AHP to optimize multi-criteria feasibility. *Ain Shams Engineering Journal*, 13(3), 101618. <https://doi.org/10.1016/j.asej.2021.10.013>

- Engel, T., Hoogenboom, G., Jones, J. W., & Wilkens, P. W. (1997). AEGIS/WIN: A Computer Program for the Application of Crop Simulation Models Across Geographic Areas. *Agronomy Journal*, 89(6), 919–928.
<https://doi.org/10.2134/agronj1997.00021962008900060012x>
- English, M. (1990). Deficit Irrigation. I: Analytical Framework. *Journal of Irrigation and Drainage Engineering*, 116(3), 399–412. [https://doi.org/10.1061/\(ASCE\)0733-9437\(1990\)116:3\(399\)](https://doi.org/10.1061/(ASCE)0733-9437(1990)116:3(399))
- Esavi, V., Karami, J., Alimohammadi, A., & Niknezhad, S. A. (2012). Comparison the AHP and FUZZY-AHP Decision Making Methods in Underground DAM Site Selection in Taleghan Basin. *Scientific Quarterly Journal of Geosciences*, 22(85), 27–34.
<https://doi.org/10.22071/gsj.2012.54018>
- Etikala, B., Golla, V., Li, P., & Renati, S. (2019). Deciphering groundwater potential zones using MIF technique and GIS: A study from Tirupati area, Chittoor District, Andhra Pradesh, India. *HydroResearch*, 1, 1–7. <https://doi.org/10.1016/j.hydres.2019.04.001>
- Fraga, H., Costa, R., Moutinho Pereira, J., Correia, C., L-T, D., Gonçalves, I., Silvestre, J., Eiras-Dias, J., Malheiro, A., & Santos, J. (2015). Modeling Phenology, Water Status and Yield Components of Three Portuguese Grapevines Using the STICS Crop Model. *American Journal of Enology and Viticulture*. <https://doi.org/10.5344/ajev.2015.15031>
- Furtak, K., & Wolińska, A. (2023). The impact of extreme weather events as a consequence of climate change on the soil moisture and on the quality of the soil environment and agriculture – A review. *CATENA*, 231, 107378.
<https://doi.org/10.1016/j.catena.2023.107378>
- Gan, Y., Zhang, Y., Kongoli, C., Grassotti, C., Liu, Y., Lee, Y.-K., & Seo, D.-J. (2021). Evaluation and blending of ATMS and AMSR2 snow water equivalent retrievals over the conterminous United States. *Remote Sensing of Environment*, 254, 112280.
<https://doi.org/10.1016/j.rse.2020.112280>
- Geerts, S., & Raes, D. (2009). Deficit irrigation as an on-farm strategy to maximize crop water productivity in dry areas. *Agricultural Water Management*, 96(9), 1275–1284.
<https://doi.org/10.1016/j.agwat.2009.04.009>
- Gigović, L., Pamučar, D., Bajić, Z., & Drobnjak, S. (2017). Application of GIS-Interval Rough AHP Methodology for Flood Hazard Mapping in Urban Areas. *Water*, 9(6), Article 6.
<https://doi.org/10.3390/w9060360>
- Gömann, H. (2015). How Much did Extreme Weather Events Impact Wheat Yields in Germany? - A Regionally Differentiated Analysis on the Farm Level. *Procedia Environmental Sciences*, 29, 119–120. <https://doi.org/10.1016/j.proenv.2015.07.197>
- Gomboš, M., Pavelková, D., Kandra, B., & Tall, A. (2019). Impact of Soil Texture and Position of Groundwater Level on Evaporation from the Soil Root Zone. In A. M. Negm & M. Zeleňáková (Eds.), *Water Resources in Slovakia: Part I: Assessment and Development* (pp. 167–181). Springer International Publishing. https://doi.org/10.1007/698_2017_181

- Govindaraj, M., Vetriventhan, M., & Srinivasan, M. (2015). Importance of genetic diversity assessment in crop plants and its recent advances: An overview of its analytical perspectives. *Genetics Research International*, 2015, 431487. <https://doi.org/10.1155/2015/431487>
- Grassini, P., Cassman, K. G., & van Ittersum, M. (2017). *Exploring Maize Intensification with the Global Yield Gap Atlas*. 101(2).
- Groffman, P. M., Driscoll, C. T., Fahey, T. J., Hardy, J. P., Fitzhugh, R. D., & Tierney, G. L. (2001). Colder soils in a warmer world: A snow manipulation study in a northern hardwood forest ecosystem. *Biogeochemistry*, 56(2), 135–150. <https://doi.org/10.1023/A:1013039830323>
- Guitouni, A., & Martel, J.-M. (1998). Tentative guidelines to help choosing an appropriate MCDA method. *European Journal of Operational Research*, 109(2), 501–521. [https://doi.org/10.1016/S0377-2217\(98\)00073-3](https://doi.org/10.1016/S0377-2217(98)00073-3)
- Gutjahr, O., Putrasahan, D., Lohmann, K., Jungclaus, J. H., von Storch, J.-S., Brüggemann, N., Haak, H., & Stössel, A. (2019). Max Planck Institute Earth System Model (MPI-ESM1.2) for the High-Resolution Model Intercomparison Project (HighResMIP). *Geoscientific Model Development*, 12(7), 3241–3281. <https://doi.org/10.5194/gmd-12-3241-2019>
- Hadley, K., Talbott, J., Reddy, S., & Wheat, S. (2023). Impacts of climate change on food security and resulting perinatal health impacts. *Seminars in Perinatology*, 151842. <https://doi.org/10.1016/j.semperi.2023.151842>
- Hajkowicz, S., & Higgins, A. (2008). A Comparison of Multiple Criteria Analysis Techniques for Water Resource Management. *European Journal of Operational Research*, 184, 255–265. <https://doi.org/10.1016/j.ejor.2006.10.045>
- Hall, D. K., Foster, J. L., Verbyla, D. L., Klein, A. G., & Benson, C. S. (1998). Assessment of Snow-Cover Mapping Accuracy in a Variety of Vegetation-Cover Densities in Central Alaska. *Remote Sensing of Environment*, 66(2), 129–137. [https://doi.org/10.1016/S0034-4257\(98\)00051-0](https://doi.org/10.1016/S0034-4257(98)00051-0)
- Hall, D. K., Riggs, G. A., & Salomonson, V. V. (1995). Development of methods for mapping global snow cover using moderate resolution imaging spectroradiometer data. *Remote Sensing of Environment*, 54(2), 127–140. [https://doi.org/10.1016/0034-4257\(95\)00137-P](https://doi.org/10.1016/0034-4257(95)00137-P)
- Hall, D. K., Riggs, G. A., Salomonson, V. V., DiGirolamo, N. E., & Bayr, K. J. (2002). MODIS snow-cover products. *Remote Sensing of Environment*, 83(1), 181–194. [https://doi.org/10.1016/S0034-4257\(02\)00095-0](https://doi.org/10.1016/S0034-4257(02)00095-0)
- Hammer, G. L., Hansen, J. W., Phillips, J. G., Mjelde, J. W., Hill, H., Love, A., & Potgieter, A. (2001). Advances in application of climate prediction in agriculture. *Agricultural Systems*, 70(2), 515–553. [https://doi.org/10.1016/S0308-521X\(01\)00058-0](https://doi.org/10.1016/S0308-521X(01)00058-0)
- Hansen, J. W., Potgieter, A., & Tippet, M. K. (2004). Using a general circulation model to forecast regional wheat yields in northeast Australia. *Agricultural and Forest Meteorology*, 127(1), 77–92. <https://doi.org/10.1016/j.agrformet.2004.07.005>

- Höök, M., Sivertsson, A., & Aleklett, K. (2010). Validity of the Fossil Fuel Production Outlooks in the IPCC Emission Scenarios. *Natural Resources Research*, 19, 63–81.
<https://doi.org/10.1007/s11053-010-9113-1>
- Ilbeyi, A., Ustun, H., Oweis, T., Pala, M., & Benli, B. (2006). Wheat water productivity and yield in a cool highland environment: Effect of early sowing with supplemental irrigation. *Agricultural Water Management*, 82(3), 399–410.
<https://doi.org/10.1016/j.agwat.2005.08.005>
- IPCC. (n.d.). *IPCC 5th Assessment Synthesis Report “Future changes, risks and impacts.”* IPCC 5th Assessment Synthesis Report. Retrieved November 7, 2023, from http://ar5-syr.ipcc.ch/topic_futurechanges.php
- Jenssen, R. O. R., & Jacobsen, S. K. (2021). Measurement of Snow Water Equivalent Using Drone-Mounted Ultra-Wide-Band Radar. *Remote Sensing*, 13(13), Article 13.
<https://doi.org/10.3390/rs13132610>
- Jha, M., Chowdary, V., & Chowdhury, A. (2010). Groundwater assessment in Salboni Block, West Bengal (India) using remote sensing, geographical information system and multi-criteria decision analysis techniques. *Hydrogeology Journal*, 18, 1713–1728.
<https://doi.org/10.1007/s10040-010-0631-z>
- Jones, H. G., Pomeroy, J. W., Walker, D. A., & Hoham, R. W. (2001). *Snow Ecology: An Interdisciplinary Examination of Snow-Covered Ecosystems*. Cambridge University Press.
- Jozaghi, A., Alizadeh, B., Hatami, M., Flood, I., Khorrami, M., Khodaei, N., & Ghasemi Tousi, E. (2018). A Comparative Study of the AHP and TOPSIS Techniques for Dam Site Selection Using GIS: A Case Study of Sistan and Baluchestan Province, Iran. *Geosciences*, 8(12), Article 12. <https://doi.org/10.3390/geosciences8120494>
- Kabir, M., Habiba, U. E., Khan, W., Shah, A., Rahim, S., Rios-Escalante, P. R. D. los, Farooqi, Z.-U.-R., Ali, L., & Shafiq, M. (2023). Climate change due to increasing concentration of carbon dioxide and its impacts on environment in 21st century; a mini review. *Journal of King Saud University - Science*, 35(5), 102693.
<https://doi.org/10.1016/j.jksus.2023.102693>
- Kadam, A., Kale, S., Pande, N., Pawar, N., & Sankhua, R. (2012). Identifying Potential Rainwater Harvesting Sites of a Semi-arid, Basaltic Region of Western India, Using SCS-CN Method. *Water Resources Management: An International Journal, Published for the European Water Resources Association (EWRA)*, 26(9), 2537–2554.
- Kang, S., Zhang, L., Liang, Y., Hu, X., Cai, H., & Gu, B. (2002). Effects of limited irrigation on yield and water use efficiency of winter wheat in the Loess Plateau of China. *Agricultural Water Management*, 55(3), 203–216. [https://doi.org/10.1016/S0378-3774\(01\)00180-9](https://doi.org/10.1016/S0378-3774(01)00180-9)
- Karatayev, M., Clarke, M., Salnikov, V., Bekseitova, R., & Nizamova, M. (2022). Monitoring climate change, drought conditions and wheat production in Eurasia: The case study of Kazakhstan. *Heliyon*, 8(1), e08660. <https://doi.org/10.1016/j.heliyon.2021.e08660>

- Karthikeyan, R., Venkatesan, K., & Chandrasekar, A. (2019). A Comparison of Strengths and Weaknesses for Analytical Hierarchy Process. *Journal of Chemical and Pharmaceutical Sciences*, 9, S-12 S.
- Kim, D., Jung, H.-S., & Kim, J.-C. (2017). Comparison of Snow Cover Fraction Functions to Estimate Snow Depth of South Korea from MODIS Imagery. *Korean Journal of Remote Sensing*, 33(4), 401–410. <https://doi.org/10.7780/kjrs.2017.33.4.6>
- Kumar, R., Manzoor, S., Vishwakarma, D. K., Al-Ansari, N., Kushwaha, N. L., Elbeltagi, A., Sushanth, K., Prasad, V., & Kuriqi, A. (2022). Assessment of Climate Change Impact on Snowmelt Runoff in Himalayan Region. *Sustainability*, 14(3), Article 3. <https://doi.org/10.3390/su14031150>
- Lal, H., Calixte, J.-P., Jones, J., & Beinroth, F. (1993). Using Crop Simulation Models and GIS for Regional Productivity Analysis. *Transactions of the ASAE*, 36, 175–184. <https://doi.org/10.13031/2013.28328>
- Lemmetyinen, J., Kontu, A., Pulliainen, J., Vehviläinen, J., Rautiainen, K., Wiesmann, A., Mätzler, C., Werner, C., Rott, H., Nagler, T., Schneebeli, M., Proksch, M., Schüttemeyer, D., Kern, M., & Davidson, M. W. J. (2016). Nordic Snow Radar Experiment. *Geoscientific Instrumentation, Methods and Data Systems*, 5(2), 403–415. <https://doi.org/10.5194/gi-5-403-2016>
- Lentswe, G., & Molwalefhe, L. (2020). Delineation of potential groundwater recharge zones using analytic hierarchy process-guided GIS in the semi-arid Motloutse watershed, eastern Botswana. *Journal of Hydrology: Regional Studies*, 28. <https://doi.org/10.1016/j.ejrh.2020.100674>
- Lettenmaier, D. P., Alsdorf, D., Dozier, J., Huffman, G. J., Pan, M., & Wood, E. F. (2015). Inroads of remote sensing into hydrologic science during the WRR era. *Water Resources Research*, 51(9), 7309–7342. <https://doi.org/10.1002/2015WR017616>
- Lin, J., Feng, X., Xiao, P., Li, H., Wang, J., & Li, Y. (2012). Comparison of Snow Indexes in Estimating Snow Cover Fraction in a Mountainous Area in Northwestern China. *IEEE Geoscience and Remote Sensing Letters - IEEE GEOSCI REMOTE SENS LETT*, 9, 725–729. <https://doi.org/10.1109/LGRS.2011.2179634>
- Liu, J., Williams, J. R., Zehnder, A. J. B., & Yang, H. (2007). GEPIC – modelling wheat yield and crop water productivity with high resolution on a global scale. *Agricultural Systems*, 94(2), 478–493. <https://doi.org/10.1016/j.agsy.2006.11.019>
- Long, X.-X., Ju, H., Wang, J.-D., Gong, S.-H., & Li, G.-Y. (2022). Impact of climate change on wheat yield and quality in the Yellow River Basin under RCP8.5 during 2020–2050. *Advances in Climate Change Research*, 13(3), 397–407. <https://doi.org/10.1016/j.accre.2022.02.006>
- Magesh, S., Chandrasekar, N., & Prince, J. (2012). Delineation of groundwater potential zones in Theni district, Tamil Nadu, using remote sensing, GIS and MIF techniques. *Geoscience Frontiers*, 3, 189–196. <https://doi.org/10.1016/j.gsf.2011.10.007>

- Maina, C., & Raude, J. (2016). Assessing Land Suitability for Rainwater Harvesting Using Geospatial Techniques: A Case Study of Njoro Catchment, Kenya. *Applied and Environmental Soil Science*, 2016, 1–9. <https://doi.org/10.1155/2016/4676435>
- Malczewski, J. (2006). GIS-based multicriteria decision analysis: A survey of the literature. *International Journal Geographical Information Science*, 20, 703–726. <https://doi.org/10.1080/13658810600661508>
- Malhi, G. S., Kaur, M., & Kaushik, P. (2021). Impact of Climate Change on Agriculture and Its Mitigation Strategies: A Review. *Sustainability*, 13(3), Article 3. <https://doi.org/10.3390/su13031318>
- Mehdaoui, R., Anane, M., Cañas Kurz, E. E., Hellriegel, U., & Hoinkis, J. (2022). Geospatial Multi-Criteria Approach for Ranking Suitable Shallow Aquifers for the Implementation of an On-Farm Solar-PV Desalination System for Sustainable Agriculture. *Sustainability*, 14(13), Article 13. <https://doi.org/10.3390/su14138113>
- Mekdaschi Studer, R., & Liniger, H. (2013). *Water Harvesting: Guidelines to Good Practice*.
- Melese, T., & Belay, T. (2022). Groundwater Potential Zone Mapping Using Analytical Hierarchy Process and GIS in Muga Watershed, Abay Basin, Ethiopia. *Global Challenges*, 6(1), 2100068. <https://doi.org/10.1002/gch2.202100068>
- Mirzabaev, A., Bezner Kerr, R., Hasegawa, T., Pradhan, P., Wreford, A., Cristina Tirado von der Pahlen, M., & Gurney-Smith, H. (2023). Severe climate change risks to food security and nutrition. *Climate Risk Management*, 39, 100473. <https://doi.org/10.1016/j.crm.2022.100473>
- Mishra, A., Hansen, J. W., Dingkuhn, M., Baron, C., Traoré, S. B., Ndiaye, O., & Ward, M. N. (2008). Sorghum yield prediction from seasonal rainfall forecasts in Burkina Faso. *Agricultural and Forest Meteorology*, 148(11), 1798–1814. <https://doi.org/10.1016/j.agrformet.2008.06.007>
- Mote, P. W., Hamlet, A. F., Clark, M. P., & Lettenmaier, D. P. (2005). DECLINING MOUNTAIN SNOWPACK IN WESTERN NORTH AMERICA*. *Bulletin of the American Meteorological Society*, 86(1), 39–50. <https://doi.org/10.1175/BAMS-86-1-39>
- Mubeen, M., Ahmad, A., Hammad, H. M., Awais, M., Farid, H. U., Saleem, M., Din, M. S. U., Amin, A., Ali, A., Fahad, S., & Nasim, W. (2020). Evaluating the climate change impact on water use efficiency of cotton-wheat in semi-arid conditions using DSSAT model. *Journal of Water and Climate Change*, 11(4), 1661–1675. <https://doi.org/10.2166/wcc.2019.179>
- Murken, L., & Gornott, C. (2022). The importance of different land tenure systems for farmers' response to climate change: A systematic review. *Climate Risk Management*, 35, 100419. <https://doi.org/10.1016/j.crm.2022.100419>
- Murmu, P., Kumar, M., Lal, D., Sonker, I., & Singh, S. K. (2019). Delineation of groundwater potential zones using geospatial techniques and analytical hierarchy process in Dumka district, Jharkhand, India. *Groundwater for Sustainable Development*, 9, 100239. <https://doi.org/10.1016/j.gsd.2019.100239>

- Musa, J. J., Anijofor, S. C., Obasa, P., & Avwevuruvwe, J. J. (2017). Effects of soil physical properties on erodibility and infiltration parameters of selected areas in Gidan Kwano. *Nigerian Journal of Technological Research*, 12(1), Article 1. <https://doi.org/10.4314/njtr.v12i1.8>
- Negi, H., Kulkarni, A., & Semwal, B. (2009). Study of contaminated and mixed objects snow reflectance in Indian Himalaya using spectroradiometer. *International Journal of Remote Sensing*, 30, 315–325. <https://doi.org/10.1080/01431160802261197>
- Negi, H. S., Singh, S. K., Kulkarni, A. V., & Semwal, B. S. (2010). Field-based spectral reflectance measurements of seasonal snow cover in the Indian Himalaya. *International Journal of Remote Sensing*, 31(9), 2393–2417. <https://doi.org/10.1080/01431160903002417>
- Ngaba, M. J. Y., Uwiragiye, Y., Bol, R., de Vries, W., Jian, J., & Zhou, J. (2023). Global cross-biome patterns of soil respiration responses to individual and interactive effects of nitrogen addition, altered precipitation, and warming. *Science of The Total Environment*, 858, 159808. <https://doi.org/10.1016/j.scitotenv.2022.159808>
- Nolan, B., Healy, R., Taber, P., Perkins, K., Hitt, K., & Wolock, D. (2006). *Factors influencing groundwater recharge in the eastern United States*. <https://www.semanticscholar.org/paper/Factors-influencing-groundwater-recharge-in-the-Nolan-Healy/71f78873853b429dc9b7913858c4afa432e65b9c>
- Noorollahi, E., Fadaei, D., Akbarpour Shirazi, M., & Ghodsipour, S. H. (2016). Land Suitability Analysis for Solar Farms Exploitation Using GIS and Fuzzy Analytic Hierarchy Process (FAHP)—A Case Study of Iran. *Energies*, 9(8), Article 8. <https://doi.org/10.3390/en9080643>
- North Kazakhstan Agricultural Experimental Station. (2022, February 1). *Features of cultivation of agricultural crops in the North Kazakhstan region" for 2022*. <https://sk-shos.kz/>
- Nugroho, A. D., Prasada, I. Y., & Lakner, Z. (2023). Comparing the effect of climate change on agricultural competitiveness in developing and developed countries. *Journal of Cleaner Production*, 406, 137139. <https://doi.org/10.1016/j.jclepro.2023.137139>
- Nunes, L. J. R. (2023). The Rising Threat of Atmospheric CO₂: A Review on the Causes, Impacts, and Mitigation Strategies. *Environments*, 10(4), Article 4. <https://doi.org/10.3390/environments10040066>
- Nurbatsina, A., Salavatova, Z., Tursunova, A., Didovets, I., Huthoff, F., Rodrigo-Clavero, M.-E., & Rodrigo-Ilarri, J. (2025). Flood Modelling of the Zhabay River Basin Under Climate Change Conditions. *Hydrology*, 12(2), Article 2. <https://doi.org/10.3390/hydrology12020035>
- Ongdas, N., Akiyanova, F., Karakulov, Y., Muratbayeva, A., & Zinabdin, N. (2020). Application of HEC-RAS (2D) for Flood Hazard Maps Generation for Yesil (Ishim) River in Kazakhstan. *Water*, 12(10), Article 10. <https://doi.org/10.3390/w12102672>

- Ouma, Y. O., & Tateishi, R. (2014). Urban Flood Vulnerability and Risk Mapping Using Integrated Multi-Parametric AHP and GIS: Methodological Overview and Case Study Assessment. *Water*, 6(6), Article 6. <https://doi.org/10.3390/w6061515>
- Pandey, V., Sharma, M., Deeba, F., Maurya, V. K., Gupta, S. K., Singh, S. P., Mishra, A., & Nautiyal, C. S. (2017). Impact of Elevated CO₂ on Wheat Growth and Yield under Free Air CO₂ Enrichment. *American Journal of Climate Change*, 6(4), Article 4. <https://doi.org/10.4236/ajcc.2017.64029>
- Pangapanga-Phiri, I., & Mungatana, E. D. (2021). Adoption of climate-smart agricultural practices and their influence on the technical efficiency of maize production under extreme weather events. *International Journal of Disaster Risk Reduction*, 61, 102322. <https://doi.org/10.1016/j.ijdr.2021.102322>
- Patrick, E. (2017). *Drought characterization and management in Central Asia Region and Turkey*. FAO. <https://www.fao.org/documents/card/en/c/d2da11f3-4d0c-4f30-ab8d-fe6a0cd348ab/>
- Perondi, D., de Souza Nôia Júnior, R., Zotarelli, L., Mulvaney, M. J., & Fraisse, C. W. (2022). Soybean maturity groups and sowing dates to minimize ENSO and extreme weather events effects on yield variability in the Southeastern US. *Agricultural and Forest Meteorology*, 324, 109104. <https://doi.org/10.1016/j.agrformet.2022.109104>
- Pielke Jr., R., Burgess, M. G., & Ritchie, J. (2021). *Most plausible 2005-2040 emissions scenarios project less than 2.5 degrees C of warming by 2100*. SocArXiv. <https://doi.org/10.31235/osf.io/m4fdu>
- Pilon, C. E., Côté, B., & Fyles, J. W. (1994). Effect of snow removal on leaf water potential, soil moisture, leaf and soil nutrient status and leaf peroxidase activity of sugar maple. *Plant and Soil*, 162(1), 81–88. <https://doi.org/10.1007/BF01416092>
- Popova, V. V., Morozova, P. A., Titkova, T. B., Semenov, V. A., Cherenkova, E. A., Shiryayeva, A. V., & Kitaev, L. M. (2015). Regional features of present winter snow accumulation variability in the North Eurasia from data of observations, reanalysis and satellites. *Ice and Snow*, 55(4), Article 4. <https://doi.org/10.15356/2076-6734-2015-4-73-86>
- Powell, J. P., & Reinhard, S. (2016). Measuring the effects of extreme weather events on yields. *Weather and Climate Extremes*, 12, 69–79. <https://doi.org/10.1016/j.wace.2016.02.003>
- Rahman, A. (2017). Recent Advances in Modelling and Implementation of Rainwater Harvesting Systems towards Sustainable Development. *Water*, 9(12), Article 12. <https://doi.org/10.3390/w9120959>
- Raihan, A., & Tuspekova, A. (2022). Dynamic impacts of economic growth, energy use, urbanization, agricultural productivity, and forested area on carbon emissions: New insights from Kazakhstan. *World Development Sustainability*, 1, 100019. <https://doi.org/10.1016/j.wds.2022.100019>
- Ravier, E., & Buoncristiani, J.-F. (2018). Chapter 12—Glaciohydrogeology. In J. Menzies & J. J. M. van der Meer (Eds.), *Past Glacial Environments (Second Edition)* (pp. 431–466). Elsevier. <https://doi.org/10.1016/B978-0-08-100524-8.00013-0>

- Rehman, A., Ma, H., & Ulucak, R. (2021). Sustainable development and pollution: The effects of CO₂ emission on population growth, food production, economic development, and energy consumption in Pakistan. *Environmental Science and Pollution Research*, 29. <https://doi.org/10.1007/s11356-021-16998-2>
- Romanov, P. (2003). Mapping and monitoring of the snow cover fraction over North America. *Journal of Geophysical Research*, 108(D16), 8619. <https://doi.org/10.1029/2002JD003142>
- Romanov, P., & Tarpley, D. (2004). Estimation of snow depth over open prairie environments using GOES imager observations. *Hydrological Processes*, 18, 1073–1087. <https://doi.org/10.1002/hyp.5508>
- Rood, S. B., Pan, J., Gill, K. M., Franks, C. G., Samuelson, G. M., & Shepherd, A. (2008). Declining summer flows of Rocky Mountain rivers: Changing seasonal hydrology and probable impacts on floodplain forests. *Journal of Hydrology*, 349(3), 397–410. <https://doi.org/10.1016/j.jhydrol.2007.11.012>
- Saaty, T. (2008). Decision making with the Analytic Hierarchy Process. *Int. J. Services Sciences*, 1, 83–98. <https://doi.org/10.1504/IJSSCI.2008.017590>
- Saaty, T. L. (1986). Axiomatic Foundation of the Analytic Hierarchy Process. *Management Science*, 32(7), 841–855. <http://dx.doi.org/10.1287/mnsc.32.7.841>
- Saaty, T., & Vargas, L. (2001). *Models, Methods, Concepts & Applications of the Analytic Hierarchy Process*. <https://doi.org/10.1007/978-1-4614-3597-6>
- Saboori, B., Radmehr, R., Zhang, Y. Y., & Zekri, S. (2022). A new face of food security: A global perspective of the COVID-19 pandemic. *Progress in Disaster Science*, 16, 100252. <https://doi.org/10.1016/j.pdisas.2022.100252>
- Salomonson, V. V., & Appel, I. (2004). Estimating fractional snow cover from MODIS using the normalized difference snow index. *Remote Sensing of Environment*, 89(3), 351–360. <https://doi.org/10.1016/j.rse.2003.10.016>
- Sarwar, A., Ahmad, S. R., Rehmani, M. I. A., Asif Javid, M., Gulzar, S., Shehzad, M. A., Shabbir Dar, J., Baazeem, A., Iqbal, M. A., Rahman, M. H. U., Skalicky, M., Brestic, M., & EL Sabagh, A. (2021). Mapping Groundwater Potential for Irrigation, by Geographical Information System and Remote Sensing Techniques: A Case Study of District Lower Dir, Pakistan. *Atmosphere*, 12(6), Article 6. <https://doi.org/10.3390/atmos12060669>
- Sayl, K., Adham, A., & Ritsema, C. J. (2020). A GIS-Based Multicriteria Analysis in Modeling Optimum Sites for Rainwater Harvesting. *Hydrology*, 7(3), Article 3. <https://doi.org/10.3390/hydrology7030051>
- Schlenker, W., Hanemann, W. M., & Fisher, A. C. (2006). The Impact of Global Warming on U.S. Agriculture: An Econometric Analysis of Optimal Growing Conditions. *The Review of Economics and Statistics*, 88(1), 113–125.
- Schmitt, J., Offermann, F., Söder, M., Frühauf, C., & Finger, R. (2022). Extreme weather events cause significant crop yield losses at the farm level in German agriculture. *Food Policy*, 112, 102359. <https://doi.org/10.1016/j.foodpol.2022.102359>

- Şener, E., Şener, Ş., & Davraz, A. (2018). Groundwater potential mapping by combining fuzzy-analytic hierarchy process and GIS in Beyşehir Lake Basin, Turkey. *Arabian Journal of Geosciences*, 11. <https://doi.org/10.1007/s12517-018-3510-x>
- Shaheen, H., Mustafa, A., & Ulfat, A. (2022). Chapter 6 - Crop production in response to elevated CO₂: Grain yield and quality. In F. Liu, X. Li, P. Hogg, D. Jiang, M. Brestic, & B. Liu (Eds.), *Sustainable Crop Productivity and Quality Under Climate Change* (pp. 91–101). Academic Press. <https://doi.org/10.1016/B978-0-323-85449-8.00009-9>
- Shelia, V., Hansen, J., Sharda, V., Porter, C., Aggarwal, P., Wilkerson, C. J., & Hoogenboom, G. (2019). A multi-scale and multi-model gridded framework for forecasting crop production, risk analysis, and climate change impact studies. *Environmental Modelling & Software*, 115, 144–154. <https://doi.org/10.1016/j.envsoft.2019.02.006>
- Shen, Z., Zhang, Q., Singh, V. P., Sun, P., Song, C., & Yu, H. (2019). Agricultural drought monitoring across Inner Mongolia, China: Model development, spatiotemporal patterns and impacts. *Journal of Hydrology*, 571, 793–804. <https://doi.org/10.1016/j.jhydrol.2019.02.028>
- Shmelev, S. E., Salnikov, V., Turulina, G., Polyakova, S., Tazhibayeva, T., Schnitzler, T., & Shmeleva, I. A. (2021). Climate Change and Food Security: The Impact of Some Key Variables on Wheat Yield in Kazakhstan. *Sustainability*, 13(15), Article 15. <https://doi.org/10.3390/su13158583>
- Shoukat, M. R., Cai, D., Shafeeque, M., Habib-ur-Rahman, M., & Yan, H. (2022). Warming Climate and Elevated CO₂ Will Enhance Future Winter Wheat Yields in North China Region. *Atmosphere*, 13(8), Article 8. <https://doi.org/10.3390/atmos13081275>
- Sindhu, S., Nehra, V., & Luthra, S. (2017). Investigation of feasibility study of solar farms deployment using hybrid AHP-TOPSIS analysis: Case study of India. *Renewable and Sustainable Energy Reviews*, 73, 496–511. <https://doi.org/10.1016/j.rser.2017.01.135>
- Smith, L. (2015). Hydrogeology☆. In *Reference Module in Earth Systems and Environmental Sciences* (p. B9780124095489094690). Elsevier. <https://doi.org/10.1016/B978-0-12-409548-9.09469-0>
- State Commission for Variety Testing of Agricultural Crops of the Ministry of Agriculture of the Republic of Kazakhstan. (2006). *Improved Shortlandy 95 wheat variety*. <https://sortcom.kz/%D0%A8%D0%9E%D0%A0%D0%A2%D0%90%D0%9D%D0%94%D0%98%D0%9D%D0%A1%D0%9A%D0%90%D0%AF-95-%D0%A3%D0%9B%D0%A3%D0%A7%D0%A8%D0%95%D0%9D%D0%9D%D0%90%D0%AF/>
- Steinbach, S. (2023). The Russia–Ukraine war and global trade reallocations. *Economics Letters*, 226, 111075. <https://doi.org/10.1016/j.econlet.2023.111075>
- Sturm, M. (2015, June 24). *White water: Fifty years of snow research in WRR and the outlook for the future*. <https://agupubs.onlinelibrary.wiley.com/doi/full/10.1002/2015WR017242>
- Subbarayan, S., Thiagarajan, S., Jesudasan, J., Singh, L., Ayyakkanu, S., & Devanatham, A. (2020). Delineation of groundwater potential zone using analytical hierarchy process and

- GIS for Gundihalla watershed, Karnataka, India. *Arabian Journal of Geosciences*, 13. <https://doi.org/10.1007/s12517-020-05712-0>
- Sugiura, T., Sumida, H., Yokoyama, S., & Ono, H. (2012). Overview of Recent Effects of Global Warming on Agricultural Production in Japan. *Japan Agricultural Research Quarterly: JARQ*, 46(1), 7–13. <https://doi.org/10.6090/jarq.46.7>
- Suleimenov, M., Saparov, A., Akshalov, K., & Kaskarbayev, Z. (2012). Land Degradation Issues in Kazakhstan and Measures to Address Them: *Land Degradation and Pedology*, 55(3), 373–381. https://doi.org/10.18920/pedologist.55.3_373
- Supit, I. (1997). Predicting national wheat yields using a crop simulation and trend models. *Agricultural and Forest Meteorology*, 88(1), 199–214. [https://doi.org/10.1016/S0168-1923\(97\)00037-3](https://doi.org/10.1016/S0168-1923(97)00037-3)
- Tan, M. L., Ficklin, D. L., Ibrahim, A. L., & Yusop, Z. (2014). Impacts and uncertainties of climate change on streamflow of the Johor River Basin, Malaysia using a CMIP5 General Circulation Model ensemble. *Journal of Water and Climate Change*, 5(4), 676–695. <https://doi.org/10.2166/wcc.2014.020>
- Teleubay, Z. (2023). *Source codes for snow depth and snow water equivalent calculation on Google Earthe Enigne platform using Sentinel-2 MSI images*. [JavaScript]. <https://code.earthengine.google.com/>
- Teleubay, Z., Yermekov, F., Rustembayev, A., Topayev, S., Zhabayev, A., Tokbergenov, I., Garkushina, V., Igilmanov, A., Shelia, V., & Hoogenboom, G. (2024). Comparison of Climate Change Effects on Wheat Production under Different Representative Concentration Pathway Scenarios in North Kazakhstan. *Sustainability*, 16(1), Article 1. <https://doi.org/10.3390/su16010293>
- Teleubay, Z., Yermekov, F., Tokbergenov, I., Toleubekova, Z., Igilmanov, A., Yermekova, Z., & Assylkhanova, A. (2022). Comparison of Snow Indices in Assessing Snow Cover Depth in Northern Kazakhstan. *Sustainability*, 14(15), Article 15. <https://doi.org/10.3390/su14159643>
- Terekhov, A. G., Abayev, N. N., Tillakarim, T. A., & Serikbay, N. T. (2023). Interrelation between snow cover depth and spring flooding in Northern Kazakhstan. *Sovremennye problemy distantsionnogo zondirovaniya Zemli iz kosmosa*, 20(1), 323–328. <https://doi.org/10.21046/2070-7401-2023-20-1-323-328>
- The GFDL Earth System Model Version 4.1 (GFDL-ESM 4.1): Overall Coupled Model Description and Simulation Characteristics—Dunne—2020—Journal of Advances in Modeling Earth Systems—Wiley Online Library*. (n.d.). Retrieved October 19, 2023, from <https://agupubs.onlinelibrary.wiley.com/doi/10.1029/2019MS002015>
- Thomas, S., Seitonen, O., & Herva, V.-P. (2016). Nazi memorabilia, dark heritage and treasure hunting as “alternative” tourism: Understanding the fascination with the material remains of World War II in Northern Finland. *Journal of Field Archaeology*, 41(3), Article 3. <https://doi.org/10.1080/00934690.2016.1168769>

- Upwanshi, M., Damry, K., Pathak, D., Tikle, S., & Das, S. (2023). Delineation of potential groundwater recharge zones using remote sensing, GIS, and AHP approaches. *Urban Climate*, 48, 101415. <https://doi.org/10.1016/j.uclim.2023.101415>
- U.S. Department of Agriculture. (2022, August). *Kazakhstan: Wheat production forecast lowered due to dryness in the north*. International Production Assessment Division. <https://ipad.fas.usda.gov/highlights/2022/08/Kazakhstan/index.pdf>
- U.S. Department of Agriculture. (2023, July 20). *Kazakhstan: Grain and Feed Update | USDA Foreign Agricultural Service*. <https://www.fas.usda.gov/data/kazakhstan-grain-and-feed-update-25>
- Uyan, M. (2013). GIS-based solar farms site selection using analytic hierarchy process (AHP) in Karapinar region, Konya/Turkey. *Renewable and Sustainable Energy Reviews*, 28, 11–17. <https://doi.org/10.1016/j.rser.2013.07.042>
- van der Velde, M., van Diepen, C. A., & Baruth, B. (2019). The European crop monitoring and yield forecasting system: Celebrating 25 years of JRC MARS Bulletins. *Agricultural Systems*, 168, 56–57. <https://doi.org/10.1016/j.agsy.2018.10.003>
- van Vuuren, D. P., Edmonds, J., Kainuma, M., Riahi, K., Thomson, A., Hibbard, K., Hurtt, G. C., Kram, T., Krey, V., Lamarque, J.-F., Masui, T., Meinshausen, M., Nakicenovic, N., Smith, S. J., & Rose, S. K. (2011). The representative concentration pathways: An overview. *Climatic Change*, 109(1), 5. <https://doi.org/10.1007/s10584-011-0148-z>
- Vavrus, S. (2007). The role of terrestrial snow cover in the climate system. *Climate Dynamics*, 29(1), 73–88. <https://doi.org/10.1007/s00382-007-0226-0>
- Vogeler, I., Cichota, R., Langer, S., Thomas, S., Ekanayake, D., & Werner, A. (2023). Simulating water and nitrogen runoff with APSIM. *Soil and Tillage Research*, 227, 105593. <https://doi.org/10.1016/j.still.2022.105593>
- Vojtek, M., & Vojteková, J. (2019). Flood Susceptibility Mapping on a National Scale in Slovakia Using the Analytical Hierarchy Process. *Water*, 11(2), Article 2. <https://doi.org/10.3390/w11020364>
- Wageningen University & Research, University of Nebraska-Lincoln. (n.d.). *Global yield gap atlas*. Global Yield Gap Atlas. Retrieved November 7, 2023, from <https://www.yieldgap.org/>
- Wang, D., Li, R., Gao, G., Jiakula, N., Toktarbek, S., Li, S., Ma, P., & Feng, Y. (2022). Impact of Climate Change on Food Security in Kazakhstan. *Agriculture*, 12(8), Article 8. <https://doi.org/10.3390/agriculture12081087>
- Weber, L., Bartek, L., Brancoli, P., Sjölund, A., & Eriksson, M. (2023). Climate change impact of food distribution: The case of reverse logistics for bread in Sweden. *Sustainable Production and Consumption*, 36, 386–396. <https://doi.org/10.1016/j.spc.2023.01.018>
- Wimalasiri, E., Ampitiyawatta, A., Dissanayake, P., & Karunaratne, A. (2022). Impact of climate change adaptation on paddy yield in dry zone Sri Lanka: A case study using agricultural production systems simulator (APSIM) model. *IOP Conference Series Earth and Environmental Science*, 1016. <https://doi.org/10.1088/1755-1315/1016/1/012036>

- Wu, R.-S., Molina, G. L. L., & Hussain, F. (2018). Optimal Sites Identification for Rainwater Harvesting in Northeastern Guatemala by Analytical Hierarchy Process. *Water Resources Management*, 32(12), 4139–4153. <https://doi.org/10.1007/s11269-018-2050-1>
- Xiang, Z., Bailey, R. T., Nozari, S., Husain, Z., Kisekka, I., Sharda, V., & Gowda, P. (2020). DSSAT-MODFLOW: A new modeling framework for exploring groundwater conservation strategies in irrigated areas. *Agricultural Water Management*, 232, 106033. <https://doi.org/10.1016/j.agwat.2020.106033>
- Xiao, X., Shen, Z., & Qin, X. (2001). Assessing the potential of VEGETATION sensor data for mapping snow and ice cover: A Normalized Difference Snow and Ice Index. *International Journal of Remote Sensing*, 22(13), 2479–2487. <https://doi.org/10.1080/01431160119766>
- Xu, T., Shi, Z., & An, Z. (2018). Responses of ENSO and NAO to the external radiative forcing during the last millennium: Results from CCSM4 and MPI-ESM-P simulations. *Quaternary International*, 487, 99–111. <https://doi.org/10.1016/j.quaint.2017.12.038>
- Yasser, M., Jahangir, K., & Mohmmad, A. (2013). Earth dam site selection using the analytic hierarchy process (AHP): A case study in the west of Iran. *Arabian Journal of Geosciences*, 6(9), 3417–3426. <https://doi.org/10.1007/s12517-012-0602-x>
- Yeh, H.-F., Cheng, Y.-S., Lin, H.-I., & Lee, C.-H. (2016). Mapping groundwater recharge potential zone using a GIS approach in Hualian River, Taiwan. *Sustainable Environment Research*, 26(1), 33–43. <https://doi.org/10.1016/j.serj.2015.09.005>
- Yifru, B. A., Chung, I.-M., Kim, M.-G., & Chang, S. W. (2021). Assessing the Effect of Land/Use Land Cover and Climate Change on Water Yield and Groundwater Recharge in East African Rift Valley using Integrated Model. *Journal of Hydrology: Regional Studies*, 37, 100926. <https://doi.org/10.1016/j.ejrh.2021.100926>
- Zhang, H., & Oweis, T. (1999). Water–yield relations and optimal irrigation scheduling of wheat in the Mediterranean region. *Agricultural Water Management*, 38(3), 195–211. [https://doi.org/10.1016/S0378-3774\(98\)00069-9](https://doi.org/10.1016/S0378-3774(98)00069-9)
- Zhang, T. (2005). Influence of the seasonal snow cover on the ground thermal regime: An overview. *Reviews of Geophysics*, 43(4). <https://doi.org/10.1029/2004RG000157>
- Zhang, T., He, Y., DePauw, R., Jin, Z., Garvin, D., Yue, X., Anderson, W., Li, T., Dong, X., Zhang, T., & Yang, X. (2022). Climate change may outpace current wheat breeding yield improvements in North America. *Nature Communications*, 13(1), Article 1. <https://doi.org/10.1038/s41467-022-33265-1>
- Zhang, Y., Kendy, E., Qiang, Y., Changming, L., Yanjun, S., & Hongyong, S. (2004). Effect of soil water deficit on evapotranspiration, crop yield, and water use efficiency in the North China Plain. *Agricultural Water Management*, 64(2), 107–122. [https://doi.org/10.1016/S0378-3774\(03\)00201-4](https://doi.org/10.1016/S0378-3774(03)00201-4)
- Zhou, Y., Zhu, X., Guo, W., & Feng, C. (2023). Effects of Climate Change on Wheat Yield and Nitrogen Losses per Unit of Yield in the Middle and Lower Reaches of the Yangtze River in China. *Atmosphere*, 14(5), Article 5. <https://doi.org/10.3390/atmos14050824>

Zhumabayev, E. (2023). *Strategic measures to combat desertification in the Republic of Kazakhstan until 2025 | United Nations Development Programme*. UNDP.
<https://www.undp.org/ru/kazakhstan>

Összefoglaló

A disszertáció középpontjában Észak-Kazahsztán mezőgazdasági termelésének klímaváltozáshoz való alkalmazkodása áll, különös tekintettel a tavaszi hóolvadásból származó vízkészletek fenntartható hasznosítására. A térség búzatermelése az ország gazdasága és Közép-Ázsia élelmezésbiztonsága szempontjából meghatározó, ugyanakkor egyre nagyobb veszélyt jelentenek a gyakori aszályok, a hirtelen hóolvás okozta árvizek, valamint a hiányos vízgazdálkodási infrastruktúra. A tanulmány újszerű megközelítése abban rejlik, hogy a hóolvadást nem kockázati tényezőként, hanem stratégiai vízforrásként értelmezi, amely hozzájárulhat a klímaturóbb mezőgazdaság kialakításához.

A kutatás három fő pillére: (1) klímaváltozási forgatókönyvek hatásának vizsgálata a tavaszi búza hozamaira a DSSAT modell segítségével, (2) távérzékelési módszerek fejlesztése a hóvastagság és a hóvíz-egyenérték (SWE) pontos becslésére Sentinel-2 műholdfelvételek és terepi mérések alapján, valamint (3) egy térinformatikai, AHP-alapú döntéstámogató rendszer kidolgozása kis léptékű víztározók optimális helyének kijelölésére.

Az eredmények szerint a század közepére a várható hozamsökkenés 9% (RCP2.6), 17% (RCP4.5) és 26% (RCP8.5), különösen a déli és középső, gyengébb vízmegtartó képességű talajokkal rendelkező régiókban. A távérzékelési vizsgálatok alapján a DSI-2 index bizonyult a legpontosabbnak ($R^2 > 0,88$), lehetővé téve a hóborítás és a SWE nagyfelbontású térképezését. A térinformatikai elemzés 3,3%-ot jelölt „nagyon magas”, 35,5%-ot „magas”, és 56,5%-ot „közepes” alkalmasságú területként tározók létesítésére. A vízmérlegek szerint 5 hektár hófogó terület elegendő vízhozamot biztosíthat 1 hektár teljes, vagy 2 hektár részleges öntözéséhez, ami a terület szántóterületeinek mintegy egynegyedét láthatná el kiegészítő öntözéssel.

A disszertáció fő hozzájárulása, hogy a hóolvadást integrálja a regionális vízgazdálkodási stratégiákba, és ezzel új utakat nyit a szárazföldi, hideg sztyeppi rendszerek klímaadaptív mezőgazdasági fejlesztésében. Az interdiszciplináris módszertan és a gyakorlati alkalmazhatóság révén a kutatás nemcsak tudományos értéket hordoz, hanem közvetlen gyakorlati ajánlásokat is ad a vízbiztonság és az élelmiszer-termelés stabilitásának erősítésére Észak-Kazahsztánban.